To the Graduate Council:

I am submitting herewith a dissertation written by Richard Steward Hutchings, entitled "Thermodynamics of Binary n-Alkane Mixtures; Partial Molar Volumes and Free Energies." I have examined the final copy of this dissertation for form and content and recommend that it be accepted in partial fulfillment of the requirements for the degree of Doctor of Philosophy, with a major in Chemistry.

Alexander Van Hook, Major Professor

We have read this dissertation
and recommend its acceptance:

C R Brooks

Jeffrey Kovac

J. Alexander

John E. Bloor

Accepted for the Council:

The Graduate School

4

THERMODYNAMICS OF BINARY n-ALKANE MIXTURES; PARTIAL MOLAR VOLUMES AND FREE ENERGIES

A Dissertation

Presented for the

Doctor of Philosophy

Degree

The University of Tennessee, Knoxville

Richard Steward Hutchings

March 1984

ACKNOWLEDGEMENT

The author wishes to give his most sincere thanks to Dr. W. Alexander Van Hook for the strong guidance, inspiration, and friendship given during the course of this work. Also, the assistance of Dr. J. Kovac and Dr. G. Jakli is greatly appreciated. Special thanks are extended to the National Science Foundation and Dupont Company for financial assistance.

To Pedro Bernal, Betty Williams and Rajiv Singh, the author would like to express his appreciation for the support and friendship given over the years. He is also indebted to Mr. Paul Beal for the fine work and valuable knowledge shared over the course of this work. Finally, but in no way least, the author wishes to thank Mr. George McGhee for the extraordinary typing of this dissertation.

The author dedicates this work to his loving mother, Mrs. Lena C. Hutchings.

ABSTRACT

Excess partial molar free energies and excess volumes of n-alkane/n-alkane mixtures were investigated, with special emphasis placed on the low concentration regions. Using a vibrating tube densitometer, the excess volumes of the following systems are reported; $n\text{-}C_8 + n\text{-}C_9$ and $n\text{-}C_8 + n\text{-}C_{10}$, at 288.15 K, and $n\text{-}C_8 + n\text{-}C_9$, $n\text{-}C_8 + n\text{-}C_{10}$ and $n\text{-}C_9 + n\text{-}C_{11}$ at 298.15 K across the entire concentration range; and $n\text{-}C_8 + n\text{-}C_{10}$, $n\text{-}C_9 + n\text{-}C_{11}$ and $n\text{-}C_9 + n\text{-}C_{13}$ at 298.15 K at low concentrations (characterized by a particularly high density of data points). The excess partial molar free energies were measured with a continuous dilution vapor pressure apparatus. Limiting activity coefficients are reported for $n\text{-}C_6 + n\text{-}C_7$ and $n\text{-}C_7 + n\text{-}C_8$ at 303.15 K, and $n\text{-}C_6 + n\text{-}C_5$, $n\text{-}C_7 + n\text{-}C_6$, $n\text{-}C_8 + n\text{-}C_7$, $n\text{-}C_9 + n\text{-}C_8$ and $n\text{-}C_9 + n\text{-}C_7$ at 323.15 K. Activity coefficients are also reported for the benzene-cyclohexane and benzene-cyclohexane-water test systems.

Correlations between the excess properties and carbon number are given. The data are interpreted and the observations are compared with the predictions of the various theories of binary n-alkane mixtures.

TABLE OF CONTENTS

LIST OF TABLES

TABLE PAGE

TABLE PAGE

TABLE PAGE

LIST OF FIGURES

FIGURE PAGE

CHAPTER I

INTRODUCTION

One goal of solution chemistry is the formulation of laws to quantitatively describe the behavior of liquids and liquid mixtures. A first step toward realization of this goal is to gain an understanding of the properties of liquids and their mixtures which are structurally simple and free of those factors, such as electrostatic or chemical interactions, that complicate the interpretation of observed liquid phase behavior. Consequently, the thermodynamic properties of straight chain hydrocarbons and their mixtures have been the object of intense theoretical and experimental investigation for many decades. Consisting only of end methyl, $-CH_3$, and repeating middle methylene, $-CH_2-$, groups, n-hydrocarbons are ideal for scientific investigation. Also, because n-hydrocarbons are major constituents of our fossil fuels and are used in today's polymer industries, the understanding of their thermodynamic properties has recently become increasingly important. Although considerable progress has been made toward understanding the properties of n-hydrocarbons, the door to complete understanding has barely been opened.

The magnitude of the observed thermodynamic properties of n-hydrocarbon mixtures is small and therefore extremely difficult to measure. This fact accounts for the lack of systematic experimental studies of the quality required for a comprehensive interpretation of the liquid phase behavior. Furthermore, theoreticians are hindered by this lack of precise experimental data with which the theories concerning the thermodynamics of n-hydrocarbons can be developed and tested.

The present theoretical framework used for the interpretation of the thermodynamics of n-hydrocarbons is dominated by four approaches, which are not necessarily mutually exclusive. They are the principle of congruence; the corresponding states theory; Flory's theory; and the theoretical work of Patterson. The principle of congruence, originally due to Brønsted,[1] is an empirical statement which qualitatively describes the excess thermodynamic properties of a mixture of n-alkanes purely in terms of the average chain length of its components. The principle of corresponding states[2,3] was an early attempt to describe quantitatively what occurs on a microscopic level in n-alkane mixtures. This principle assumed that if reduced quantities are used, then a universal equation of state may be written to describe the physical behavior of the substances involved. The theory of Flory and coworkers,[4-7] which was derived from the corresponding states theory, was based on the assumption that the intermolecular energy depended only on the volume and that it was permissible to adopt a hard sphere repulsive potential for the segments of the chain when developing an equation of state for n-hydrocarbons. Most recently, the theoretical work of Patterson and coworkers[8-11] has incorporated the notion of a correlation of molecular orientations into a theory developed by Flory in an attempt to better represent the observed thermodynamic trends. These various approaches will be discussed in turn in the following material.

It is interesting to note that the theoretical studies on n-hydrocarbons progressed at a much more rapid pace than the experimental investigations and when compared with the experimental data

available, the theories agreed more closely with themselves than with the experimental facts they were designed to interpret. As will be seen in the following historical review, each theoretical approach has some serious inherent flaw. Furthermore, with every new experimental measurement the rationale with which the data is interpreted changes. Clearly, further understanding of the thermodynamic behavior of n-hydrocarbons rest not just with theory but also, and more importantly, in the acquisition of accurate and precise experimental data.

A. PRINCIPLE OF CONGRUENCE

The basic assumption underlying the early theories concerning n-hydrocarbons and their binary solutions was that, in these liquids, thermodynamic behavior was governed by $-CH_2-$ (midchain) and $-CH_3$ (terminal) segment interactions. It was assumed that the $-CH_2-$ and $-CH_3$ segments, rather than the individual molecules, were the basic elements governing the thermodynamics of the pure liquid or mixture.

In 1937, Hildebrand[12] investigated the thermodynamic properties of n-paraffin mixtures, and from the standpoint of statistical mechanics and many simplifying assumptions, derived the ideal value, $-R\ln x_i$, for the entropy of a paraffin component i in the mixture. Later, Fowler and Rushbrooke[13] made an attempt to extend the statistical theory of perfect solutions to mixtures in which the molecules were distinctly unequal in size. They reduced the liquid arrangements to those of a simple regular lattice and represented a change of size by requiring the larger molecule to occupy two or more adjacent lattice

sites. Furthermore, all configurations were assumed to have the same energy. On the basis of these simplifying assumptions, they showed that deviations from the ideal vapor pressure curves may be due to the components of the mixtures differing widely in molecular size and not necessarily due to the influence of intermolecular forces.

Utilizing the basic assumptions described in the last paragraph, Brønsted and Koefoed[1] formulated the "Concept of Congruence" for mixtures of normal paraffins. The theory assumed that a mixture of components A_1, A_2,... containing n_1, n_2,... carbon atoms per molecule, respectively, and present in the mixture in mole fractions x_1, x_2,... may be characterized by an index n, and that mixtures with the same index be considered congruent. These congruent solutions were postulated to have the same equilibrium properties. An equivalent statement of the principle of congruence[14] is that any excess thermodynamic property of a mixture of n-alkanes should be determined at a given temperature and pressure entirely by the average chain length x_i n_i, where x_i is the mole fraction of an n-alkane containing n_i carbon atoms. Then if the excess Gibbs function, G^E, for a binary mixture is parabolic in the mole fraction x_i for any one pair of n-alkanes (i.e., form a regular or simple mixture,[15]) then G^E should also be parabolic for any other pair, and for each pair, the height of the parabola should be proportional to the square of the difference between the n_1 and n_2 of the carbon atoms in the two n-alkanes. That is to say,

$$G^E = (n_1-n_2)^2 Ax(1-x) \qquad 1$$

where A depends on temperature and pressure, but not on n_1 or n_2. So from basic thermodynamic relationships, assuming eqn. (1) is obeyed, the heat of mixing H^E and the volume of mixing V^E must obey the relationships

$$H^E = (n_1-n_2)^2Bx(1-x) \qquad 2$$

and

$$V^E = (n_1-n_2)^2Cx(1-x) \qquad 3$$

where $B = A-T\partial A/\partial T$ and $C = \partial A/\partial P$.

In an attempt to verify their theoretical results, Brønsted and Koefoed[1] found the values of G^E, obtained from their vapor pressure measurements for the three pairs of n-alkanes 6 + 16, 7 + 16, and 6 + 12 at 20°C, could be fitted by equation (1) with A = -2.69 J/mole. Van der Waals[16] found that his measurements of the heats of mixing H^E for five pairs of n-alkanes at 20°C could be roughly fitted by eqn. (2) with B = 5.1 J/mole. McGlashan and Morcom[17] also chose eqn. (2) to fit their data and concluded that the principle of congruence satisfactorily interpreted their data. In a later work, Harrison and Winnick[18] chose to fit their excess volumes of mixing for binary n-alkane mixtures, utilizing eqn. (4)

$$V^E = A_1(N_2-N)(N-N_2)/(N-2)(N_1-2)(N_2-2) + A_2(N_2-N)(N-N_1)/(N-2)(N_1-2)(N_2) \times (1/(N-2) + 1/(N_1-2) + 1/(N_2-2)) \qquad 4$$

for the excess volume, derived by Hijmans and Holleman,[19] which is based on the principle of congruence.

B. PRINCIPLE OF CORRESPONDING STATES

Although the data of McGlashan,[17] Van der Waals,[16] along with that of others[19] were satisfactorily fitted by the principle of congruence,[1] the fact remains that the principle is purely empirical and makes no attempt to quantitatively describe what occurs on a microscopic level in n-alkane mixtures.

The principle of corresponding states introduced by Pitzer[2] and Guggenheim,[3] is often used for correlating the thermodynamic properties of simple substances. For approximately spherical molecules it may be assumed that the intermolecular interaction potential for a pair of molecules depends only on their distance apart, r, and is of the form

$$\psi(r) = \varepsilon\psi^*(r/\sigma), \qquad 5$$

where ψ^* is a universal function of the reduced distance, $r^* = r/\sigma$, and where ε and σ are scale factors determining the overall strength and the range of the interaction. Pitzer[2] and later Guggenheim[3] showed that for all substances satisfying the requirement, eqn. (5), a principle of corresponding states is valid. A universal equation of state, $p^*(v^*,T^*)$, valid for any of these substances, was obtained when the pressure, volume and temperature were replaced by the reduced quantities

$$p^* = p\sigma^3/\varepsilon;\ v^* = v/N\sigma^3;\ T^* = kT/\varepsilon \qquad 6$$

Prigogine, Bellemans, and Narr-Colin[20] extended the principle of corresponding states to liquids of chain molecules such as the

members of the normal alkane series. They stressed that care must be taken when selecting the corresponding properties because the theory is only applicable to condensed states. It does not work at the critical point nor in the gaseous state.

The essential step in the generalization of Prigogine and coworkers[20,21] is the introduction of three dimensionless parameters q, r, and c, each having the significance of an effective number of segments per molecule and depending only on the chain length n. Thus the energy, volume and entropy become

$$U_0(n) = q(n)N\varepsilon;\ V_0(n) = r(n)N\sigma^3;\ S_0(n) = c(n)Nk \qquad 7$$

where k is Boltzmann's constant and ε and σ characterize the strength and range of the interactions between segments, respectively. By using the quantities of equation (7), and the corresponding units for temperature and pressure;

$$T_0(n) = q(n)/c(n)\ x\ \varepsilon/K;\ p_0(n) = q(n)/r(n)\ x\ \varepsilon/\sigma^3 \qquad 8$$

various thermodynamic relations such as the molar volume, the "external" potential energy, or the compressibility as functions of the temperature, could be reduced to universal relations, valid for any value of the chain length.

Holleman and Hijmans[22] developed a principle of corresponding states for the thermodynamic excess functions of binary mixtures of chain molecules which is based on the theory of congruence[1] and a phenomenological formulation of the principle of corresponding states[23]. First, consider some extensive thermodynamic quantity A

and consider its dependence on temperature for all members of a homologous series at zero pressure. From the principle of corresponding states the authors were able to write,

$$A(n,T) = A_0(n) \times A^*(T^*) \qquad 9$$

where T* is defined by

$$T = T_0(n) \times T^* \qquad 10$$

and where $A_0(n)$ and $T_0(n)$ are the reduction factors for the quantity A. $A^*(T^*)$ is a universal function of chain length. It follows that the excess functions of property A for a binary mixture is defined as

$$A^E(n_1,n_2,x_1,x_2,T) = A(n_1,n_2x_1,x_2,T)-Ax_1(n_1,T)-x_2A(n_2,T) \qquad 11$$

where $A\ (n_1,n_2,x_1,x_2,T)$ is the property of the mixture. Utilizing Brønsted's principle of congruence,[1] eqn. (11) may be written as

$$A^E(n_1,n_2,n,T) = A(n,T)-n_2-n_1/((n_2-n_1) \times (n-n_1)/(n_2-n_1) \times A(n_2,T)) \qquad 12$$

Now by applying eq. (9) to eqn. (12), the authors obtained

$$A^E(T_1^*,T_2^*) = A_0(n) \times (A^*(T^*)-x_1A^*(T_1^*)-x_2A^*(T_2^*)) \qquad 13$$

with

$$T^* = T/T_0(n);\ T_1^* = T/T_0(n_1);\ T_2^* = T/T_0(n_2) \qquad 14$$

and

$$x_1 = (n_2-n)/(n_2-n_1)*A_0(n_1)/A_0(n);\ x_2 = (n-n_1)/(n_2-n_1)*A_0(n_2)/A_0(n) \qquad 15$$

Now recall that a function obeys a principle of corresponding states if it takes the form of eqn (5). Therefore the excess function will obey a principle of corresponding states if the reduced excess function

$$A^E(T_1^*,T_2^*,T^*) = A^*(T)-x_1A(T_1^*)-x_2A^*(T_2^*)) \quad 16$$

can be expressed as a universal function of T_1^*, T_2^* and T^*, not explicitly involving n, n_1, and n_2. This requirement was found to be satisfied if the molecular units $A_0(n)$ and $T_0(n)$ are special functions of the chain length n.

The formal derivation of the principle for excess function can be found in reference (22). The conclusions reached are that for the principle of corresponding states to be applicable to an excess quantity $A^E(n_1, n_2, x_2, x_2, T)$;

(a). the molecular unit for the temperature as a function of chain length is of the form

$$T_0(n) = \text{const. } ((1-\alpha)/(1-\beta n))^u \quad 17$$

where $\alpha = \dfrac{q_m/q_e}{2(1-q_m/q_e)}$ and $\beta = \dfrac{c_m}{2-3c_m}$,

and (b). The molecular unit for the property A whose behavior is studied is of the form

$$A^0(n) = \text{const. } ((1+\alpha n)/(1-\beta(n))^v x(1-\alpha n) \quad 18$$

Holleman and Hijmans[22] tested the theory by using heats of mixing data from McGlashan[17] and Van der Waals[16,24]. It was found that by utilizing the conditions described previously, the theory worked reasonably well in fitting the experimental data. As will be seen in the following section, problems resulted from the use of the cell

model. The model proved to be inadequate when the theory was expanded to rationalize more of the observed characteristics of n-hydrocarbons and their binary mixtures.

C. FLORY'S EQUATION OF STATE

The difficulty experienced by Prigogine and coworkers[20,21] resulted from the use of a cell model which fixed the nearest neighbors of a given molecule at their mean positions and suppressed randomness. By fixing the positions of the molecules, the intermolecular energy obtained from the model was not representative of the actual energy.

Using statistical thermodynamics, Flory and coworkers[4] developed an equation of state for n-hydrocarbons. They assumed the intermolecular energy to depend only on the volume and adopted a hard sphere repulsive potential for segments of the chain. The number of external degrees of freedom was introduced as a parameter on the premise that the corresponding modes could be separated from the internal degrees of freedom of the molecules.

Start the derivation by considering normal hydrocarbons consisting of repeating $-CH_2-$ groups, the number of which depending on the specific hydrocarbon. The terminal groups, $-CH_3$, are assumed to exert intermolecular forces differing from those of the midchain segments. Also, the chain is assumed to be flexible and capable of assuming a variety of spatial configurations. Now imagine the chain to be divided into x segments. Although the segment need not be defined, the authors[4] specified that x be linear with n for homologous members of the series or more particularly, proportional to the "hard core" molecular volume $V^* = xv^*$, where v^* is the net volume of the segment.

To represent the mean number of external contact sites per segment of the molecule, the authors[4] used the relationship

$$x_s = xs_m + x_e \qquad 19$$

where s_m is the number of contacts for an internal segment and s_e is the contribution due to chain ends. Thus x_s could be regarded as a measure of molecular surface.

The modes of motion were defined by assuming that the normal oscillatory modes of the isolated chain molecules could be separated into internal (intramolecular) and external (intermolecular) modes. Since the internal modes were considered not to be affected appreciably by neighboring molecules, they were disregarded. On the other hand, the intermolecular modes are subject to greater perturbation by interaction with neighbors. Thus the intermolecular modes could be treated as translational (external) motions. By adding the three degrees of freedom of the molecular center of gravity and the intermolecular modes, the total number of intermolecular degrees of freedom is

$$3xc = 3(xc_m + c_e) \qquad 20$$

per molecule. c is assumed to be independent of the temperature and volume over the range of application of the equations to follow.

Subsequently, on the assumption of hard sphere repulsion between segments and concepts discussed above, Flory and coworkers[4] were able to write the configuration partition function of the liquid

$$Z = Z^{\dagger}(r(v^{1/3}-v^{*1/3})^3)^{xNc}\exp(-E_0/kT) \qquad 21$$

where r is a geometric constant, E_0 the intermolecular energy and $Z^\dagger$ the "combinatorial factor." $Z^\dagger$ has to do with the way the molecules are arranged with respect to each other. The form of the partition function is the same as was introduced by Prigogine,[20] yet the treatment of E_0 distinguishes Flory's development.[4]

As noted above, the cell model was rejected as a base for expressing the intermolecular energy E_0. The energy of interaction between a pair of molecules is a sensitive function of the intermolecular distance. Thus the error introduced by confining the neighboring molecules to a predescribed distance introduces a large error in the energy. This prediction was justified by the authors[4] by noting that, irrespective of the density of mean displacement, one or more of the molecule's neighbors is likely to be in proximity to the distance of closest approach. Furthermore, these molecules' contribution to the energy is the most important.

Assuming the terminal segments to have different forces of attraction to neighbors than that of the midchain segments, the intermolecular energy may be written

$$E_o = -(1/v)(N_m\eta_m + N_{em}\eta_{em} + N_e\eta_e) \qquad 22$$

where η_m, η_{em} and η_e characterize interactions between sites on two neighboring midchain segments, between a midchain and a terminal segment site, and between two terminal sites respectively. The N's, which are assumed to be equal to those for random mixing of sites, denote the numbers of neighbor pairs in the respective categories. The number of terminal sites having atypical interactions is taken to be

s_e, the excess number of sites for the two end groups as required by eqn. (19).

Upon substituting the equation

$$E_o = -xNs\eta/2v \tag{23}$$

into eqn. (21) and introducing the reduced variables

$$\tilde{V} = v/v^* \tag{24}$$

and

$$\tilde{T} = T/T^* = 2v^*ckT/s\eta \tag{25}$$

Flory and coworkers[4] obtained

$$Z = Z^+(\gamma v^*)^{xNc}(\tilde{v}^{1/3}-1)^{3xNc}\exp(xNc/\tilde{v}\tilde{T}) \tag{26}$$

The equation of state obtained from eqn. (26) and expressed in reduced form is

$$\tilde{p}\tilde{V}/T = \tilde{v}^{1/3}/((\tilde{v}^{1/3}-1) - (1/\tilde{v}\tilde{T})) \tag{27}$$

with the reduced pressure $\tilde{p}$ defined by

$$\tilde{p} = p/p^* = 2pv^{*2}/s\eta = pv^*/ckT^* \tag{28}$$

The reduced equation of state may also be expressed as

$$\tilde{p}/\tilde{\rho}^2 = T/(1-\tilde{\rho}^{1/3})-1 \tag{29}$$

where $\tilde{\rho} = 1/\tilde{v}$ is the reduced density.

The coefficient of thermal expansion α, the coefficient of compressibility κ, and the thermal pressure coefficient γ may be expressed in terms of the reduced variables as

$$\alpha = v^{-1}/(\partial v/\partial T)p = (\tilde{T}/T\tilde{v})(\partial\tilde{V}/\partial\tilde{T})\tilde{p} \qquad 30$$

$$\kappa = -v^{-1}(\partial v/\partial p)T = -(\tilde{p}/p\tilde{v})(\partial\tilde{v}/\partial\tilde{p})_{\tilde{T}} \qquad 31$$

$$\text{and } \gamma = (\partial p/\partial T)_v = \alpha/\kappa = (\tilde{T}p/T\tilde{p})(\partial\tilde{p}/\partial\tilde{T})_{\tilde{v}} \qquad 32$$

By solving eqn. (29) first for $\tilde{T}$ and then for $\tilde{p}$, differentiating the results, and finally eliminating $\tilde{T}$ in each case, the following equations are obtained. These equations furnish a simple basis for evaluating the various parameters.

$$(\alpha T)^{-1} = 1/3(\tilde{v}^{1/3}-1)-1 + 2\tilde{p}\tilde{v}^2/(\tilde{p}\tilde{v}^2 + 1) \qquad 33$$

$$(\kappa p)^{-1} = (1/3(\tilde{v}^{1/3}-1)-1)(1 + 1/\tilde{p}\tilde{v}^2) + 2 \qquad 34$$

$$(\gamma T)/\rho = 1 + 1/\tilde{p}\tilde{v} \qquad 35$$

Also the values of the parameters become

$$s\eta = 2pv^2 = 2\gamma Tv^2 \qquad 36$$

and

$$c = p^*v^*/T^* = (\gamma v/\kappa) = (\alpha/T)/(3 + 4\alpha T) \qquad 37$$

Experimental verification of the results obtained above can be found in reference 6.

The statistical thermodynamic treatment outlined above is derived for pure n-hydrocarbons. Nevertheless, the rationale and equations previously described can be expanded to mixtures of n-hydrocarbons.[5]

The authors rationalized that since the two types of segments ($-CH_2-$ and $-CH_3$) were assumed to be distributed randomly for the pure components, it was valid to apply the assumptions to their mixtures. The only drawback noted was that differences in the two species might introduce different correlations between terminal and midchain segments.

By making the proper analogies, the authors[5] were able to write

$$E_o = -\bar{x}Np^*v^*/\tilde{v} = -\bar{x}Ns\eta/2v \qquad 38$$

where E_o is the intermolecular energy, and $\bar{x}$ is the number average defined by

$$\bar{x} = \Sigma x_l N_l/\Sigma N_l = \Sigma x_l N_l/N \qquad 39$$

with s and η retaining their previous definitions. The parameters for the pure components now become

$$1/x = \Sigma\psi_i/x_i;\ s = \Sigma\psi_i s_i;\ c = \Sigma\psi_i c_i \qquad 40$$

where ψ_i is the segment fragment for species i

$$\psi_i = x_i n_i/\Sigma x_i N_i \qquad 41$$

The derivation of the equations for the excess properties of the mixtures is relatively straight forward. Yet only the procedure for obtaining the excess volume will be outlined. For the derivation of the other excess properties, the reader is referred to reference (7).

Remembering that the hard sphere approximation was applied to the various segments, let $\tilde{v}^o$ represent the reduced volume per segment. Therefore it follows for a binary mixture that

$$V^E = \tilde{v}-\tilde{v}^o = \tilde{v}-\psi_1\tilde{v}_1-\psi_2\tilde{v}_2 \qquad 42$$

where $\tilde{v}$ is the reduced volume of the mixture.

To evaluate $\tilde{v}^E$, Flory[5] began by first noting that $1/\tilde{T}$ increased linearly with $1/x$ within experimental error. Thus it was appropriate to write

$$\tilde{T} = \tilde{T}_\infty(1 + (C_e/C_m-a)/\bar{x}) \qquad 43$$

Therefore since $1/x$ was linear in the ψ_i, it followed that $\tilde{T}$ for a binary mixture should also vary linearly with the segment fraction composition at constant T,

$$T = \psi_i\tilde{T}_i + \psi_2\tilde{T}_2 \qquad 44$$

The reduced volume $\tilde{v}^o$ for the reduced temperature $\tilde{T}$ may then be calculated from the equation of state for $p = 0$;

$$\tilde{T} = (\tilde{v}^{1/3}-1)\tilde{v}^{4/3} \qquad 45$$

Therefore, the difference compared to $\tilde{v}^o$, determined by linear interpolation from the reduced volumes v_1 and v_2 of the components, gives the excess reduced volume $\tilde{v}^E$. An alternative method for calculating the excess volume is given by the equations

$$V^E = (\partial v/\partial T)(\tilde{T}-\tilde{T}^o) = 3(\tilde{v}^o)^{7/3}(4-3(\tilde{v}^o)^{1/3})^{-1}(\tilde{T}-\tilde{T}^o) \qquad 46$$

The authors noted that the results[7] obtained from their calculations were in agreement with experimental results.[6,7] Also, Brønsted's principle of congruence[1] was acknowledged to have been reaffirmed by their data. The work of Sims and Winnick[25] further emphasized the validity of Flory's corresponding states theory. However, as will be shown in the following section, Flory's theory had several inconsistencies. The theory, as presented here, could not account for the experimentally positive excess enthalpy. Also, the reduced parameters p*, v* and T* of Flory's development, varied with temperature. It was evident that more theoretical work was needed to correct these problems.

D. PATTERSON TO PRESENT

By the end of the sixties, several treatments of the thermodynamics of n-alkanes and their mixtures had been proposed. Yet it is interesting to note that although the treatments were based on superficially different initial premises, the final relations were all similar. A study by Williamson and Scott[26] arrived at the conclusion that the differences between the theories and experimental data were major when compared with the differences between the various treatments. Therefore, it naturally followed that refinements of the existing theories, so they better agreed with existing experimental data, would be the next route of investigation.

As previously stated, Flory and coworkers concluded that their calculations were in agreement with experimental results.[6,7] However, they also found that the reduction parameters p,* v,* and T* varied with temperature, implying an imperfection in the corresponding states principle and/or the theory. The reduced pressure p,* which has the significance of intermolecular contact energy per unit volume of the alkane chain, decreased markedly with decrease of n. Whereas the excess enthalpy, H^E, is found to be positive experimentally, Flory's theory predicted H^E to be negative at all temperatures. Flory and coworkers[6,7] rationalized their H^E and p* data by assuming the force fields surrounding the methyl end groups to be weaker than those around the methylene groups in the interior of the alkane chains.

The problems pointed out by Flory[6,7] and others were investigated in more detail by Patterson and coworkers.[8,9] By using existing density, thermal expansion coefficient, and isothermal compressibility data for the n-alkane series from methane to polymethylene, Patterson and coworkers[8-10] concluded that the variation of p* with both n and T to be an artifact of the approximate Flory theory. It was found that, although the principle of corresponding states was well obeyed by the models of Flory[4] and Prigogine[2] and able to qualitatively reproduce the experimental data, characteristic errors in the models prevented quantitative agreement between theory and experiment. $\tilde{T}$ and $\tilde{V}$ increased too rapidly, and the isothermal compressibility too slowly. The result was that, in order to compensate for the effects, the reduced temperature used had to increase with temperature; p* had to decrease with increased $\tilde{T}$; and incorrectly, it had to decrease with

decreasing alkane chain length. Furthermore, the data was found to be consistent with only a very small difference in force fields surrounding methyl and methylene groups. Thus, at that time, the interpretation of the positive values of H^E remained open to question.

Patterson, Tewari and Schreiber[10] investigated the force fields surrounding the methyl and methylene groups by attempting to interpret activity coefficients obtained for normal alkanes at infinite dilution in n-C_{18} and n-C_{36} (Chruickshank and collaborators.[27]) The X_{12} parameter, "a contact interaction" term contribution to the non-combinatorial part of in γ_1^{∞}, was found to be independent of the extent of branching of the lower alkanes. This results again suggested a small methyl-methylene interchange energy.

In light of the difficulties associated with the methyl-methylene interpretation of excess functions of alkane systems, it became clear that another interpretation or method of study was warranted. Consequently, an interpretation, based on the orientational structure of these liquids extrapolated from depolarized Rayleigh scattering data, was developed.

Bothorel and collaborators[28] established depolarized Rayleigh scattering as an important technique for studying the structure of alkane systems. The apparent optical anisotropies, γ^2, obtained from such a study is representative of the chain molecule when it is unperturbed by intramolecular attractive interactions.

Bothorel and coworkers[28] obtained the apparent optical anisotropies of the n-alkanes in the pure state and in solution with spherical molecules. Although γ^2 for the short n-alkanes, $n < 7$,

showed little difference between the pure and dilute solution values, it was found that for long n-alkane molecules, e.g. n-C_{16}, there was a striking decrease of the apparent γ^2 value on passing from pure liquid to high dilution. Bothorel[28] and Nagai[29] attributed the value of for dilute solution in spherical molecule solvents to the molecular anisotropy of the long n-C_n chains.

To rationalize the results, Bothorel[28] and Nagai[29] suggested that the pure liquid value of γ^2 was raised above the dilute solution value because of a correlation of the molecular orientations (CMO) of neighboring chains or short length of these chains. Moreover, these orientations would be short range in character rather than solution wide.

Experimental results obtained by Bothorel and others[28-32] seemed to add validity to the notion of CMO. It was found that when long alkanes[30] were dissolved in a series of solvents whose molecules were increasingly less spherical, γ^2 rose from the value it would have in a spherical solvent to that for the n-alkane in the pure state. Furthermore, when measurements were made with cyclohexane, 2,2-dimethylbutane, and n-hexane as solvents,[31] there appeared to be a small CMO effect for the n-alkane chains in spherical cyclohexane and 2,2-dimethylbutane, when compared with n-hexane. These results were interpreted as showing that there was an increasing CMO between the long-chain alkane solute and the increasingly nonspherical solvent molecules.

The thermodynamic consequences of orientational order was summarized by Patterson and coworkers.[32] The orientation order would

lead to negative contributions in the configurational enthalpy and entropy of the pure n-alkanes; becoming more important with increasing n. From the experimental data,[28-31,33] it was further postulated that a corresponding positive contribution to ΔH_m and ΔS_m would occur when long n-alkanes were mixed with spherical molecules with which CMO does not occur. Therefore, the energetic weakness of a (1-2) contact relative to (1-1) and (2-2) could be caused by a relative weakness of CMO between 1 and 2 molecules, and the interchange energy and entropy would arise from the interchange correlations.

As alluded to in the previous paragraph, difficulties encountered with the methyl-methylene interpretation are not present in the CMO interpretation. For example, the thermodynamics of branched isomers would not be dictated by the increased methyl nature of the molecules, but by the increased globular shape and diminished CMO in the pure liquids and mixture. Therefore, the branching of the alkanes of lower carbon number would increase ΔH_m and ΔS_m in mixtures with a higher n-alkane and the opposite effect observed when the alkane of higher carbon number is branched.

In order to test the usefulness of the CMO interpretation of n-alkanes thermodynamics, several experiments were performed[32,34-37] and interpreted with the CMO concept. Patterson and coworkers[32] determined the heat of mixing of globular, i.e., 2,2,4-trimethylpentane, and normal alkanes. It was found that the molar heats and heats per unit volume were positive and increased rapidly with n for the n-C_n series. The branched-C_n gave a smaller positive heat and decreased with n, where n-hexane and 2,2-dimethylbutane showed

increasingly negative heats. Whereas the methyl-methylene interpretation was inconsistent with the usual positive ΔH_m in n-alkane mixtures, the CMO interpretation correctly predicted the observed experimental trends.[32]

Moreover, the CMO concept proved to be valuable in interpreting many other observed experimental phenomena. Patterson and coworkers and others[38,39] used the concept to explain enthalpy-entropy compensations,[35] excess properties,[40] temperature dependence of orientation correlations,[36] excess entropies[34] and excess heat capacities[37,41,42] in n-alkane systems.

E. STATEMENT OF PURPOSE

The theoretical successes obtained by the corresponding states principle,[2,3] CMO concept,[8-11] principle of congruence[1] and Flory theories[4-7] have established a firm foundation for studying the excess properties of normal hydrocarbons. However, as shown in the preceding discussion, there are several inconsistencies between the experimental data and the various theories. Presently, there are simply not enough experimental measurements on n-hydrocarbons to substantiate using one theory over another, or creating a new approach to explain the measured quantities.

A survey of the literature on n-alkanes and their binary mixtures reveals a shortage of experimental data. Also, the available experimental data lacks cohesiveness. Clearly, because of the importance of the experimental data to the field of solution thermodynamics, a methodical investigation of the thermodynamics of these substances is warranted.

The excess thermodynamic properties of binary n-hydrocarbon mixtures are small in magnitude and decrease as the difference in carbon number between components and the concentration of the solute, decreases. Therefore, because the effects are larger and consequently more easily studied, systems, consisting of components differing widely in carbon number and at relatively high concentrations, have received a greater amount of experimental investigation. Also, experiments at low concentrations (i.e. usually gas chromatography work) have been performed mostly on systems whose components differ widely in carbon number.

One reason to study an homologous series is that the thermodynamic properties of the series show interactions which can possibly be directly attributed to the addition of the basic unit of the series. Therefore, we have chosen those n-hydrocarbons systems which differ by only one or two methylene units and are at low ($x < .05$) concentrations. By measuring the thermodynamic properties of such systems, the effects caused by the introduction of one or two $-CH_2-$ units can be better documented and errors, introduced by extrapolation from data taken a higher concentrations or on systems whose components differ widely in carbon number, reduced.

In this context, we have chosen to study the excess volume V^E, and vapor-liquid equilibria (VLE) of binary n-hydrocarbon solutions. Furthermore, to facilitate the vapor-liquid equilibria measurements at low concentrations, a new continuous dilution vapor pressure apparatus was designed and built. Additionally, the well studied benzene-cyclohexane and benzene-cyclohexane-water systems were investigated to test

the performance and limitations of the vapor pressure apparatus and further examine the possible applications of this novel apparatus.

CHAPTER II

EXPERIMENTAL

A. MATERIALS

The normal alkanes used in this investigation were obtained from the Aldrich Chemical Company, Inc. The minimum purity of 99.9% was confirmed by G.C. analysis and density measurements to be described later. The benzene and cyclohexane were Fisher Certified A.C.S. grade. All hydrocarbons were stored over sodium wire to remove traces of water present in the substances, and used without further purification. Water was triply distilled; once from potassium permanganate and again in an all glass still.

B. DENSITY MEASUREMENTS

Density measurements were made at 288.5 K and 298.15 K with a Mettler/Paar 601 NT vibrating tube densitometer. The temperature, measured with a Pt resistance thermometer to ±0.002 and monitored with a thermistor mounted near the sample chamber, was controlled to ±0.0002 K by a circulating thermostat. The actual property obtained from the Mettler/Paar instrument was the natural vibration period of the tube, τ. By using the equation

$$d_{sample} = A + k\tau^2 \qquad 47$$

where A and k are constants characterizing the spring and τ is the period, the density of the measured substance may be obtained. By measuring water and air as standard substances, the density of the

substance in question could be obtained by rewriting equation (47) in terms of a standard

$$d_{unknown} = d_{stand} + k(\tau_{unknown}^2 - \tau_{stand}^2) \quad 48$$

where

$$k = (d_{water} - d_{air})/(\tau_{water}^2 - \tau_{air}^2) \quad 49$$

The question of whether the linear approximation given in equation (47) is appropriate was addressed by Van Hook and coworkers.[43] They found that, after calibrating with water and air, their measurements were in good agreement with that of other researchers.[44,45] Also, in this investigation, careful density measurements on the pure n-hydrocarbons, n-C_5 through n-C_{16}, showed good agreement with literature values.[46-48] As pointed out by Van Hook and coworkers,[43] density measurements usually differ between laboratories and sample lots by several parts in 10^5 or more, so that the linear hypothesis is established by this limit of 10^5 over a density range from 0.60 to 1.20 kg/m^3.

The density measurements fall into three categories. First measurements were made on the pure n-alkanes, n-C_5 through n-C_{15}, at 288.15 K and 298.15 K to determine the purity of the substances and consequently obtain the molar volumes per carbon number, (V_m/n). Second, the density of individually prepared binary solutions, n-C_8 +n-C_9, n-C_8 +n-C_{10} and n-C_9 +n-C_{11}, which covered the complete concentration range, were measured and the magnitude and dependence of the excess volume on concentration, determined. Finally, using solutions prepared from higher concentration mother solutions, the excess volumes

at low concentrations of several systems, n-C_8 +n-C_{10}, n-C_9 +n-C_{11} and n-C_9 +n-C_{13}, were extracted from the density measurements. All solutions were prepared gravimetrically and buoyancy corrections applied. Before each density measurement, the calibrating water, solvent, solute, and solutions were degassed by several freeze(liquid N2)-pump-thaw-freeze cycles on a vacuum manifold. A more detailed description of the experimental method is given in reference (43).

C. DEVELOPMENT OF VLE APPARATUS

Although gas chromatography has been established as a method of study for components differing widely in carbon number and volatility at low concentrations,[27] this method was inappropriate for this investigation because VLE data for components differing by only one or two methylene units was desired. Thus, for reasons previously discussed, it was decided that an instrument which would give the desired quantities be developed and built.

Traditionally, there are two types of equipment that are used for the measurement of VLE data;[49,50] the equilibrium still and equilibrium cell. In the equilibrium still, boiling liquid and effluent vapor are equilibrated at constant pressure or temperature. The liquid and vapor phases are separated in a disengaging chamber, and the condensed vapor and liquid recirculated back to the still pot where they are remixed and reboiled. Liquid samples are withdrawn from a small reservoir in the return leg and analysed. This procedure is repeated until the composition of the solution no longer changes with time. This solution is assumed to be composed of the equilibrium phases at the temperature and pressure of the disengaging chamber.

Thus, the mole fractions in the liquid and vapor phases are obtained at a given temperature and pressure.

The operation of the equilibrium still is slow and tedious. Furthermore, at best, this type of equipment achieves a state of dynamic equilibrium which may or may not be at the true thermodynamic equilibrium state. One also has to be wary of superheating of the solution, partial condensation of the vapor, entrainment of liquid into the condenser, and evaporation of the samples before analysis.

On the other hand, the equilibrium cell experiment, in which static equilibrium is achieved between phases, is essentially very simple. All that needs to be done is to load the sample into an evacuated thermostated cell, stir to assure equilibrium, measure the pressure in the cell, and sample the phases for analysis. Yet the equilibrium cell has two major disadvantages. First, the cell must be thoroughly evacuated and the sample degassed of all the noncondensible gases which might cause erroneous pressure readings. Secondly, sampling of the phases upsets the phase equilibrium. Thus, until recently, the more tedious equilibrium still was preferred over the equilibrium cell. However, sampling of the phases in an equilibrium cell is not necessary. With the use of the Gibbs-Duhem theorem, calculations which provide the concentrations and partial pressures of the vapor phase in terms of the total pressure and concentrations of the components in the liquid phase, can be done that require only the measurement of the total pressure and mass. The equations are complex and iterative, but with the advent of computers, the calculations are easily performed. Also, with today's high vacuum techniques and proven

experimental techniques,[51] problems with the evacuation of the system and degassing are minimized.

Having weighed the pros and cons of the two types of basic equipment, it was decided that an equilibrium cell type of apparatus was preferred for this investigation. Before the construction of such an apparatus could begin, there were several difficulties which would have to be resolved. An accurate study of the change in pressure with concentration at very low concentration and constant temperature would require making several solutions of precisely known concentrations. If solutions were made and measured individually, the time frame of the experiment would be extremely long. Also, the relative amounts of components would be required to be large in order to ensure the minimum error during the weighing process. This would make the experiments expensive and wasteful. Consequently, it was decided that, in order to alleviate these problems, a closed, continuous dilution, differential vapor pressure apparatus would be constructed. With this instrument, solutions would be prepared within the solution cell of the apparatus. By measuring the change in the vapor pressure with change in concentration at extremely low concentrations directly, errors in interpretation of infinite dilution behavior extrapolated from higher concentration data would be greatly reduced.

D. VLE APPARATUS

The continuous dilution vapor pressure apparatus consists of two separate sections connected via a six port chromatographic valve (Valco Instruments Co.). The solution section, where the solutions are

prepared and pressure change per injection measured, contains an air thermostated oven, the valve assembly, pressure transducer, magnetic stirrer, micropump, solvent addition port, and solution and reference cells. The solute section consist of the solute vessel, micropump, magnetic stirrer and solute addition port. For reasons of clarity, each section will be described separately.

1. Solution Section

Because the experiments performed are differential experiments, where the pressure readings are actually the difference between the solution and reference solvent readings, the solution section was designed so that the special solution vessel and reference vessel were connected pairwise to the valve assembly which is connected to opposite sides of the differential capacitance pressure transducer (Datametrics Inc.), Figure 1. The valve assembly, constructed of 1/4 inch 316 stainless steel tubing and Nupro high vacuum valves (Ridge Valve Inc.), and pressure transducer, are evacuated with a mercury diffusion pump and are contained within the thermostated air oven. The solution and reference cells, which extend into the thermostated water bath, are connected pairwise to the assembly through Kovar glass-metal seals. The permanent, specially designed solution cell, Figure 2, is joined to ports 1 and 2 of the chromatographic valve and micropump via 1/16 inch stainless steel capillary tubing. Below the solution cell is the water tight magnetic stirrer which is used to mix the solute into the solution. The solvent is added to the solution vessel through a zero dead volume valve (Valco Instruments Co.) which is connected to the

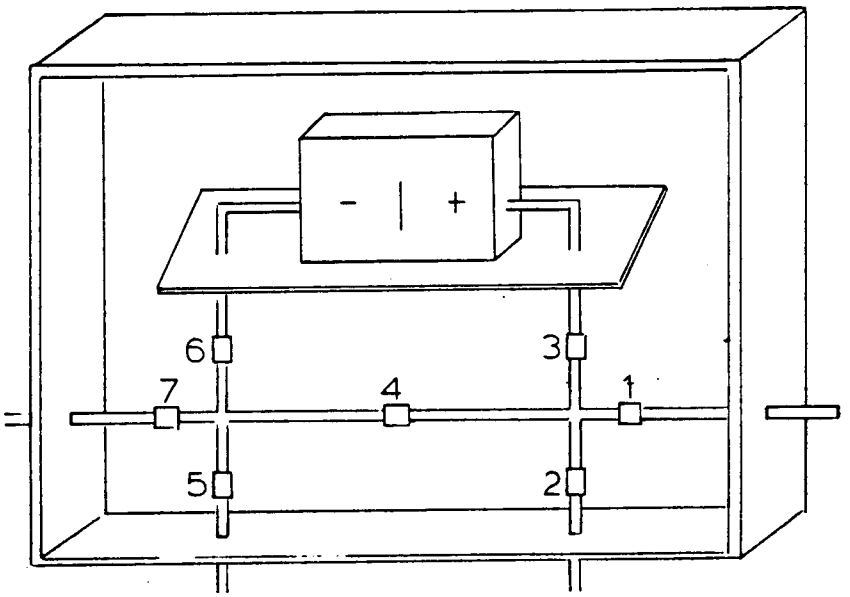

Figure 1. Pressure transducer and valve assembly.

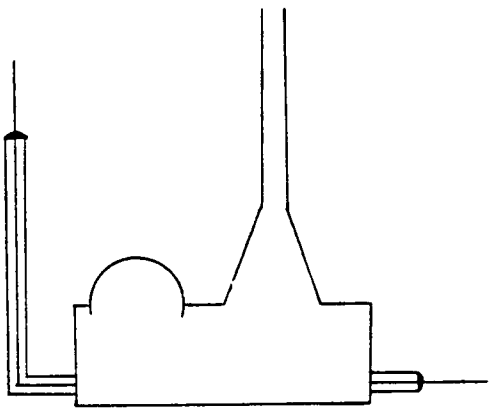

Figure 2. Solution cell.

1/16 stainless steel capillary line via a zero dead volume stainless steel tee (Valco Instruments Co.), Figure 3.

2. Solution Cell

The design of the solution cell, which was perfected by a process of trial and error, was dictated by observations made during preliminary test of the VLE apparatus and the system's experimental requirements. Solute must be added to the solution and the solution stirred in such a way as not to disturb the system beyond its ability to return to static equilibrium. The principle danger to the VLE experiments is splashing of the solution, which may cause droplets of the solution to adhere to the neck and sides of the solution cell, which in turn establish a dynamic equilibrium with the solution and vapor phase above the solution. This may consequently ruin the experiment. It was observed that when a solute of a vapor pressure which was much higher than that of the solvent was introduced into the solution cell, the change in vapor pressure caused the solute to rush into the cell and splash the contents. Also, stirring had the potential of splashing the solution up the tube connecting the vessel to the valve assembly.

As shown in Figure 2, the vessel has a wide base to accommodate the glass covered stirring bar and is connected to the valve assembly by 1/4 inch glass tubing. The inlet and outlet ports are located at the base of the cell, below the solution level, to aid in pumping and mixing. Above the inlet port on the top of the solution cell, there is a raised bubble to trap any solution which may be splashed by the introduction of solute. The opening to the valve assembly is located off center away from the inlet port and is connected to the assembly by

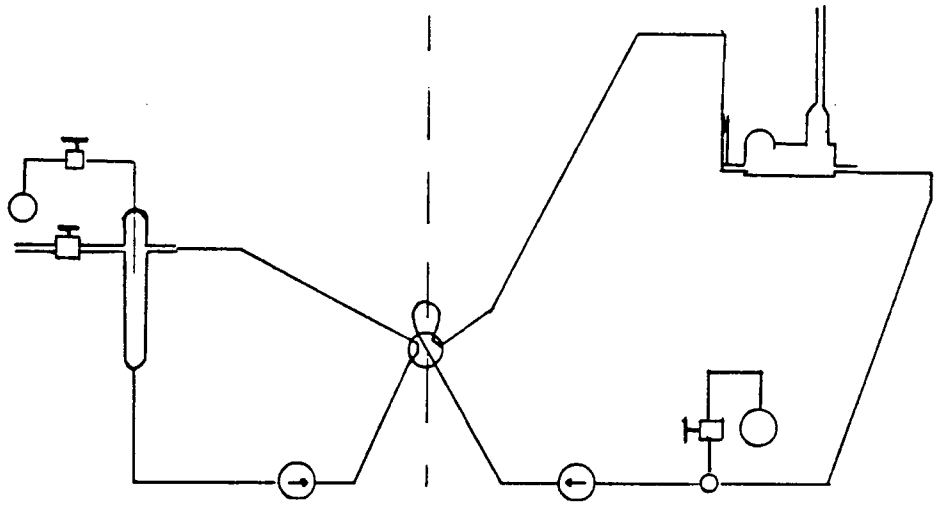

Figure 3. Solution and solute sections.

a tapered neck which is wide at the base and long enough to prevent splashing up the neck by stirring or sample introduction.

3. Chromatographic Valve

The six port chromatographic valve is an essential part of the instrument and is specifically designed so that four of the ports, 1-2-3-4(configuration 2) or 3-4-5-6(configuration 1), can be totally separated from the remaining ports, Figure 4. The valve is switched back and forth electrically between the two configurations by an air driven helical-drive air actuator (Valco Instruments Inc.). A calibrated 1/16 inch stainless steel capillary sample loop, Table 1, is connected to ports 3 and 4, and can be changed according to the dilution size required.

E. CALIBRATION OF VLE APPARATUS

The system was vacuum tested and found to be able to maintain a vacuum of < 0.001 Pa. Differential leak test revealed a leak rate of less than a micron, 0.10 Pa/day. The pressure is measured by negative(-), solution side, or positive(+), reference side, deviation of a membrane contained within the pressure transducer. Each side of the transducer was calibrated at different pressures by simultaneously measuring the pressure with the transducer and a mercury manometer, which was read with a cathetometer, Table 2. It was found that the average deviation from the actual pressure was less that ± 0.10 Pa. As can be seen in Table 2, the deviation from the actual pressure was greater at lower pressures, < 1.33 kPa. Calibration at low pressures, < 1.33 kPa, was accomplished by measuring the vapor pressure of a known

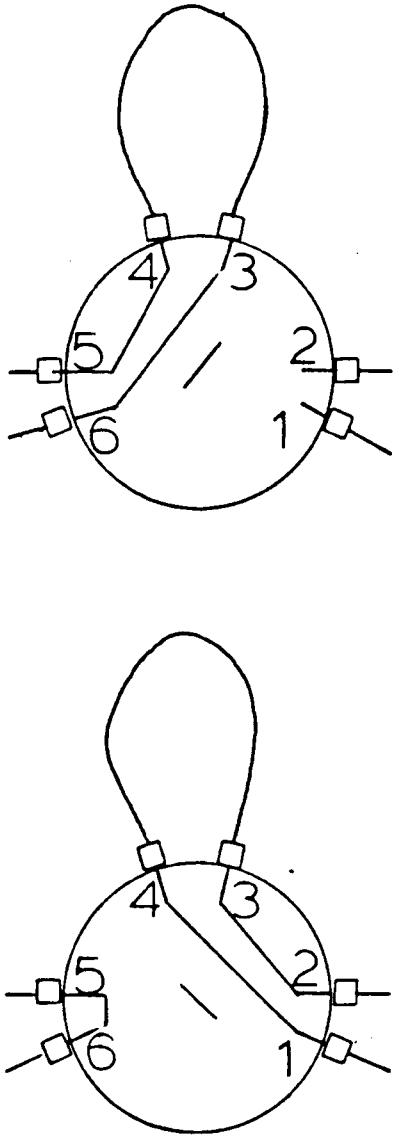

Figure 4. Chromatographic valve and connection scheme.

TABLE 1

SAMPLE LOOP VOLUME DETERMINATION

LOOP #	Trial I (cm^3)	Trial II (cm^3)	% difference	Volume Used
1	0.039169	0.039173	0.0102	0.03917
2	0.062312	0.062310	0.0032	0.06231
3	0.40152	0.40147	0.0125	0.40150

TABLE 2

CALIBRATION OF PRESSURE TRANSDUCER

P/kPa Manometer	P/kPa Transducer	Ln(Pm/Pt)	P/kPa Manometer	P/kPa Transducer	Ln(Pm/Pt)
9.6005	9.6019	-0.0001	9.3539	9.3432	0.0011
6.7568	6.7568	0.0000	6.6595	6.6581	0.0002
4.0130	4.0103	0.0007	3.8317	3.8317	0.0000
2.6584	2.6664	0.0030	2.3611	2.3678	-0.0028

substance at a constant temperature and comparing the value to the literature value. As will be seen in the following section, numerical analysis of the data of the benzene-cyclohexane system revealed a precision of better that 0.60 Pa.

The volume of each section of the apparatus was determined by injection of a gas from a vessel of known volume and constant temperature, into an isolated section of the apparatus and measuring the pressure. By assuming the ideal gas law, PV=nRT, the volume of the section in question could be determined to .02 ml. To insure precision, all volume calibrations were repeated several times.

The three sample loops used in the VLE experiments were calibrated by making at least fifty injections of a substance of known density into a special trap vessel. The vessel was weighed and the amount of substance per injection determined. The procedure was repeated until the difference between the mass per injection values was less than 0.0005g. This allowed the volumes of the sample loops to be determined to be better than ±0.05 µl.

F. VLE EXPERIMENTAL PROCEDURE

Although the experimental procedure is relatively straightforward, the success of each experiment depended upon strict adherence to the details outlined below. First, the system is cleaned and evacuated to < 0.001 Pa. The solute and solvent masses are determined gravimetrically and connected to the degassing ports of the respective sections of the apparatus. A third vessel, containing solvent, is connected to the reference side of the valve assembly. The samples are

then meticulously degassed by first cooling the samples to almost the freezing point, withdrawing the air above the liquid, and then subjecting the samples to repeated freeze-pump-thaw cycles. The procedure is repeated until all noncondensible gases are removed. Depending upon what substances are being degassed, the entire process generally requires six to ten hours.

Valves 1,2,5 and 6 of the valve assembly are then closed, thus removing the system from the vacuum, and the samples are introduced into their respective sections of the apparatus. Next the system is put into the experimental mode by exposing the solvent and reference solvent to their respective sides of the pressure transducer by closing valve 4 and opening valves 5 and 2, Figure 1 (p 31). The pressure transducer and valve assembly are maintained at a temperature of at least 353.15 K by the air oven to prevent the condensation of vapor in the transducer and assembly. The temperature bath is then elevated so as to completely cover the solution and reference cells and the temperature of the bath slowly raised over night to the desired value. After the operating temperature has been attained, the system is allowed to equilibrate for several minutes. The temperature of the bath is monitored with a Pt resistance thermometer and maintained at the desired temperature to better than ±0.0005 K.

Since this is a differential experiment, where solvent is present on both sides of the pressure transducer, the pressure reading recorded monitors directly the change in the total pressure relative to the vapor pressure of the pure solvent. Also, there is the added advantage of being able to perform experiments on substances whose vapor pressure

exceeds the 100 torr limit of one side of the pressure transducer. An acceptable reading before the dilution process begins, of not more than ±0.0667 kPa, was taken to be the zero or baseline of the experiment. The stirrers, which are present in the solute and solution cells, are activated and the micropumps switched on. Now by switching the chromatographic valve from configuration (1) to configuration (2), Figure 4, page 35, the small amount of solute present in the sample loop (the amount of which is determined by the temperature, density and size of the loop) is carried into the solution cell by the micropump, where it is thoroughly mixed into the solvent by the stirrer. The pumping and stirring are continued until all the solvent present in the pump head and connecting lines is mixed into the solution. The chromatographic valve is then switched back to configuration (1) and the solution present in the loop mixed into the solute present in the solute section. The stirring and pumping are then stopped and the solution allowed to come to equilibrium. The resulting change in pressure per injection number is recorded and the procedure repeated until the desired concentration range has been covered. The change in the mole fractions of the solute and solvent present in the solution and solute cells per injection are calculated by a mass balance computer program.

The system and experimental procedure were subjected to several test and calibrations. A blank run, where the solute and solvent were identical, showed no deviation in the measured pressure with successive injections. This indicated that the system was free of external interference and that no error in the pressure reading was introduced by the

experimental procedure. However, when a solute with a vapor pressure much greater than the solvent is injected, there is a possibility of a splash within the solute vessel which may upset the equilibrium. To test the accuracy to which an experiment could be performed with this apparatus, several experiments, using loops of differing volumes, were performed on the well studied benzene-cyclohexane system.[52-54] The error between the literature and experimental values was only 0.02%. Also, to test other possible applications of the apparatus, the benzene-cyclohexane-water system was run and the solubility of water in cyclohexane determined. The value obtained agreed well with the literature values.[56-60] The results of these and the other VLE measurements are given in the next section.

CHAPTER III

RESULTS

A. EXCESS VOLUMES

Density measurements of pure n-hydrocarbons, n-C_5 to n-C_{15}, were made at 288.15 and 298.15 K. As shown in Table 3, the agreement between our values and the literature[46-48] is excellent, within several parts in 10^5. This helped to substantiate both the purity of the substances and the experimental accuracy. Plots of the density, ρ, versus the inverse of the carbon number, 1/n, Table 4, and $\ln(V_m/n)$ versus 1/n, at 288.15 and 298.15 K are given in Figures 5 and 6 respectively. The curves at 288.15 and 298.15 K for ρ versus 1/n or $\ln (V_m/n)$ versus 1/n have the same slopes; plausibly establishing the accuracy of the density measurements at 288.15, (where there is a lack of literature values), to several parts in 10^5 (i.e. the same as at 298.15).

Excess volumes were measured over the entire composition range for the mixtures n-C_8 + n-C_9, and n-C_8 + n-C_{10} at 288.15 K, and n-C_8 + n-C_9, n-C_8 + n-C_{10} and n-C_9 + n-C_{11} at 298.15 K. The results, summarized in Tables 5 and 6, and shown in Figures 7, 8, 9, 10 and 11, were fitted to the equation

$$V^E/cm^3 mol^{-1} = x(1-x) \sum_{j=0}^{n} A_j x^{(j-1)/2}. \qquad 50$$

Table 7 summarizes the coefficients of equation 50 for the different solutions. Tables 5 and 6 include the deviations, δV^E, of the individual points from equation 50, and the mean deviation, (δV^E),

TABLE 3

DENSITIES OF PURE HYDROCARBONS AT 288.15 K and 298.15 K

Substance	ρ(288.15 K)	ρ(298.15 K)	Lit. (298.15 K)
Pentane	0.63140	0.62199	0.62140[a]
Hexane	0.66345	0.65533	0.65532[b]
Heptane	0.68753	0.67950	0.67949[c]
Nonane	0.72135	0.71398	0.71394[c]
Decane	0.73338	0.72622	0.72611[c]
Undecane	0.74355	0.73652	0.73649[a]
Dodecane	-	-	0.74530[a]
Tridecane	0.76022	0.75315	0.75311[a]
Tetradecane	-	-	0.75930[a]
Pentadecane	0.77180	0.76507	0.76500[a]

[a]Reference 46.

[b]Reference 47.

[c]Reference 48.

TABLE 4

MOLAR VOLUMES AND MOLAR VOLUMES PER CARBON NUMBER
AT 288.15 K AND 298.15 K

Substance	V_m(288.15 K)	V_m(298.15 K)	V_m/n(298.15 K)	V_m/n(298.15 K)
Pentane	114.2699	115.9987	22.8540	23.1997
Hexane	129.8922	131.5014	21.6487	21.9169
Heptane	145.7440	147.4672	20.8206	21.0667
Octane	161.7067	163.4746	20.2133	20.4343
Nonane	177.8066	179.6366	19.7556	19.9596
Decane	194.0108	195.9244	19.4011	19.5924
Undecane	210.2223	212.2288	19.1111	19.2935
Tridecane	242.5136	244.7911	18.6649	18.8301
Pentadecane	275.2225	277.6446	18.3482	18.5096

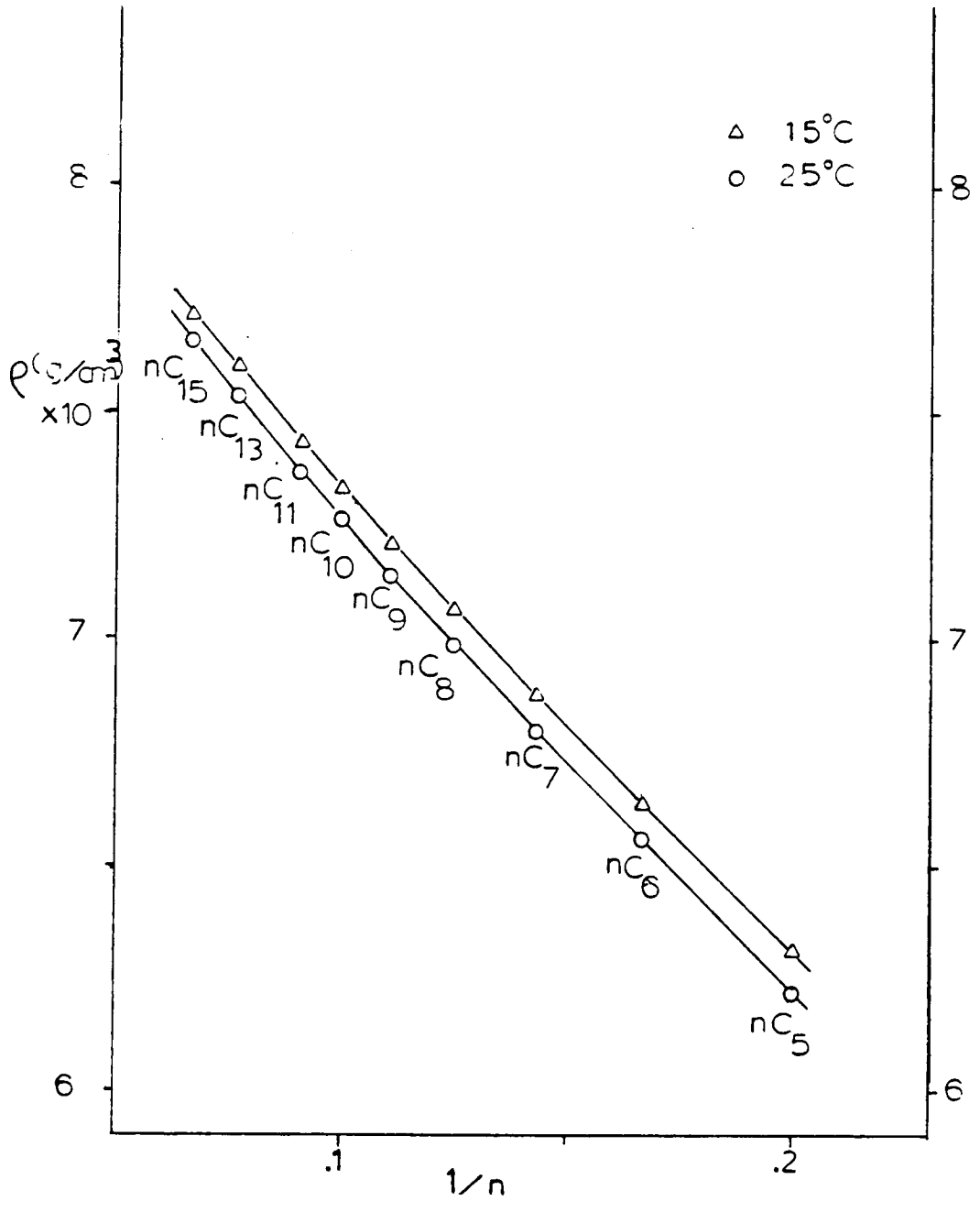

Figure 5. Plots of the density versus the inverse carbon number at 288.15 K and 298.15 K.

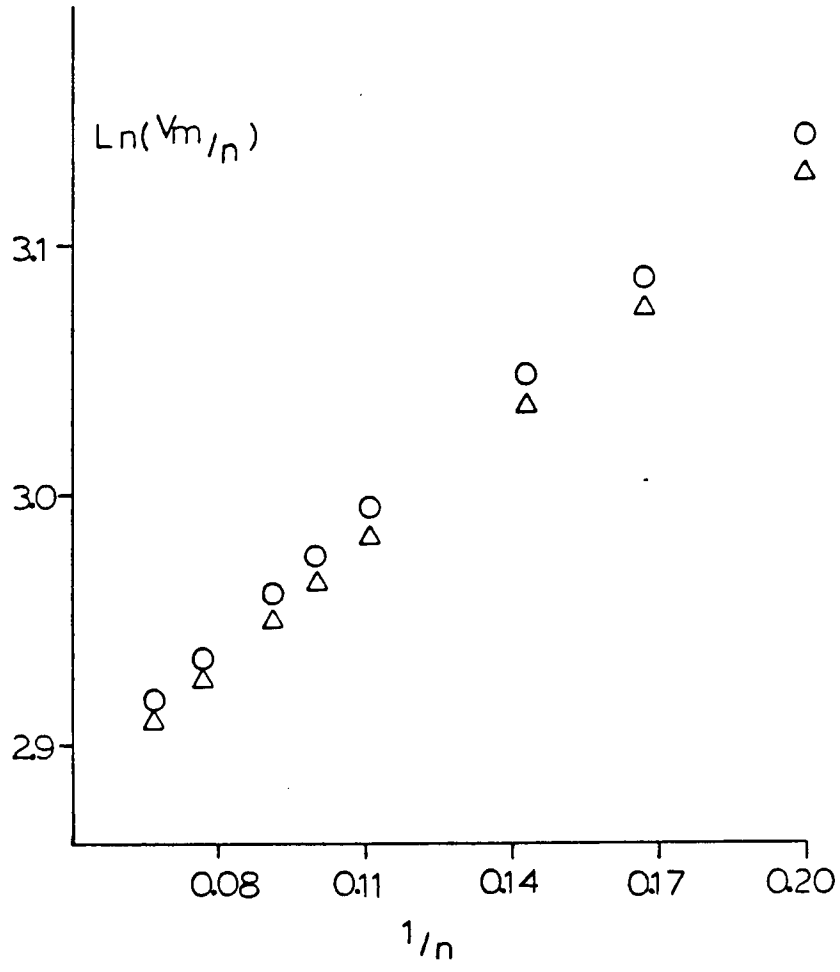

Figure 6. Plots of the logarithm of the molar volume per carbon number versus the inverse carbon number at 288.15 K and 298.15 K.

TABLE 5

EXCESS VOLUMES OVER THE ENTIRE CONCENTRATION RANGE FOR $n\text{-}C_8 + n\text{-}C_9$ SYSTEM AT 288.15 K AND 298.15 K

$xC_8H_{16} + (1-x)C_9H_{20}$							
x	ρ	V^E	$\sigma(V^E)$	x	ρ	V^E	$\sigma(V^E)$
			288.15 K				
0	0.72135	-	-	0.63638	0.71222	-0.01148	-0.00152
0.05333	0.72060	0.00407	0.00297	0.84262	0.70897	-0.00541	-0.00010
0.098385	0.72008	-0.00435	0.00136	0.91305	0.70783	-0.00305	0.00007
0.09989	0.71997	-0.00448	-0.00415	0.91771	0.70775	-0.00174	0.00123
0.36160	0.71630	-0.00935	0.00081	0.95442	0.70715	-0.00191	0.00022
0.55294	0.71348	-0.01011	-0.00152	1	0.70640	-	-
			298.15 K				
0	0.71390	-	-	0.51223	0.70651	-0.01093	-0.00099
0.00869	0.71374	0.00896	0.00743	0.77055	0.70247	-0.00746	-0.00031
0.05767	0.71310	0.00007	0.00270	0.91435	0.70010	-0.00299	0.00088
0.26629	0.71015	-0.00696	-0.00066	1	0.69868	-	-
0.42825	0.70777	-0.00930	-0.00076				

TABLE 6

EXCESS VOLUMES OVER THE ENTIRE CONCENTRATION RANGE FOR $n-C_8 + n-C_{10}$ SYSTEM AT 288.15 K AND $n-C_9 + n-C_{11}$ SYSTEM AT 298.15 K

$xC_8H_{10} + (1-x)C_{10}H_{22}$							
x	ρ	V^E	$\sigma(V^E)$	x	ρ	V^E	$\sigma(V^E)$
			288.15 K				
0	0.73339	-	-	0.72665	0.71492	0.02754	0.00002
0.01787	0.73299	-0.00081	0.00121	0.83054	0.71181	0.02162	0.00044
0.02281	0.73288	-0.00152	0.00107	0.92286	0.70893	0.01420	0.00176
0.05886	0.73209	-0.00658	0.00327	0.93212	0.70862	0.00937	0.00182
0.09445	0.73126	-0.00797	0.00210	0.97224	0.70733	0.00469	0.00033
0.16193	0.72771	-0.01594	-0.00044	0.98666	0.706861	0.00419	0.00169
0.26386	0.72727	-0.02117	0.00033	1	0.706404	-	-
0.56116	0.71959	-0.02940	-0.00015				

TABLE 6 (CONTINUED)

$xC_8H_{10} + (1-x)C_{10}H_{22}$							
x	ρ	V^E	$\sigma(V^E)$	x	ρ	V^E	$\sigma(V^E)$
			298.15 K				
0	0.72613	-	-	0.67134	0.70896	0.02851	0.00003
0.02949	0.72545	0.00122	0.00204	0.76039	0.70631	0.02115	0.00122
0.096689	0.72391	-0.00725	-0.00123	0.87334	0.70282	0.01356	0.00126
0.16624	0.72227	-0.01411	-0.00121	0.91654	0-.70143	0.00716	0.00094
0.24219	0.72043	-0.01887	0.00140	0.97810	0.69942	0.00231	0.00022
0.45164	0.71508	-0.03082	0.00182	1	0.69870	-	-
0.52543	0.71310	-0.03575	-0.00254				
			$xC_9H_{20} + (1-x)C_{11}H_{24}$				
			298.15 K				
0	0.73645	-	-	0.42959	0.72775	-0.02073	0.00120
0.01664	0.73613	0.00187	0.00971	0.53876	0.72532	-0.02257	-0.00063
0.01774	0.72611	0.00182	0.00067	0.63845	0.72302	-0.02113	0.00008
0.07645	0.73499	-0.00486	-0.00187	0.80424	0.71900	-0.01810	0.00066
0.11998	0.73414	-0.00564	-0.00179	0.95701	0.71505	-0.00433	0.00162
0.23515	0.73184	-0.01810	-0.00066	1	0.71390	-	-

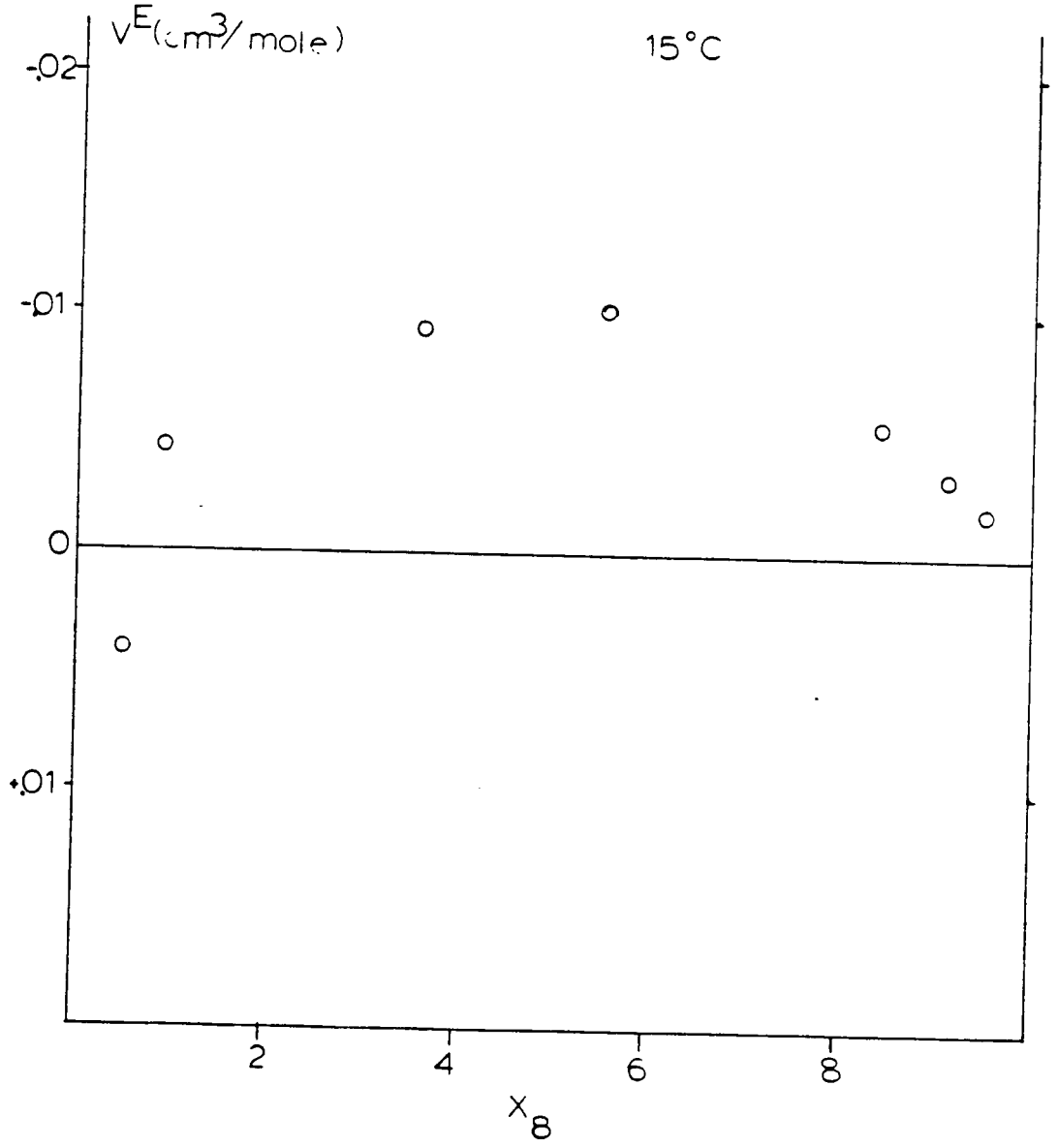

Figure 7. Excess volumes for the n-C_8 + n-C_9 system at 288.15 K.

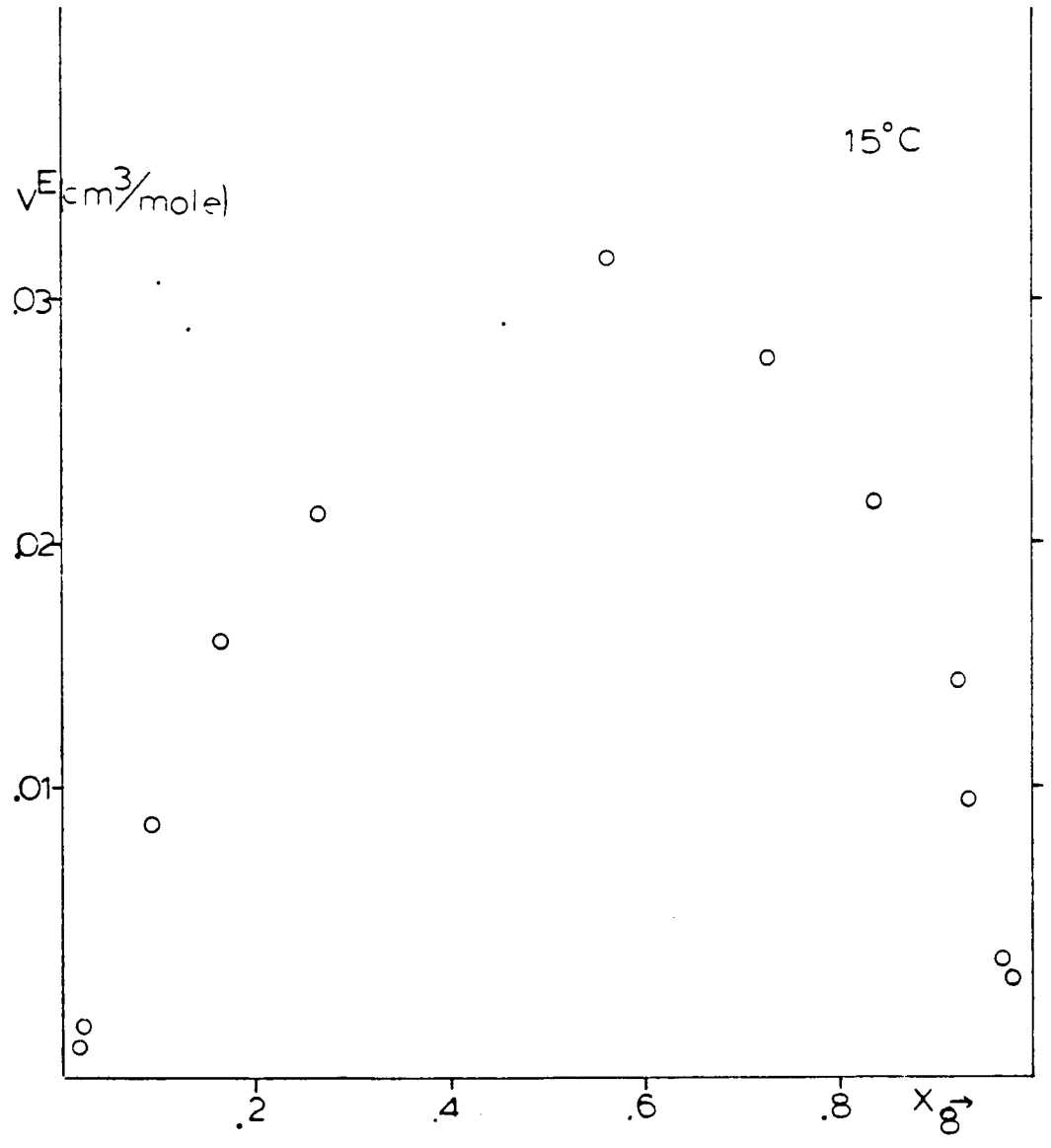

Figure 8. Excess volumes for the n-C_8 + n-C_{10} system at 288.15 K.

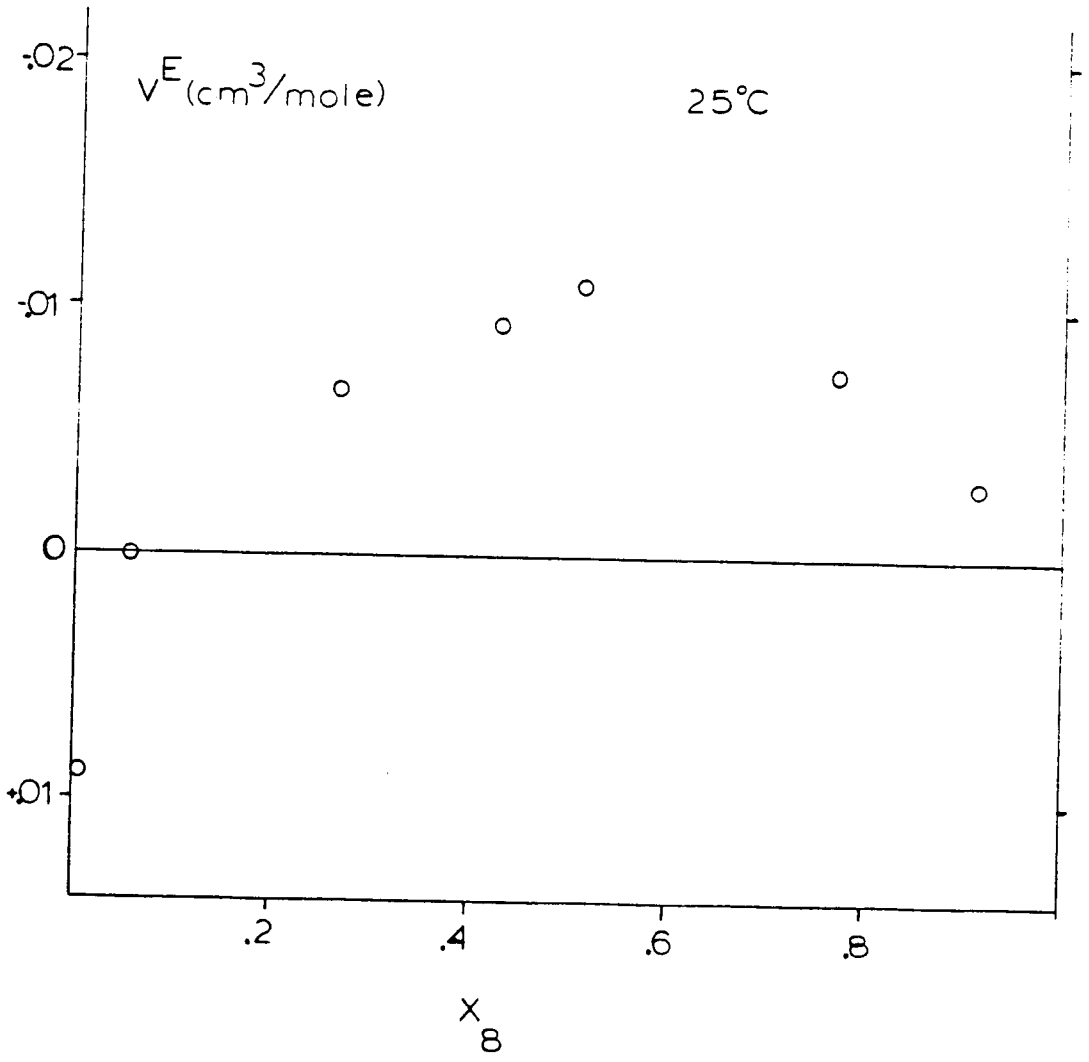

Figure 9. Excess volumes for the n-C_8 + n-C_9 system at 298.15 K.

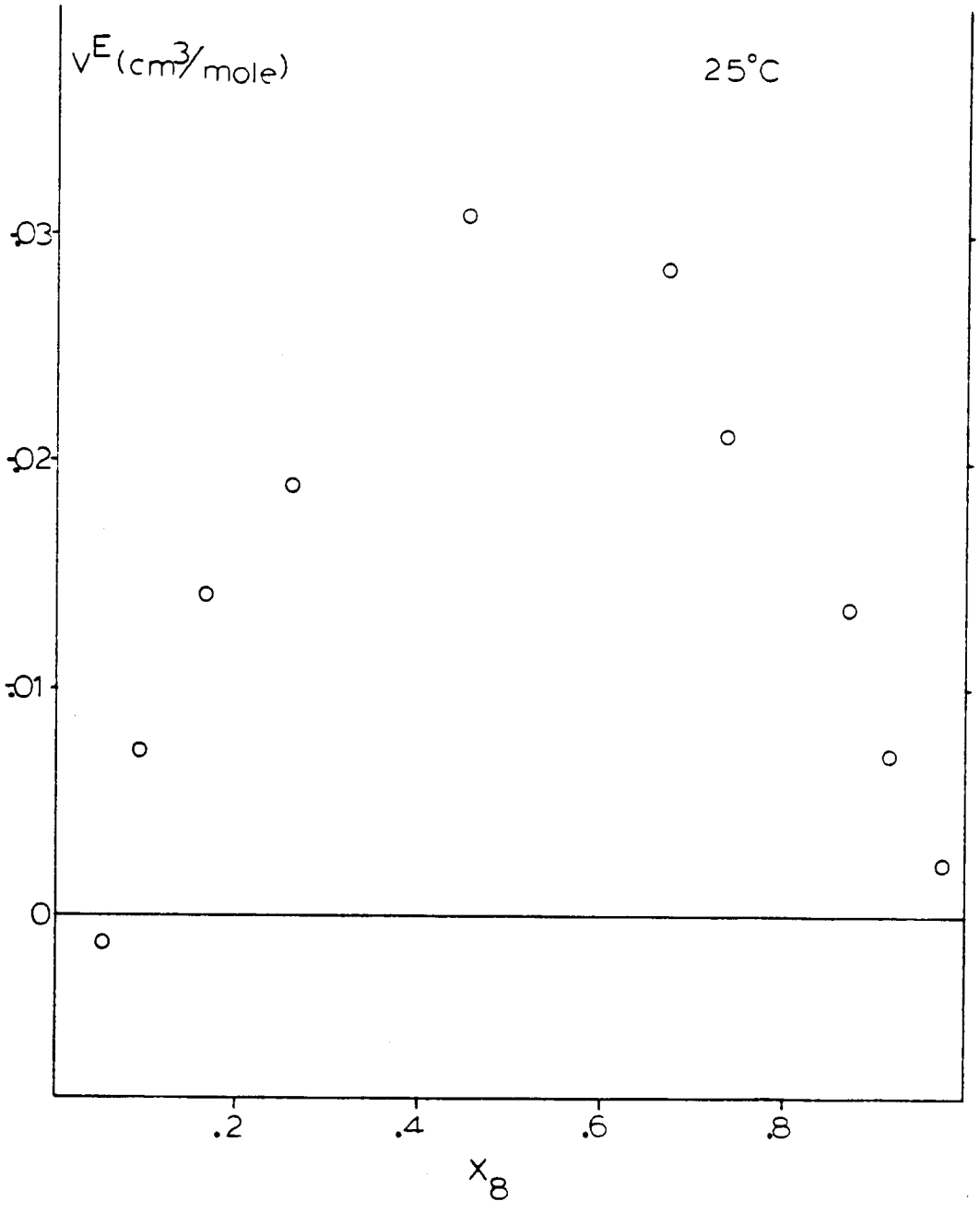

Figure 10. Excess volumes for the n-C_8 + n-C_{10} system at 298.15 K.

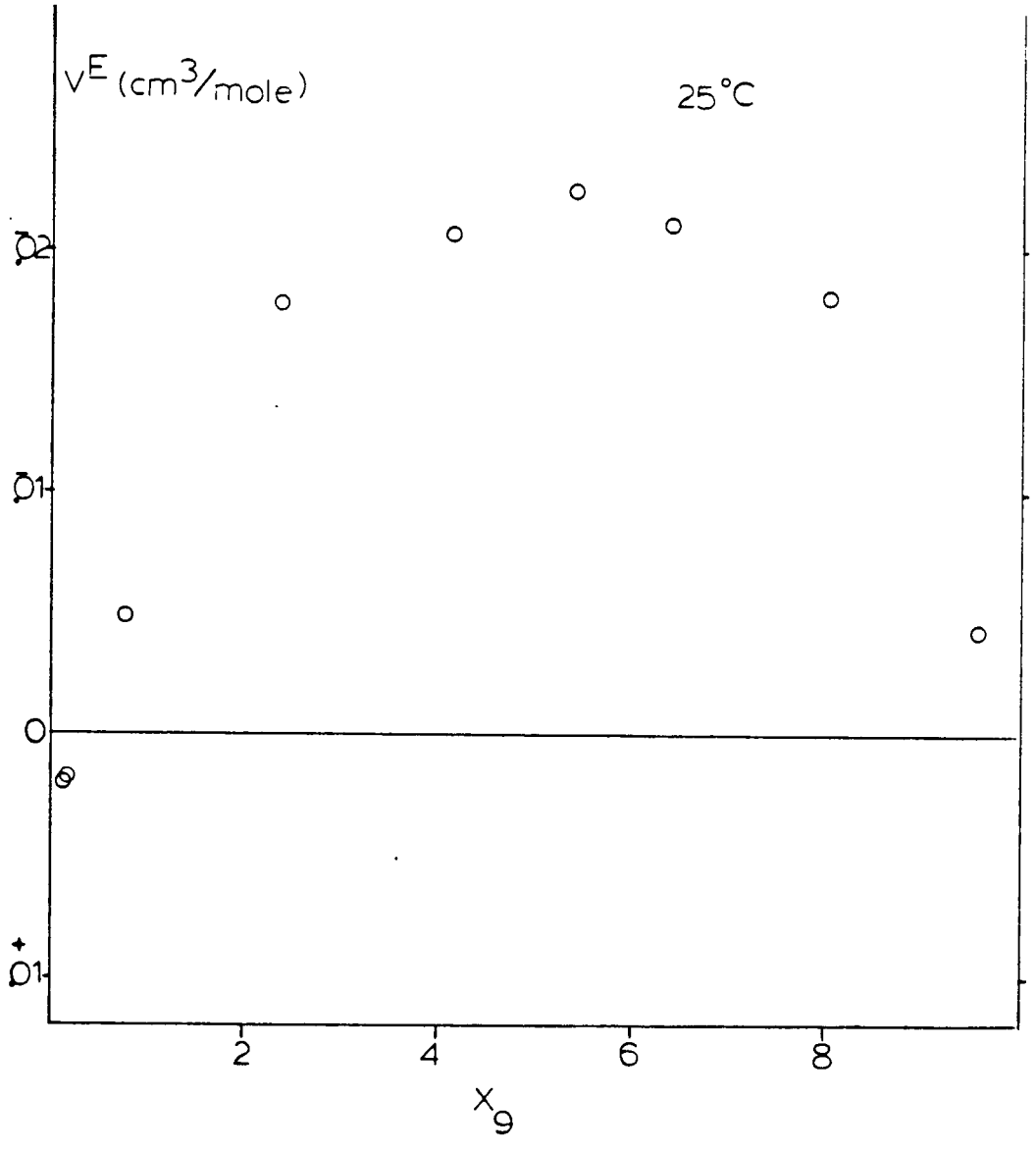

Figure 11. Excess volumes for the n-C_9 + n-C_{11} system at 298.15 K.

TABLE 7

PARAMETERS FROM LEAST SQUARES FIT OF EXCESS VOLUMES

System	Parameter 1	Parameter 2	Parameter 3	Parameter 4
		Entire Concentration Range		
$n\text{-}C_8 + n\text{-}C_9$	0.14499	-0.71979	0.88705	-0.35128
$n\text{-}C_8 + n\text{-}C_{10}$	-0.32612	1.85532	-3.60970	2.10523
$n\text{-}C_8 + n\text{-}C_9$	0.28762	-1.47939	2.12293	-0.99832
$n\text{-}C_8 + n\text{-}C_{10}$	0.25439	-0.31644	-0.02914	0.22606
$n\text{-}C_9 + n\text{-}C_{11}$	0.24919	-1.72184	2.83300	-1.51720
		Low Concentration		
$n\text{-}C_8 + n\text{-}C_{10}$	13.91147	457.7454	4922.9020	-17408.0435
$n\text{-}C_9 + n\text{-}C_{11}$	34.54379	-1261.0449	12341.4621	-
$n\text{-}C_9 + n\text{-}C_{13}$	2.06875	37.4371	131.9826	-

for each mixture. The agreement between literature values[7,61-64] and the excess volumes obtained in this study was determined by making a plot of the excess volume at 0.50 mole fraction and 298.15 K versus the negative of the difference between the carbon numbers of the shorter and longer components. The value of the excess volume at the maximum should have been used in the plot. However, since the V^E curves are not greatly skewed, the difference between the maximum and the value at 0.50 mole is small. Also, the majority of the literature data on the excess volumes of binary n-alkane systems are presented only for 0.50 mole fraction. As shown in Figure 12 and discussed thoroughly in the following chapter, the points, for a given shorter component fall on straight lines whose respective slopes decrease with increasing length of the shorter components. The present data are in good agreement with literature values.[61-64] The excess volumes for the systems, $n\text{-}C_8$ + $n\text{-}C_{10}$, $n\text{-}C_9$ + $n\text{-}C_{11}$, and $n\text{-}C_9$ + $n\text{-}C_{13}$ at very low concentrations of the shorter components and 298.15 K, are reported in Table 8 and Figures 13, 14 and 15. The present study is distinguished by the high density of data points in the low concentration range where little or no literature data in this region exist for comparison.

We find that the excess volumes are negative for each system at concentrations greater than 0.10 mole fraction of the shorter component. However, and most importantly, the excess volumes are positive at low concentrations ($x < .07$) of the shorter component; thus, the curves are S shaped, albeit strongly skewed. In agreement with the observed trends established by the literature data, the

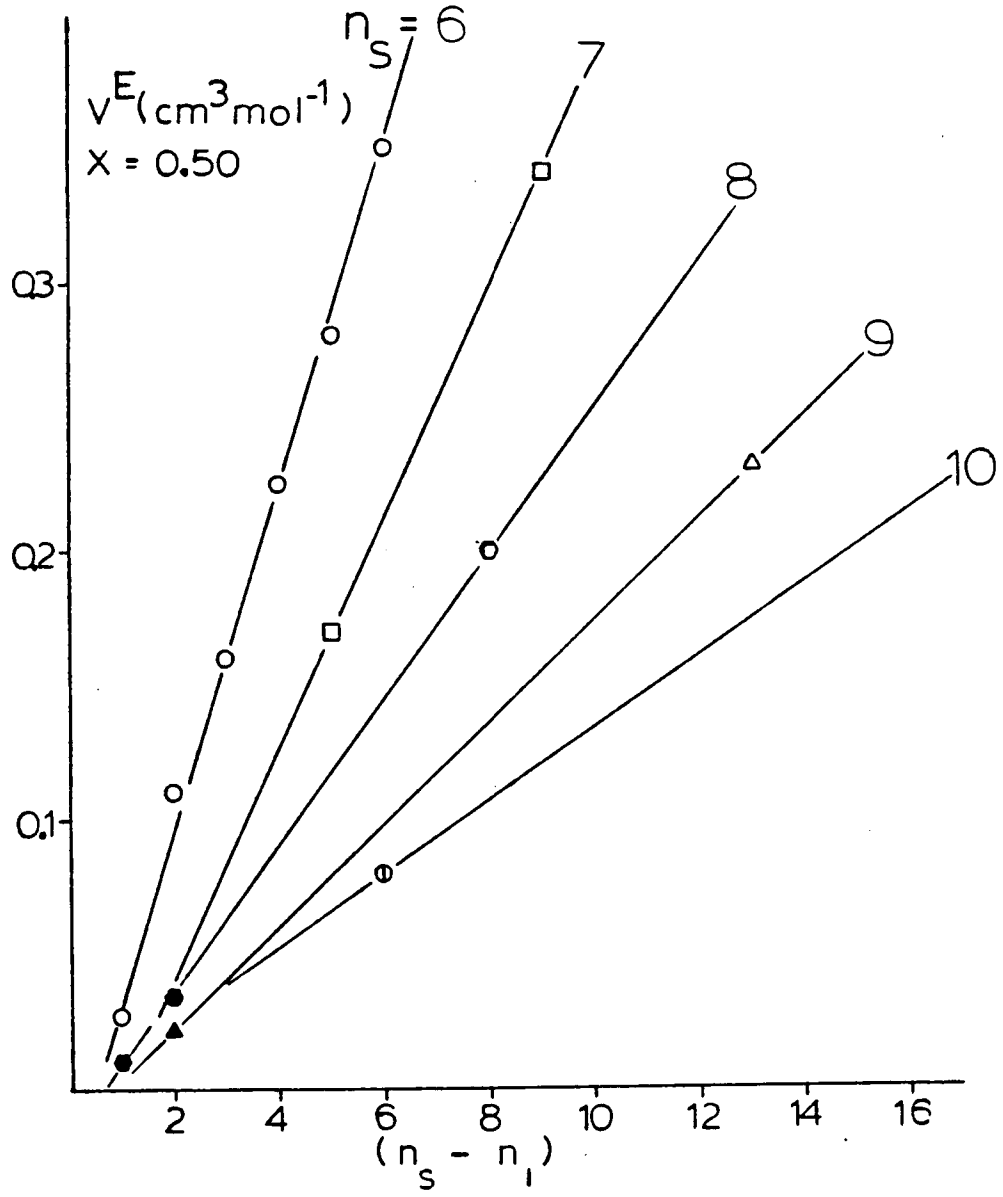

Figure 12. Plots of excess volumes at 0.50 mole fraction versus $-(n_{small} - n_{larger})$ at 298.15 K. O-(References 48, 72); []-(References 7, 64); ⬡-(Reference 63); Δ and ⏀-(Reference 7). Filled shapes, this work.

TABLE 8

EXCESS VOLUMES AT LOW CONCENTRATIONS FOR $n\text{-}C_8 + n\text{-}C_{10}$, $n\text{-}C_9 + n\text{-}C_{11}$ AND $n\text{-}C_9 + n\text{-}C_{13}$ SYSTEMS AT 298.15 K

			$xC_8H_{18} + (1-x)C_{10}H_{22}$				
x	ρ	V^E	$\sigma(V^E)$	x	ρ	V^E	$\sigma(V^E)$
			298.15 K				
0	0.726136	-	-	1.54E-3	0.726088	3.45E-3	0.00036
1.34E-4	0.726114	3.25E-3	0.00050	1.83E-3	0.726081	3.54E-3	-0.00007
6.91E-4	0.726107	3.55E-3	0.00012	5.38E-3	0.726013	-7.58E-5	0.00018
9.77E-4	0.726100	3.67E-3	-0.00012	9.68E-3	0.725916	-5.69E-4	-0.00009
1.24E-3	0.726093	3.97E-3	0.00008	1.38E-2	0.725826	-2.00E-3	0.00002
		ρ_8^0 = .698681			ρ_{10}^0 = .726136		
			$xC_9H_{20} + (1-x)C_{11}H_{24}$				
			298.15				
0	0.736467	-	-	1.27E-3	0.736418	7.11E-3	0.00037
2.73E-4	0.736442	5.70E-3	-0.00104	1.60E-3	0.736415	6.20E-3	-0.00003
4.83E-4	0.736437	5.99E-3	-0.00019	1.91E-3	0.736410	5.94E-3	-0.00010
7.31E-4	0.736430	6.65E-3	-0.00029	2.23E-3	0.736403	6.18E-3	0.00044
1.00E-3	0.73624	6.31E-3	-0.00072	2.59E-3	0.736397	5.90E-3	-0.00033
		ρ_9^0 = .713922			ρ_{11}^0 = .736467		

TABLE 8 (CONTINUED)

$xC_9H_{20} + (1-x)C_{13}H_{28}$

x	ρ	V^E	$\sigma(V^E)$	x	ρ	V^E	$\sigma(V^E)$
			298.15 K				
0	0.753113	-	-	-	0.753044	1.99E-3	0.00043
5.41E-4	0.753095	7.87E-4	0.00009	2.18E-3	0.753036	8.13E-4	-0.00083
8.36E-4	0.753087	6.31E-4	0.00032	2.59E-3	0.753021	1.53E-3	-0.00016
1.15E-3	0.753078	6.48E-4	0.00051	3.03E-3	0.753006	2.02E-3	0.00031
1.46E-3	0.753066	1.65E-3	0.00034	3.50E-3	0.752856	1.36E-3	-0.00022
1.80E-3	0.753055	2.02E-3	0.00053	8.77E-3	0.752682	2.92E-3	0.00001
		ρ_9^0 = .713920			ρ_{13}^0 = .753113		

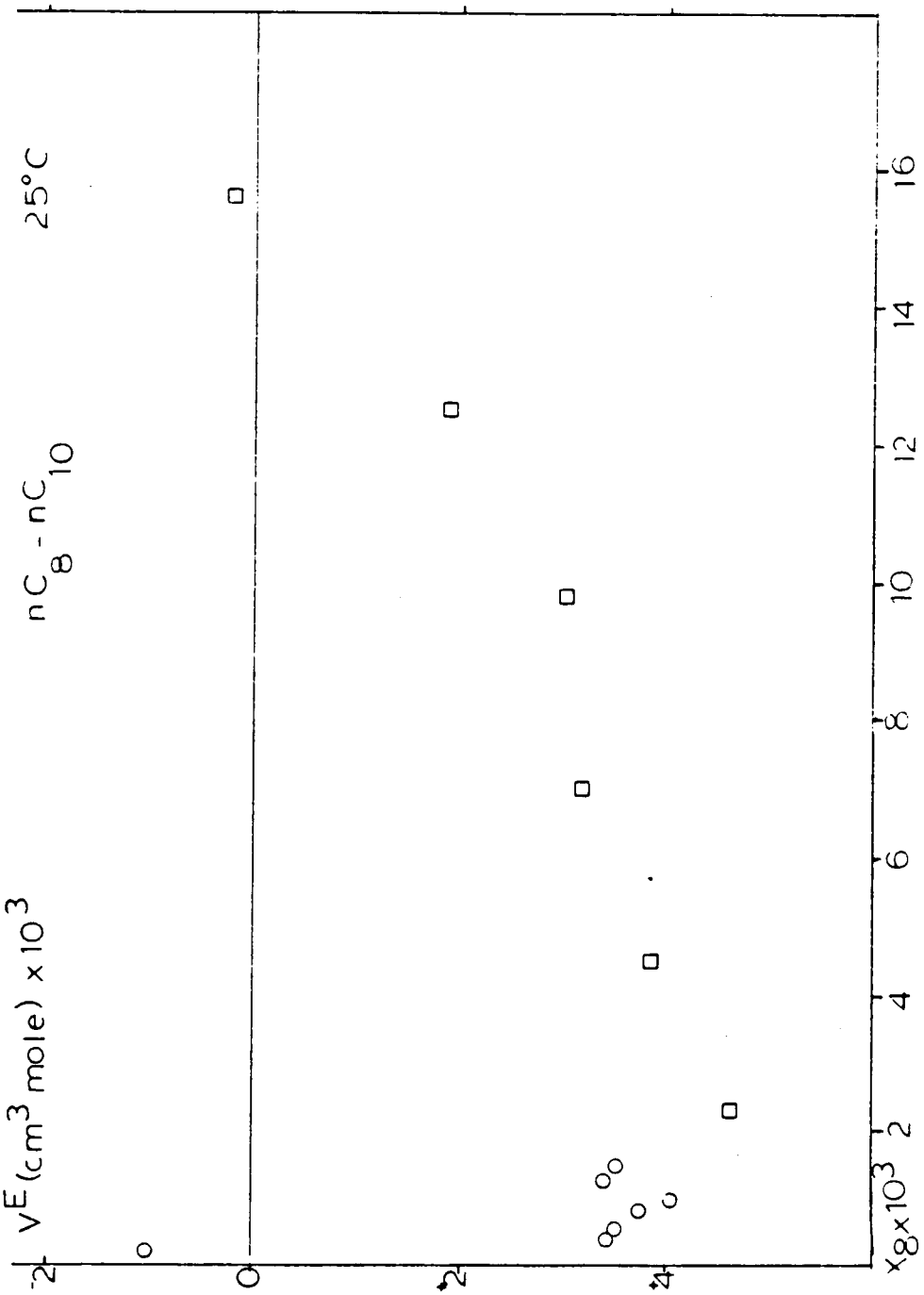

Figure 13. Excess volumes for the $n\text{-}C_8$ + $n\text{-}C_{10}$ system at low concentrations and at 298.15 K.

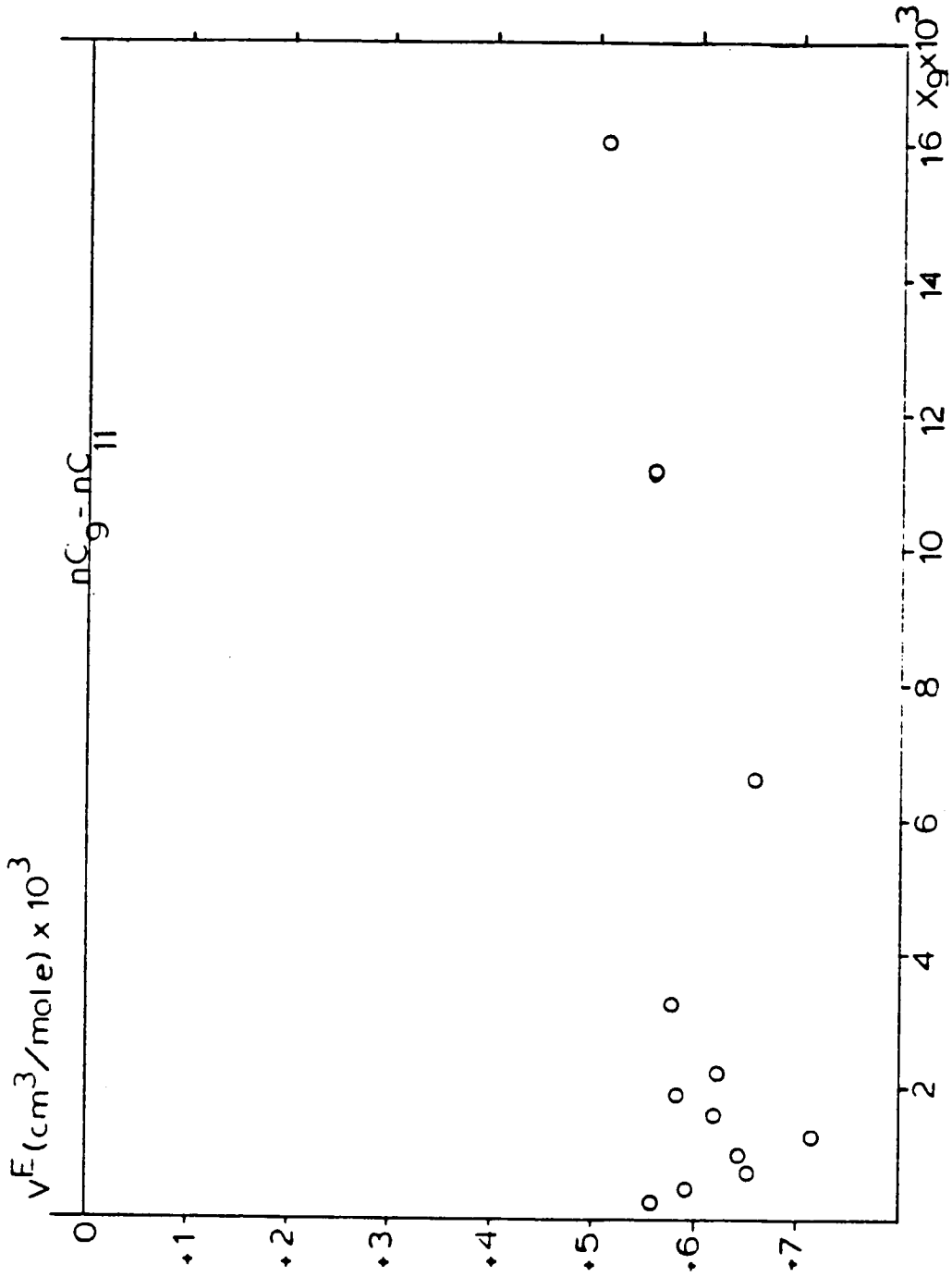

Figure 14. Excess volumes for the n-C_9 + n-C_{11} system at low concentrations and at 298.15 K.

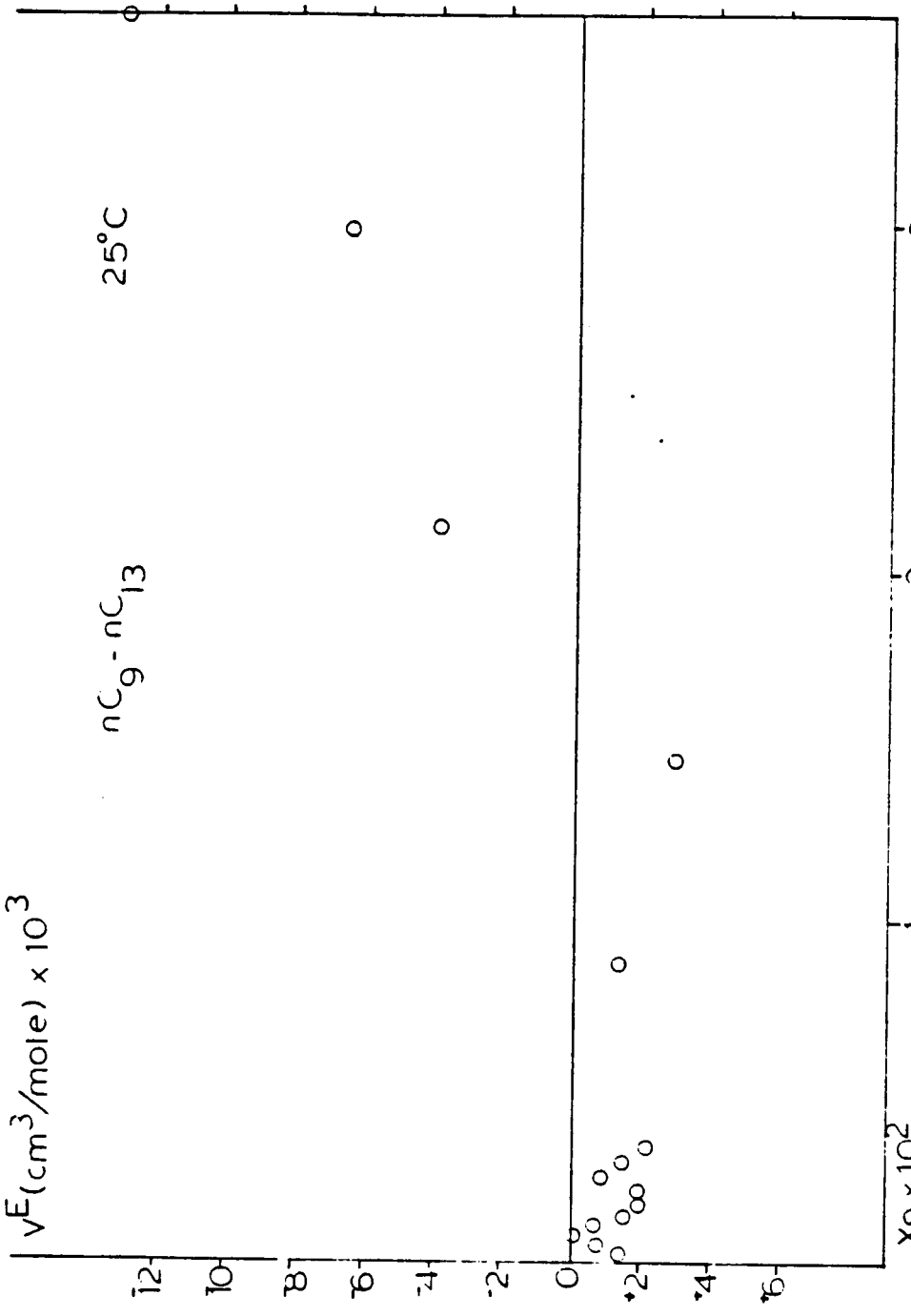

Figure 15. Excess volumes for the n-C_9 + n-C_{13} system at low concentrations and at 298.15 K.

temperature coefficient of all the systems were negative, i.e. V^E is larger (less negative) at the lower temperature.

B. PRELIMINARY VLE EXPERIMENTS

The benzene-cyclohexane system has been thoroughly studied by several laboratories and its thermodynamic properties well documented.[15,52-54,65-71] This system is quite nonideal and the magnitude of the excess thermodynamic properties large. The benzene-cyclohexane system was therefore chosen to determine the precision and accuracy of the new VLE apparatus. Utilizing the experimental method previously described, several experiments were performed at 323.15 K on the benzene-cyclohexane system using injection loops of 0.039 and 0.062 ml. The actual experimental quantities obtained, the mole fractions of the components and the change in the total pressures with the change in solution concentration, were analysed by the method of Boissonnas.[72]

The method of Boissonnas, which is particularly suited for analysis of highly nonideal systems, is an iterative method derived from the Gibbs-Duhem equation. The method is defined by the equation,

$$\partial p_2/\partial x_2 = 1/(1-p_1x_2/p_2x_1)\cdot\partial p/\partial x_2 \qquad 51$$

where p_2 and p_1 are the partial pressures of the solute and solvent respectively, and p is the solution total pressure. If the total pressure and the change in the total pressure with solute mole fraction, dp_2/dx_2, are known, and if the partial pressure of the solute is known for the composition x_2 under consideration, then the coefficient, $(\partial p_2/\partial x_2)$ can be used to calculate p_2 at an adjacent composition. Thus

by proceeding from point to point, it is possible to calculate p_2 over the entire concentration range. The method makes only two assumptions. First, the vapor phase is assumed to be ideal. Secondly, if the change in the mole fraction, ∂x_2, is small enough, then it may be replaced by the quantity Δx_2. Since the change in the mole fraction, x_2, was on the order of 10^{-3} for our experiment, and the deviation from ideality large for the C_6H_6-C_6H_{12} system, the method of Boissonnas was deemed appropriate for data reduction in this case. (A formal derivation of the method of Boissonnas is given in Appendix 1.)

Consider the case where the solution formed by injection of the first solute aliquot is sufficiently dilute, so that we may use the ideal relation to obtain a starting point for the calculation,

$$P_1 = P_1^0 x_1 \qquad 52$$

or

$$dp_1 = p_1^0 dx_1 \text{ and } dp_2 = dp - dp_1 = dp + p_1^0 dx_2 \qquad 53$$

The Boissonnas equations can then be iterated by computer to yield the partial pressures of the components using approximate equations

$$\Delta P_2 = \Delta P/(1-P_1 x_2/P_2 x_1) \qquad 54$$

and

$$\Delta P_2 = \Delta P + P_1^0 \Delta x_2, \text{ for } x_2 = 0 \qquad 55$$

An average of 20 to 25 data points over a concentration range of 0.00 to 0.025 were taken per experiment. The results of the data analysis are shown in Tables 9 through 12 and in Figures 16 and 17. When the data were compared with the literature values,[52-54] it was

TABLE 9

VAPOR PRESSURES, ACTIVITY COEFFICIENTS AND EXCESS FREE ENERGIES FOR EXPERIMENT 1, (LOOP VOLUME, 0.062 ml), FOR C_6H_6-C_6H_{12} SYSTEM AT 323.15 K, C_6H_6 SOLUTE

$X \times 10^3$	P/kPa	$\ln\gamma_1 \times 10^3$	$\ln\gamma_2$	G^E/J mole^{-1}
0	36.1745	-	-	0
3.110	36.2397	0.25048	0.40503	4.055
9.238	36.3490	0.36693	0.39373	10.749
12.258	36.4022	0.34021	0.39588	13.941
15.249	36.4553	0.30742	0.39799	17.119
18.211	36.5067	0.36210	0.39504	20.284
21.144	36.5569	0.43699	0.39157	23.394
24.050	36.6054	0.54620	0.38712	26.447
26.929	36.6534	0.61898	0.38449	29.437
29.780	36.7032	0.52599	0.38752	32.377
32.605	36.7491	0.67586	0.38306	35.313
35.403	36.7960	0.69370	0.38258	38.188
38.174	36.8414	0.77790	0.38045	41.032
40.921	36.8856	0.88294	0.37798	43.833
43.641	36.9307	0.88887	0.37785	46.589
46.337	36.9728	1.05273	0.37448	49.319
49.008	37.0155	1.12686	0.37304	51.998
51.654	37.0563	1.28284	0.37017	54.642
54.277	37.0957	1.47547	0.36681	57.240
56.875	37.1371	1.48999	0.36657	59.791
59.450	37.1765	1.60136	0.36480	62.316
62.002	37.2136	1.83357	0.36128	64.805
64.531	37.2539	1.79327	0.36187	67.247
67.037	37.2893	2.06145	0.35813	69.671
69.520	37.3280	2.05274	0.35824	72.047

TABLE 10

VAPOR PRESSURES, ACTIVITY COEFFICIENTS AND EXCESS FREE ENERGIES FOR EXPERIMENT 2, (LOOP VOLUME, 0.062 ml), FOR C_6H_6-C_6H_{12} SYSTEM AT 323.15 K, C_6H_6 SOLUTE

$X \times 10^3$	P/kPa	$\ln\gamma_1 \times 10^3$	$\ln\gamma_2$	G^E/J mole^{-1}
0	36.1745	-	-	-
2.286	36.2306	0.40809	0.40581	3.587
4.557	36.2725	0.36843	0.41443	6.060
6.814	36.3122	0.48586	0.39717	8.568
9.057	36.3522	0.46149	0.39983	10.958
11.285	36.3912	0.49890	0.39655	13.349
13.499	36.4295	0.53337	0.39403	15.704
15.699	36.4673	0.57359	0.39150	18.030
17.885	36.5045	0.61219	0.38938	20.327
20.057	36.5414	0.64279	0.38788	22.595
22.216	36.5761	0.77977	0.38184	24.840
24.362	36.6134	0.70185	0.38495	27.036
26.493	36.6489	0.74561	0.38334	29.237
28.612	36.6840	0.78099	0.38214	31.415
30.718	36.7176	0.89275	0.37861	33.572
32.810	36.7523	0.90126	0.37836	35.696
34.890	36.7859	0.96118	0.37670	37.805
36.957	36.8195	0.99655	0.37578	39.891
39.011	36.8528	1.02923	0.37497	41.960
41.053	36.8856	1.07713	0.37385	44.011
43.082	36.9182	1.12141	0.37287	46.044

TABLE 11

VAPOR PRESSURES, ACTIVITY COEFFICIENTS AND EXCESS FREE ENERGIES FOR EXPERIMENT 3, (LOOP VOLUME, 0.039 ml), FOR C_6H_6-C_6H_{12} SYSTEM AT 323.15 K, C_6H_6 SOLUTE

$X \times 10^3$	P/kPa	$\ln\gamma_1 \times 10^3$	$\ln\gamma_2$	G^E/J mole^{-1}
0	36.1745	-	-	-
1.425	36.2281	0.76818	0.40647	3.617
2.842	36.2547	0.79582	0.40576	5.230
4.252	36.2807	0.80884	0.40571	6.799
5.656	36.3057	0.81329	0.40406	8.313
7.053	36.3302	0.84697	0.39931	9.826
8.443	36.3537	0.91444	0.39135	11.313
9.826	36.3781	0.88592	0.39422	12.764
11.202	36.4018	0.90798	0.39227	14.218
12.571	36.4260	0.87914	0.39453	15.658
13.934	36.4496	0.89520	0.39340	17.010
15.291	36.4725	0.93393	0.39090	18.530
16.640	36.4961	0.92101	0.39166	19.944
17.983	36.5183	0.98156	0.38835	21.354
19.320	36.5413	0.97748	0.38856	22.745
20.650	36.5640	0.98357	0.38827	24.130
21.974	36.5867	0.98347	0.38827	25.508
23.291	36.6089	1.01032	0.38715	26.879
24.603	36.6310	1.02600	0.38652	28.239
25.907	36.6528	1.06476	0.38507	29.589
27.206	36.6747	1.05877	0.38528	30.930

TABLE 12

VAPOR PRESSURES, ACTIVITY COEFFICIENTS AND EXCESS FREE ENERGIES FOR EXPERIMENT 4, (LOOP VOLUME, 0.062 ml), FOR C_6H_6-C_6H_{12} SYSTEM AT 323.15 K, C_6H_{12} SOLUTE

$X \times 10^3$	P/kPa	$\ln\gamma_1 \times 10^3$	$\ln\gamma_2$	G^E/J mole^{-1}
0	36.1836	-	-	-
1.085	36.2161	0.00009	0.46179	1.347
2.166	36.2434	0.02701	0.46055	2.688
3.242	36.2690	0.24767	0.45374	4.019
4.313	36.2929	0.40314	0.45014	5.325
5.380	36.3167	0.48414	0.44864	6.614
6.442	36.3410	0.21150	0.45284	7.894
7.499	36.3651	0.83245	0.45454	9.180
8.552	36.3893	-0.04164	0.45598	10.466
9.600	36.4119	0.55170	0.44984	11.749
10.643	36.4345	0.98114	0.44584	13.010
11.682	36.4567	1.43770	0.44197	14.254
12.716	36.4791	1.63149	0.44047	15.482
13.746	36.5022	1.37095	0.44233	16.700
14.772	36.5249	1.35004	0.44247	17.919
15.793	36.5481	1.01841	0.44454	19.132
16.809	36.5702	1.23988	0.44324	20.346
17.822	36.5929	1.11021	0.44396	21.551
18.829	36.6134	2.03352	0.43913	22.752
19.833	36.6358	1.82872	0.44015	23.936
20.832	36.6579	1.74570	0.44054	25.117

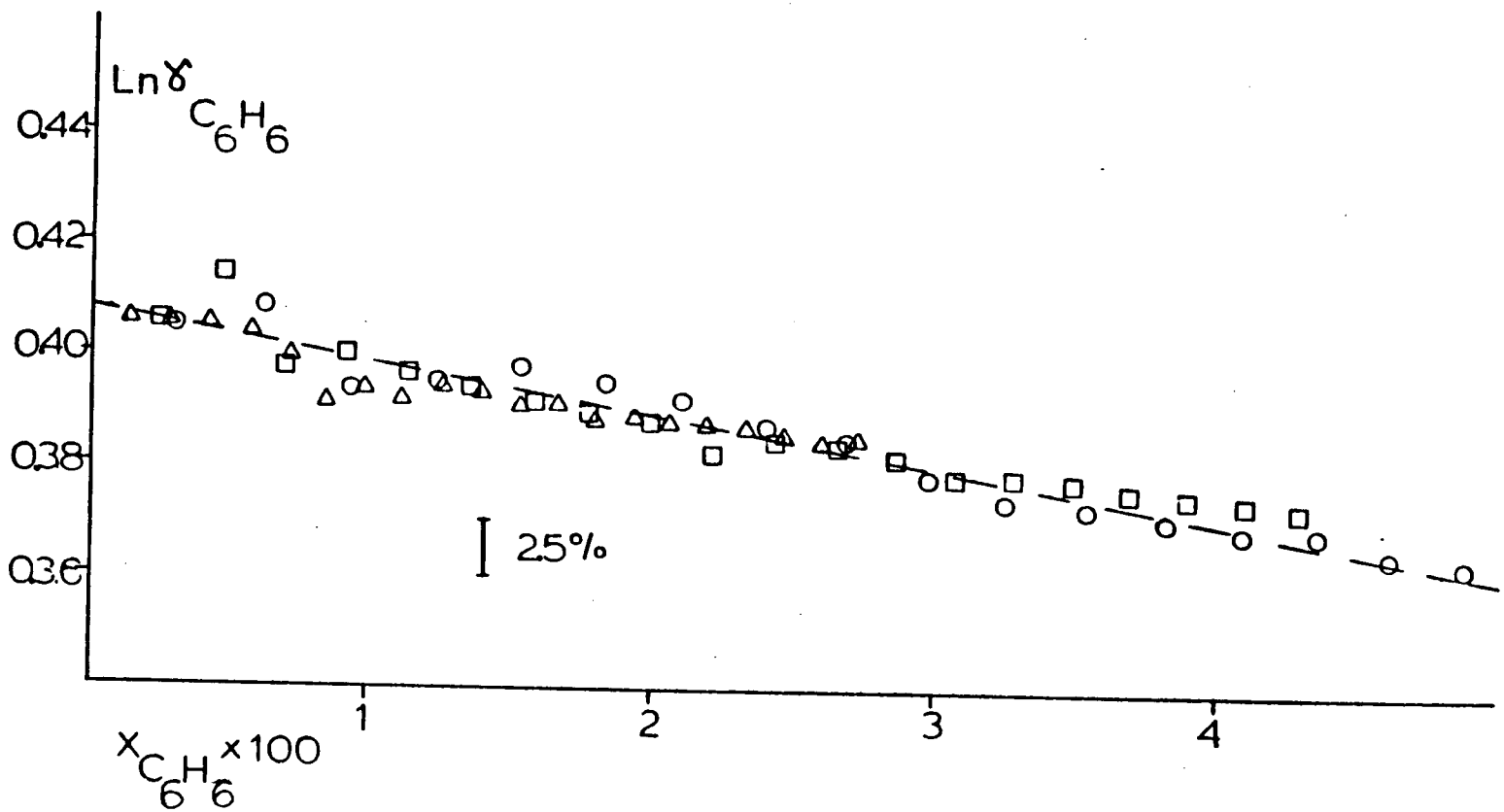

Figure 16. Logarithm of the activity coefficient of C_6H_6 at 323.15 K for preliminary experiments 1-O, 2-[] and 3-Δ. (----) literature values, Reference 52.

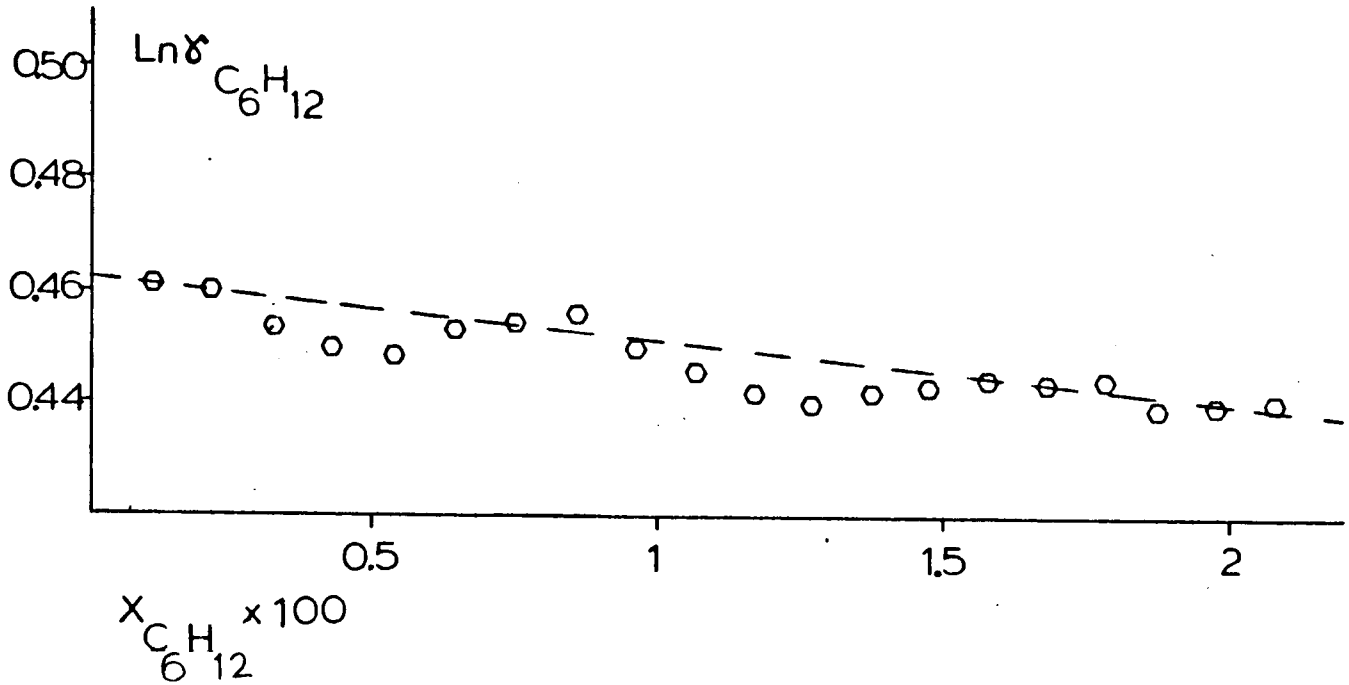

Figure 17. Logarithm of the activity coefficients of C_6H_{12} at 323.15 K for preliminary experiment 4. (----) literature values, Reference 53.

found that the logarithm of the activity coefficient of the solute, in both benzene and cyclohexane rich solutions, was determined to an precision of better than 2.5% in ln γ. For the solutions ln γ° was approximately 0.4. As can be seen in Figure 16, ln γ was reproduced to better than 0.5%, which corresponds to a precision in ΔP, $P_{soln} - P^{\circ}$, of ± 0.006 kPa.

The calibration experiments were a success. The results establish the new continuous dilution-vapor pressure apparatus as an accurate, precise instrument capable of measuring the change in the total pressure with the change in the mole fraction at low concentrations ($x < 0.05$). Also, the method used for the calculation of the moles of solute and solvent, via a mass balance computer program, was proven to be correct.

It was decided that the most likely impurity present in the system or in the samples would be water. Therefore, an experiment was performed on a benzene-cyclohexane-water system to determine what effect trace water present in the system might have on the experiments and to further investigate possible applications of the new VLE apparatus. The experiment was performed as described previously; but the manner of sample preparation was altered. The solubility of water in benzene and cyclohexane is very low; however, water is about 10 times more soluble in benzene than in cyclohexane.[56] A measured trace amount of water was added to the previously dried benzene and the resulting solution used as the solute. Dry cyclohexane was used as the solvent. The concentrations of the ternary solution were approximately; benzene, 0.02; cyclohexane, 0.98; and water, 10^{-5}.

Using the method of Boissonnas, the data for this experiment was first analyzed as if the water was not present in the benzene, Table 13. As can be seen in Figure 18, the apparent activity of the system, $\ln \gamma_{app}$, is parallel to, but higher than the literature values.[52-54] By modifying the mass balance computer program used to calculate the moles of the components present after each injection, the mole fractions of the water, benzene and cyclohexane present were calculated, Table 14. In order to determine the effects of the water present, the following assumption was made. By assuming the effects of the water and the benzene with the cyclohexane to be additive, Table 15, it was possible to extract the effect of the water and to treat the benzene as simply an inert carrier for the water, $x_{BEN.} \ll x_{CYC.}$. Since the values of the activity coefficients for the benzene-cyclohexane system have been established in this and other investigations,[52-54] and because, within experimental error, the plot of $\ln \gamma_{app}$ was parallel to the plot of the literature values, this assumption is shown to be valid. Thus by calculating the partial pressure of the benzene and cyclohexane, Table 16, and subtracting the partial pressure of benzene from the total experimental pressure, the partial pressure of the water present was obtained, Table 17. Analysis of the resulting data by the method of Boissonnas yielded an interesting artifact. It was found that the first point of the calculated $\ln \gamma_2$ was larger than could be attributed to the experiment error (curve 1, Figure 19). Also, since each successive point depended upon the preceding point, the error was cumulative. By arbitrarily decreasing the pressure of only the first point in the computer program, and analyzing the data with the method

TABLE 13

APPARENT MOLE FRACTIONS, VAPOR PRESSURES AND ACTIVITIES COEFFICIENTS FOR THREE COMPONENT MIXTURE (H_2O-C_6H_6-C_6H_{12}) AT 323.15 K, H_2O-C_6H_6 SOLUTE, (LOOP VOLUME, 0.039 ml)

Apparent X x 10^3	P/kPa	$\ln\gamma_1$ x 10^5	$\ln\gamma_2$	LV = .03917 cm^3 @ 323 K
0	36.1745	-	-	
1.409	36.2227	0.00615	0.50000	
2.812	36.2556	0.10787	0.49960	
4.207	36.2890	2.56261	0.50590	
5.596	36.3218	-1.41367	0.50385	
6.977	36.3530	5.12692	0.49450	
8.352	36.3841	8.48120	0.49051	
9.721	36.4134	17.40119	0.48138	
11.082	36.4439	17.3537	0.48142	
12.437	36.4743	16.89278	0.48179	
13.786	36.5041	18.91674	0.48034	
15.128	36.5331	22.92133	0.47773	
16.463	36.5630	21.55911	0.47854	
17.792	36.5916	26.07412	0.47605	
19.115	36.6201	29.07243	0.47451	
20.431	36.6473	37.08296	0.47066	

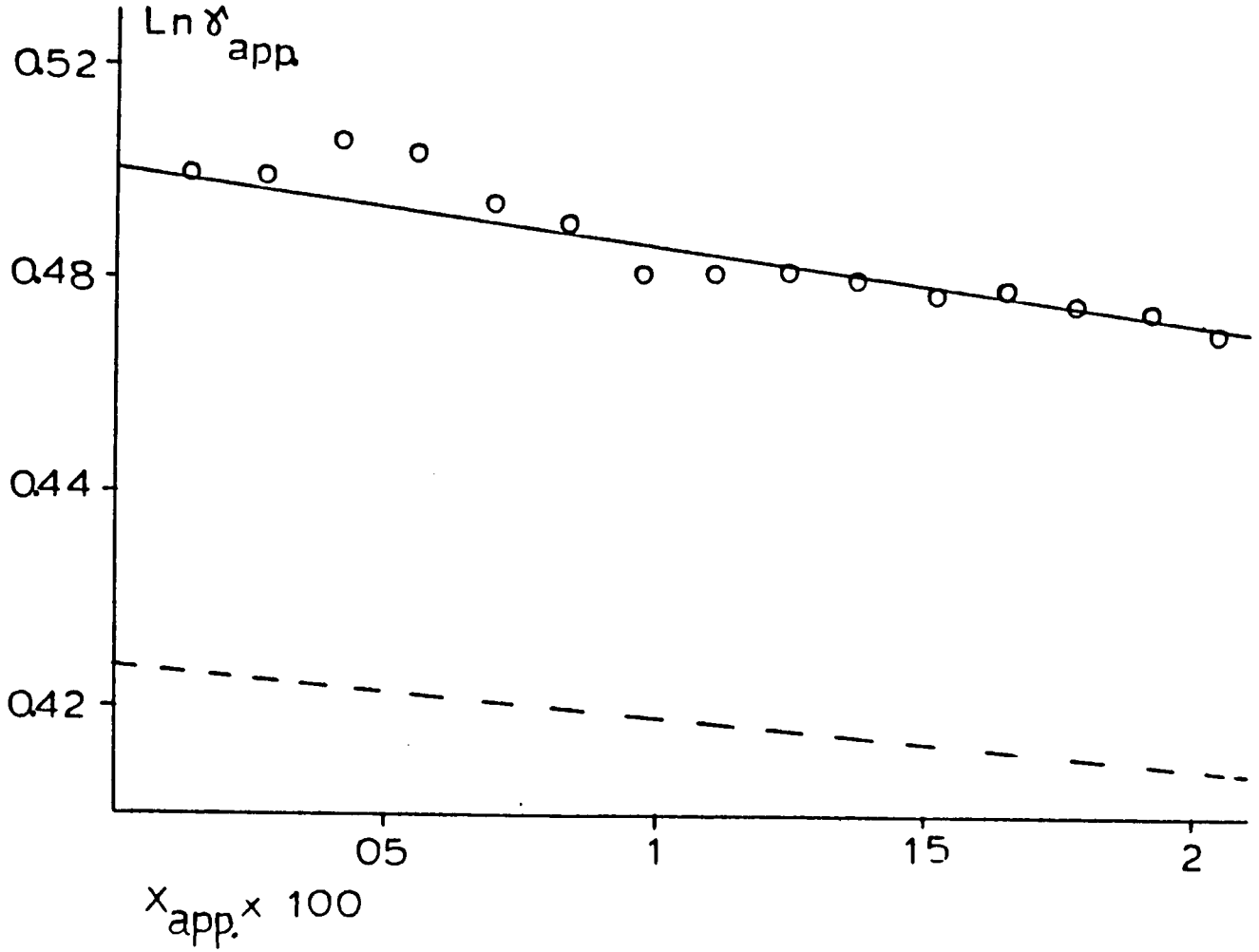

Figure 18. Apparent logarithms of the activity coefficients for three component system. (----) literature values, Reference 53.

TABLE 14

MOLE FRACTIONS OF BENZENE, WATER AND CYCLOHEXANE IN THREE COMPONENT MIXTURE

$X_B \times 10^3$	$X_H \times 10^6$	X_C
1.4093	0.98396	0.99859
2.8116	1.72629	0.99719
4.2071	2.46657	0.99579
5.5956	3.20483	0.99440
6.9773	3.94107	0.99302
8.3522	4.67530	0.99164
9.7205	5.40755	0.99027
11.0821	6.13782	0.98891
12.4371	6.86612	0.98156
13.7855	7.59247	0.98621
15.1275	8.31688	0.98486
16.4629	9.03936	0.98353
17.7920	9.75992	0.98220
19.1146	10.47858	0.98087
20.4310	11.19534	0.97956

TABLE 15

COMPARISON OF APPARENT ACTIVITY COEFFICIENTS WITH LITERATURE VALUES FOR THE TWO COMPONENT C_6H_6-C_6H_{12} SYSTEM AT 323.15 K

	$\ln \gamma_{H_2O}$ Spiked	$\ln \gamma_{C_6H_6}$	$\Delta \ln \gamma$
1	0.4999	0.4060	0.0940
2	0.4996	0.4050	0.0946
3	0.5059	0.4038	0.1021
4	0.5039	0.4020	0.1019
5	0.4945	0.4010	0.0935
6	0.4905	0.3998	0.0907
7	0.4814	0.3985	0.0829
8	0.4814	0.3970	0.0844
9	0.4818	0.3960	0.0858
10	0.4803	0.3946	0.0871
11	0.4777	0.3932	0.0845
12	0.4785	0.3920	0.0865
13	0.4760	0.3910	0.0850
14	0.4745	0.3899	0.0846
15	0.4707	0.3885	0.0822

TABLE 16

EXPERIMENTAL TOTAL PRESSURES, AND PARTIAL PRESSURES OF BENZENE, CYCLOHEXANE AND WATER PRESENT IN THREE COMPONENT SYSTEM

P_{Total}/kPa	$(X_B P^o_B \gamma_B)$/kPa	$X_C P^o_C \gamma_C$/kPa	$(X_\omega P^o_\omega)$/Pa
36.2227	0.07657	36.1235	0.01214
36.2556	0.15258	36.0729	0.02129
36.2890	0.22804	36.0225	0.03042
36.3218	0.30295	36.9725	0.03953
36.3530	0.37731	35.9227	0.04861
36.3841	0.45115	35.8733	0.05766
36.4134	0.52445	35.8241	0.06669
36.4439	0.59723	35.7753	0.07570
36.4743	0.66950	35.7267	0.08468
36.5041	0.74125	35.6784	0.09364
36.5331	0.81250	35.6304	0.10258
36.5630	0.88324	35.5827	0.11149
36.5916	0.95350	35.5353	0.12038
36.6201	1.02326	35.4882	0.12924
36.6473	1.09254	35.4413	0.13808

TABLE 17

MOLE FRACTIONS, ACTIVITY COEFFICIENTS AND PARTIAL PRESSURES OF H_2O

$X_{H_2O}(x10^6)$	$\ln\gamma_{H_2O}$	P_{H_2O}/kPa
0.9840	7.5294	0.02260
1.7263	7.2558	0.03015
2.4666	7.1409	0.03840
3.2048	7.0675	0.04637
3.9411	6.9938	0.05298
4.6753	6.9417	0.05965
5.4076	6.8794	0.06483
6.1378	6.8490	0.07138
6.8661	6.8269	0.07811
7.5925	6.8037	0.08439
8.3169	6.7791	0.09019
9.0394	6.7690	0.09704
9.7599	6.7494	0.10275
10.4786	6.7344	0.10867
11.1953	6.7114	0.11346

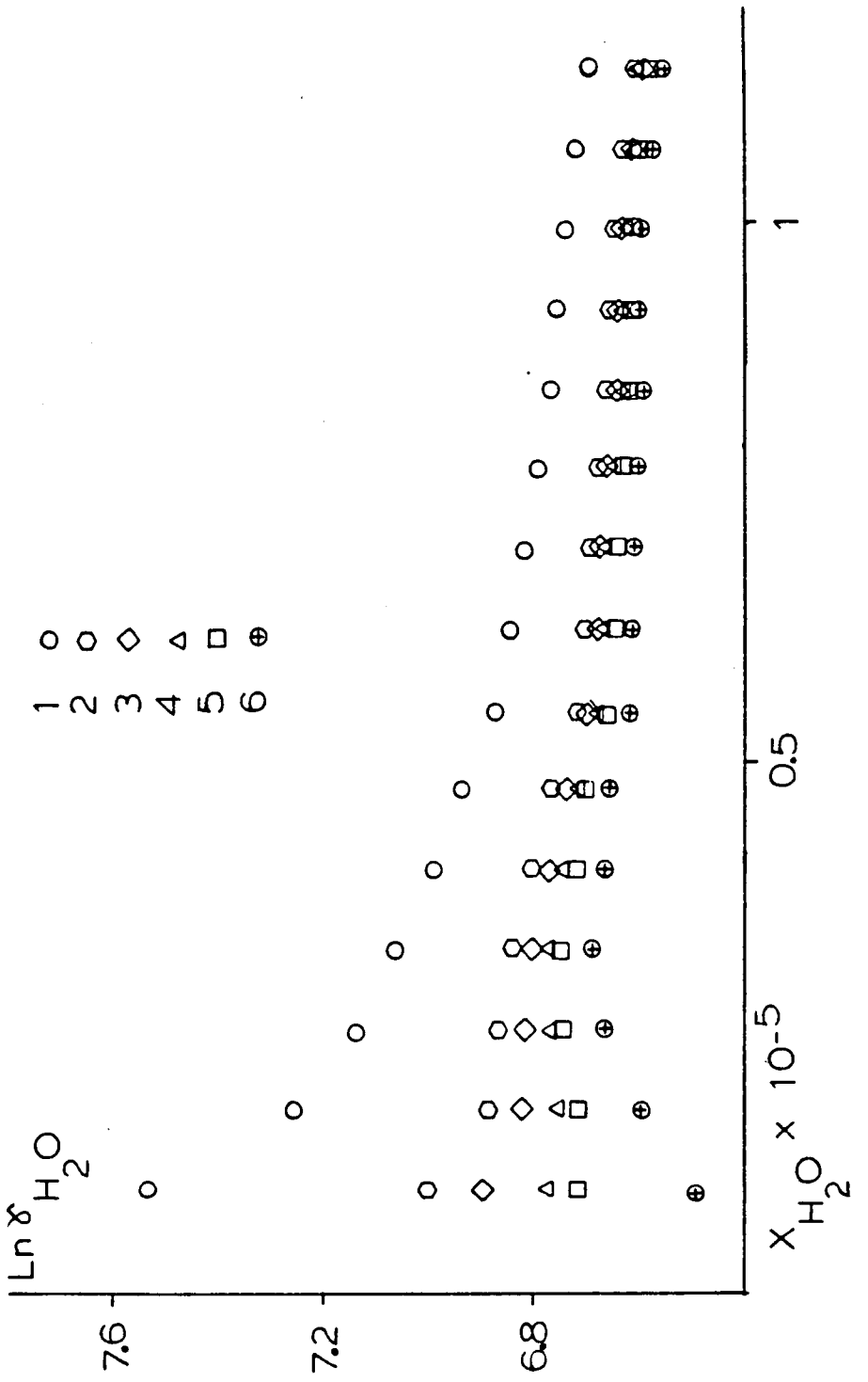

Figure 19. Boissonnas analysis of the logarithms of the activity coefficients of H_2O.

of Boissonnas, Table 18 and Figure 19, a profile of the effect of the first point on the remaining data was obtained. An investigation of this mathematical phenomenon showed that the problem rested in the initial assumption used in the method of Boissonnas, equations 52 and 53. This assumption attributes all the nonideality to the solute and may lead to erroneous results. (The importance of this observation is further emphasized in the following section). By altering the first point until the error was minimized and using the resulting activities, the logarithm of the activity coefficient at infinite dilution, $\ln \gamma_2^0$, was determined. Van Hook and coworkers established that the water-benzene system did not obey Henry's law.[51] However, at our level of precision, it is valid to assume that the water-cyclohexane system obeys Henry's law.[57] By using the relationships,

$$P = K_H x = P^0 x\gamma \qquad 56$$

and

$$K_H = \gamma^0 P^0 \qquad 57$$

the Henry's law constant was calculated and found to have the value 11241.1313 kPa. From equations 56 and 57, the solubility of water in cyclohexane at 323.15 K was determined to be 1.0972×10^{-3} mole fraction. As can be seen in Figure 20, the agreement between the literature values for the solubility of water in cyclohexane[56] and the value determined in this work was excellent.

From the results of the benzene-cyclohexane-water experiment, it is obvious that any water present or introduced into the hydrocarbon

TABLE 18

BOISSONNAS ANALYSIS OF THE CHANGE IN THE ACTIVITY COEFFICIENTS WITH A DECREASE IN THE TOTAL PRESSURE OF THE FIRST EXPERIMENTAL POINT

	P_T/kPa	$\ln\gamma_1$	$\ln\gamma_2$	$\ln\gamma_3$	$\ln\gamma_4$	$\ln\gamma_5$	$\ln\gamma_6$
0.98346	36.1971	7.5296	7.0004	6.8950	6.7772	6.7127	6.4895
1.73115	36.2047	7.2545	6.8868	6.8211	6.7507	6.7136	6.5933
2.47699	36.2129	7.1384	6.8622	6.8156	6.7667	6.7414	6.6614
3.22286	36.2209	7.0637	6.8409	6.8045	6.7668	6.7474	6.6869
3.96876	36.2275	6.9887	6.7967	6.7659	6.7342	6.7179	6.6676
4.714683	36.2342	6.9349	6.7663	6.7396	6.7123	6.6984	6.6554
5.46063	36.2394	6.8717	6.7178	6.6937	6.6690	6.6564	6.6178
6.20660	36.2459	6.8400	6.7013	6.6798	6.6578	6.6466	6.6124
6.95259	36.2526	6.8166	6.6907	6.6713	6.6515	6.6415	6.6109
7.69860	36.2589	6.7921	6.6762	6.6584	6.6404	6.6312	6.6033
8.44462	36.2647	6.7662	6.6582	6.6417	6.6250	6.6167	6.5908
9.19066	36.2716	6.7548	6.6549	6.6397	6.6244	6.6166	6.5929
9.93671	36.2778	6.7393	6.6458	6.6318	6.6174	6.6101	6.5881
10.68278	36.2832	6.7176	6.6289	6.6155	6.6020	6.5952	6.5744
11.14288	36.2880	6.6933	6.6085	6.5958	6.5829	6.5764	6.5567

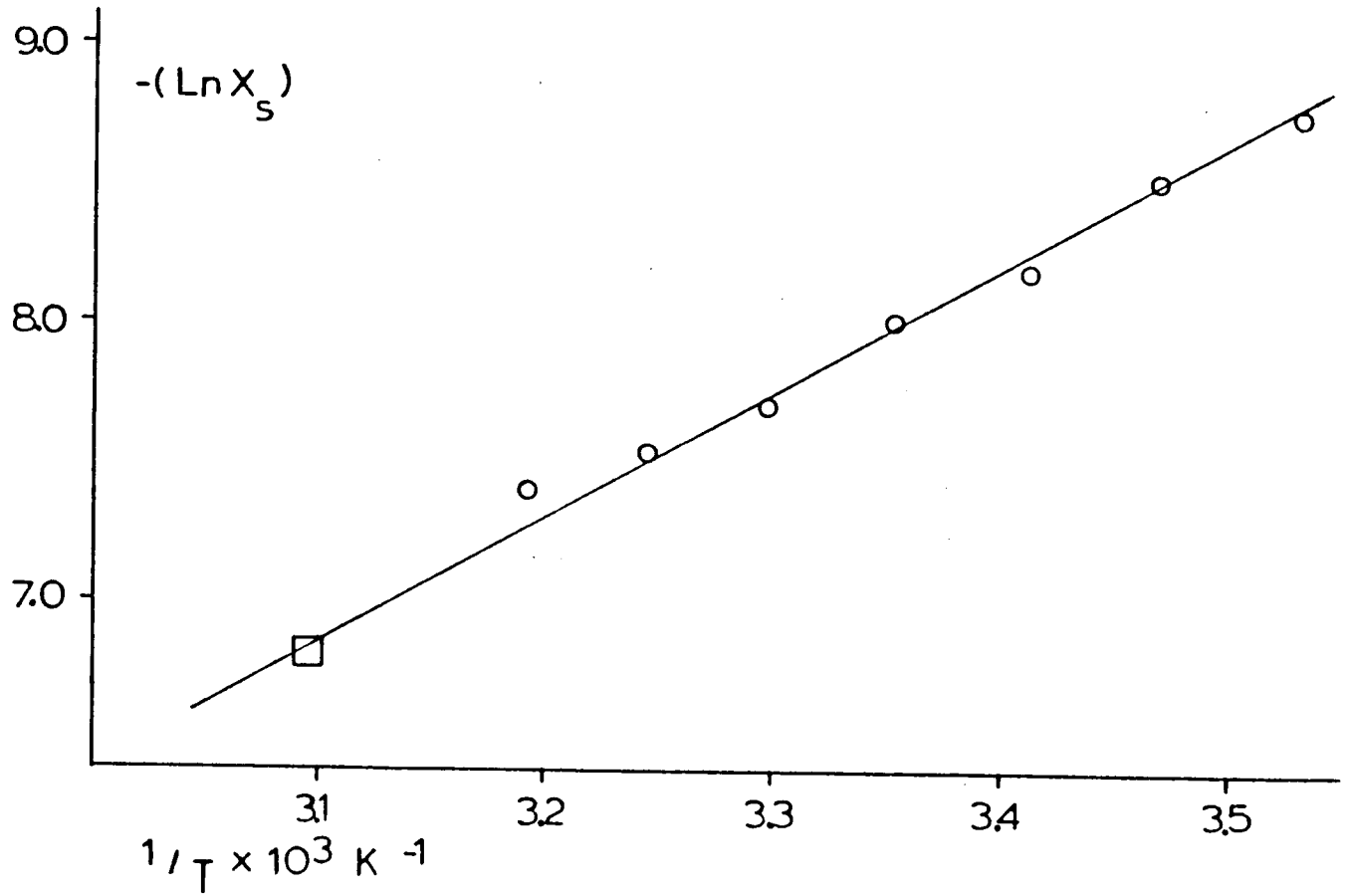

Figure 20. Solubilities of H_2O in C_6H_{12} with change in temperature. O literature values, References 56, 57. [], this work.

system would ruin an experiment by causing erroneously high pressure readings. Thus, sample drying is of the utmost importance.

As will be discussed in the following section, the problems encountered in the data reduction of the preliminary experiments present the major difficulty in the VLE experiments.

C. N-HYDROCARBON VLE MEASUREMENTS

Vapor-liquid experiments were performed on fourteen binary n-hydrocarbon systems whose components were separated by only one or two methylene, $-CH_2-$, units, Table 19. The change in the total pressure with concentration, $\partial P_T/\partial x_2$, was measured over concentration range of 0.00 to 0.025 mole fraction for injection loop volume 0.062 ml, or from 0.00 to 0.35 mole fraction for injection loop volume 0.402 ml. Preliminary analysis of the unreduced pressure data showed the systems to deviate only slightly from ideality and the data to be highly precise.

The narrow concentration range over which most experiments were performed; the wide separation in pure component vapor pressures; and the nearly ideal behavior of the experimental systems made data analysis difficult. As discussed in the preceding section and Appendix 1, the method of Boissonnas is best suited for data reduction of VLE systems which deviate markedly from ideality. Data reduction of the binary n-hydrocarbon systems by this method proved to be impossible. It was observed that the partial pressures of the solute, and consequently the activity coefficients, obtained by the method of Boissonnas were implausibly large and increased too rapidly with the change in solute concentration.

TABLE 19

N-HYDROCARBON VLE SYSTEMS STUDIED, LOOP VOLUMES AND TEMPERATURES

Solute	Solvent	Loop Volume	Temperature
Hexane	Pentane	0.06231	323.15
Hexane	Heptane	0.06231	323.15
Hexane	Heptane	0.40150	323.15
Heptane	Hexane	0.06231	323.15
Heptane	Octane	0.06231	323.15
Heptane	Octane	0.40150	323.15
Heptane	Octane	0.06231	303.15
Heptane	Octane	0.06231	303.15
Octane	Heptane	0.06231	323.15
Octane	Heptane	0.06231	323.15
Octane	Heptane	0.40150	323.15
Nonane	Heptane	0.06231	323.15
Nonane	Octane	0.06231	323.15
Nonane	Octane	0.40150	323.15

The problems encountered with the method of Boissonas were carefully analysed by a data simulation computer program. Several possible experimental conditions were postulated; solute and solvent vapor pressures equal; and, solute vapor pressure greater or less than that of the solvent (in intervals of 1.33 kPa). Data was then generated for each case by assuming several mathematical forms of the activity coefficients, systematically progressing from ideality to highly nonideal systems. The method of Boissonnas failed miserably whenever the vapor pressures of the pure components were separated by more than 2.664 kPa. Also, as discussed in the previous section, the problems due to the initial assumptions made in the method intensified as the systems became more ideal. Consequently, the method of Boissonnas was abandoned as a method of data reduction for the binary n-hydrocarbon systems.

The data was analyzed by several alternative methods; the 1,2,4 and 5 parameter Margules equations;[73] the two parameter van Laar equation;[73] the Wilson equation;[74] the Van Hook Henry's Law formalism;[51] and the modified Barker treatment.[75,76] These methods, for any given system, gave identical limiting activities coefficients and were able to precisely fit the experimental data. However, the predicted concentration dependence of the activity coefficients, differed between each method and between experiments, where the same system was run using different dilution sizes, 0.062 or 0.402 ml.

As mentioned above, the pure component vapor pressures were widely separated. It was observed that whenever a solute of a higher

vapor pressure was injected into the solution cell, the subsequent change in temperature and vapor pressure caused the solute to rush into the cell. This greatly disturbed the system's ability to re-equilibrate. Thus, the data for the systems where the solute vapor pressure was lower than that of the solvent, were more precise than the opposite situation. Using the more precise systems, a plot of the logarithm of the total experimental pressures divided by the ideal pressure versus the mole fraction x_2,

$$\ln(P_T/P_{IDEAL}) = \ln P_{exp}/(P_1^0 x_1 + P_2^0 x_2) \qquad 58$$

where p_1^0 and P_2^0 are the vapor pressures of the solvent and solute respectively, was made. As can be seen in Figure 21, the systems deviate only slightly from ideality and the differences between runs of different loop volumes agree within experimental error. Since the $\ln(P_T/P_{IDEAL})$ is a rough measure of the concentration dependence of the excess free energy, $\partial G^E/\partial x_2$, it can be surmised from the plot that the change in the activities with concentration should be small and follow approximately the trend established on Figure 21. The apparent linearity of the plot over the concentration range, 0.00 to 0.025 mole fraction, and the small deviations from ideality over that range, $\ln(P_T/P_{IDEAL})$ = 0.00 to 25×10^{-4}, suggest that the VLE data obtained for the smaller loop, 0.062 ml, is not precise enough to accurately determine the concentration dependence of the activity coefficients. Because all the methods[51,73-76] predicted the same limiting activity coefficients for each respective system, regardless of the loop volume, and also for the reasons cited above, it was

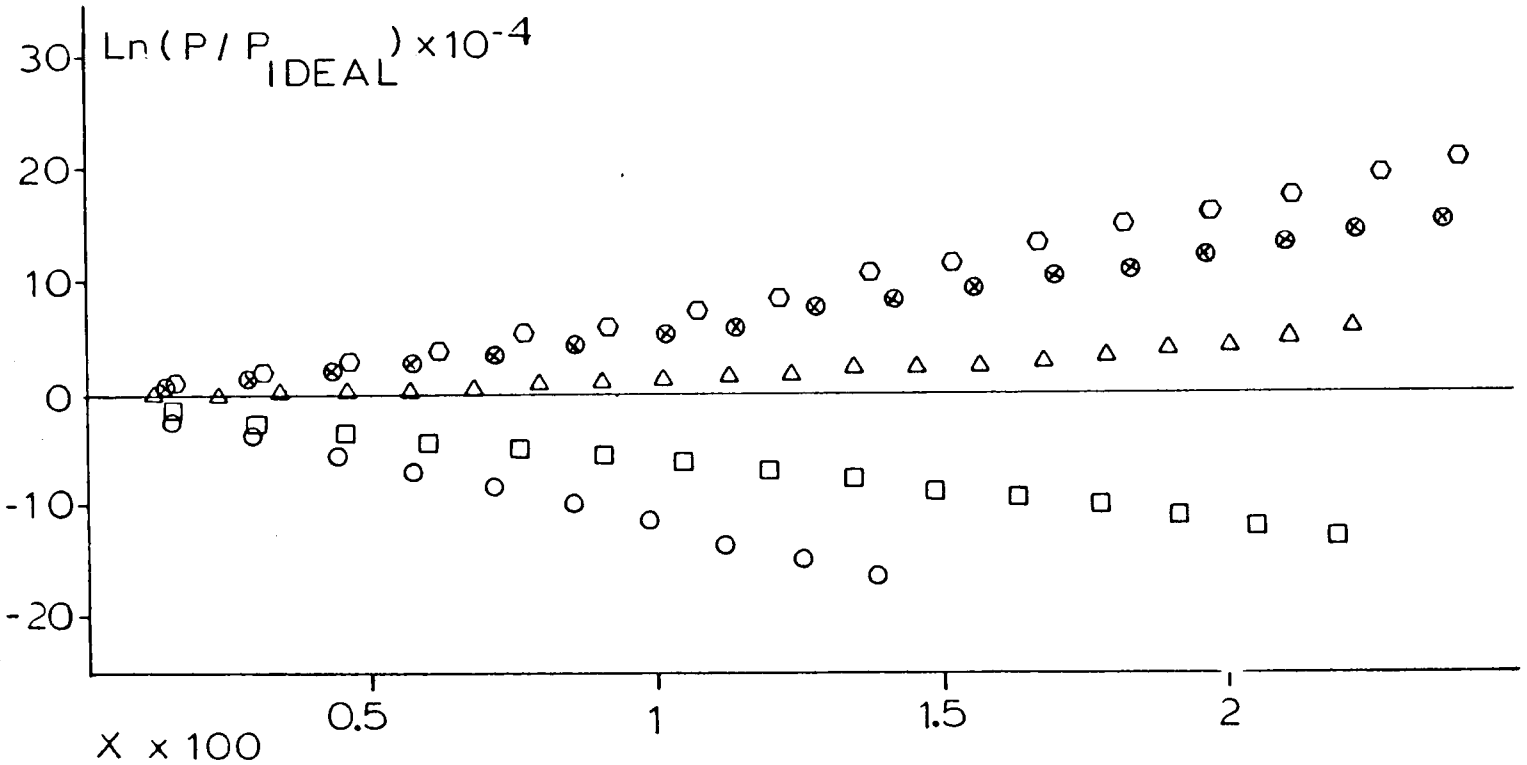

Figure 21. Ln P_T/P_{IDEAL} versus solute mole fraction for selected systems; O xn-C_6H_{14} + (1-x)n-C_5H_{12}; []xn-C_7H_{16} + (1-x)n-C_6H_{14}; Δxn-C_8H_{18} + (1-x)n-C_7H_{16}; Oxn-C_9H_{20} + (1-x)n-C_7H_{16}7; xn-C_9H_{20} + (1-x)n-C_8H_{18}.

decided that the data could be accurately represented by assuming the activity of the solvent to be a constant and that the solute obeyed Henry's law.

The data were fit to the expression

$$P_T = P_1 + P_2 = P_1^0 x_1 C + K_H x_2$$

where C is the activity of solvent and K_H is the Henry's law constant. The precision of this fit, to 10^{-3} kPa, was the same as that achieved with the more elaborate methods, and the activity coefficient of the solvent was 1.000; thus reinforcing the validity of the assumption of no apparent concentration dependence over the measured concentration range. The results of the analysis and the $\ln(P_T/P_{IDEAL})$ values are given in Tables 20 through 32, and summarized in Table 33. As shown in Table 33, the agreement between the Henry's law constants for identical systems with different loop injection volumes was excellent. Also, the sign and magnitude of the logarithm of the limiting activity coefficients, $\ln \gamma_2^0$, followed the trend established by the $\ln(P_T/P_{IDEAL})$ plot, Figure 19, p 78.

The data for the high dilution runs, 0.402 ml injection loop volume, were again analysed with the hope that the increased injection size might allow an accurate determination of the concentration dependence of the activities γ_1 and γ_2, and the excess free energies, $G^E/J\ mol^{-1}$. Since no one method fits the data best, the two parameter Margules equation was arbitrarily chosen as a method of data reduction. The two parameter Margules method is defined by the equations

TABLE 20

VAPOR PRESSURE P, AND LN(P/P_{IDEAL}) for ($xn\text{-}C_6H_{14}+(1-x)n\text{-}C_5H_{12}$) AT 323.15 K; P = P(OBS.) - P(CALC.), LOOP VOLUME, 0.062 ML

($xn\text{-}C_6H_{14}+(1-x)n\text{-}C_5H_{12}$)			
X x 10^3	P/kPa	σP/kPA	$-\ln(P/P_R) \times 10^4$
0	159.1486	-	-
1.467	158.9613	-0.0003	2.085
2.915	158.7791	-0.0030	3.977
4.345	158.6021	0.0033	5.661
5.758	158.4311	0.0002	7.089
7.152	158.2629	0.0043	8.463
8.530	158.0933	0.0049	10.038
9.890	157.9228	0.0026	11.178
11.234	157.7530	-0.0012	13.361
12.561	157.5888	-0.0016	15.191
13.871	157.4253	-0.0031	16.838
		<σP/kPa> = .0032	

TABLE 21

VAPOR PRESSURE P, AND LN(P/P_{IDEAL}) for ($xn\text{-}C_7H_{16}+(1-x)n\text{-}C_6H_{14}$) AT 323.15 K; P = P(OBS.) - P(CALC.), LOOP VOLUME, 0.062 ML

($xn\text{-}C_7H_{16}+(1-x)n\text{-}C_6H_{14}$)			
X x 10^3	P/kPa	σP/kPA	$-\ln(P/P_R) \times 10^4$
0	54.0364	-	-
1.535	53.9728	0.0010	1.779
3.060	53.9129	-0.0010	2.939
4.575	53.8554	-0.0010	3.719
6.079	53.7985	-0.0010	4.490
7.572	53.7428	-0.0004	5.085
9.056	53.6860	-0.0005	5.943
10.529	53.6311	0.0004	6.535
11.993	53.5764	0.0013	7.130
13.446	53.5210	0.0010	7.956
14.890	53.4662	0.0010	8.709
16.323	53.4117	0.0008	9.487
17.747	53.3578	0.0010	10.207
19.162	53.3036	0.0003	11.067
20.057	53.2486	-0.0014	12.127
21.961	53.1953	-0.0018	12.942
		<σP/kPa> = .0011	

TABLE 22

VAPOR PRESSURE P, AND LN(P/P_{IDEAL}) FOR ($xn-C_8H_{18}+(1-x)n-C_7H_{16}$)

AT 323.15 K; P = P(OBS.) - P(CALC.);
EXPERIMENT 1 LOOP VOLUME, 0.062 ML

($xn-C_8H_{18}+(1-x)n-C_7H_{16}$) [1]			
X x 10^3	P/kPa	σP/kPA	$-\ln(P/P_K) \times 10^4$
0	18.8740	-	-
1.150	18.8595	0.0011	-0.271
2.296	18.8495	0.0008	-0.090
3.437	18.8328	0.0010	0.289
4.574	18.8189	0.0004	0.243
5.706	18.8051	-0.0001	0.267
6.834	18.7919	-0.0002	0.533
7.958	18.7785	-0.0004	0.700
9.077	18.7653	-0.0006	0.910
10.192	28.7521	-0.0008	1.092
11.303	18.7393	-0.0006	1.475
12.409	18.7260	-0.0010	1.545
13.512	28.7136	-0.0005	2.101
14.609	18.7006	-0.0006	2.316
15.703	18.6874	-0.0011	2.375
16.793	18.6745	-0.0012	2.592
17.878	18.6627	-0.0004	3.312
18.959	18.6508	0.0004	3.990
20.036	18.6383	0.0005	4.314
21.109	18.6263	0.0009	4.854
22.177	18.6152	0.0023	5.898

$\langle \sigma P/kPa \rangle$ = .0009

TABLE 23

VAPOR PRESSURE P, AND LN(P/P_{IDEAL}) FOR ($xn\text{-}C_8H_{18}+(1-x)n\text{-}C_7H_{16}$) AT 323.15 K; P = P(OBS.) - P(CALC.); EXPERIMENT 2 LOOP VOLUME, 0.062 ML

($xn\text{-}C_8H_{18}+(1-x)n\text{-}C_7H_{16}$) [2]			
X x 10^3	P/kPa	σP/kPA	$-\ln(P/P_R) \times 10^4$
0	18.8740	-	-
1.889	18.8495	0.0029	0.831
3.764	18.8251	0.0012	1.685
5.629	18.8014	0.0002	2.191
7.483	18.7784	-0.0004	2.466
9.325	18.7555	-0.0010	2.716
11.156	18.7329	-0.0023	2.897
12.976	18.7111	-0.0012	2.723
14.785	18.6895	-0.0009	2.492
16.583	18.6680	-0.0005	2.274
18.370	18.6465	-0.0004	2.170
20.146	18.6257	0.0003	1.721
21.912	18.6038	-0.0002	1.971
23.667	18.5823	-0.0005	2.034
15.411	18.5610	-0.0006	2.081
27.145	18.5404	-0.0002	1.808
28.868	18.5199	0.0002	1.560
30.581	18.4994	0.0003	1.408
32.284	18.4257	0.0007	1.194
33.976	18.4589	0.0010	0.961
35.658	18.4382	0.0007	1.083
	<σP/kPa> = .0010		

TABLE 24

VAPOR PRESSURE P, AND LN(P/P_{IDEAL}) FOR ($xn\text{-}C_8H_{18}+(1-x)n\text{-}C_7H_{16}$) AT 323.15 K; P = P(OBS.) - P(CALC.); LOOP VOLUME, 0.402 ML

($xn\text{-}C_8H_{18}+(1-x)n\text{-}C_7H_{16}$) [LV = .4015 cm^3]			
X	P/kPa	σP/kPA	$+\ln(P/P_R) \times 10^4$
0	18.8740	-	-
0.01777	18.6581	-0.0116	0.148
0.03490	18.4495	0.0063	0.074
0.05141	18.2304	-0.0195	-9.987
0.06731	18.0506	-0.0007	-2.428
0.08264	17.8613	0.0013	-4.027
0.09741	17.6781	0.0025	-6.033
0.11164	17.5024	0.0043	-7.559
0.12535	17.3313	0.0043	-10.149
0.13856	17.1683	0.0062	-11.529
0.15129	17.0091	0.0058	-14.201
0.16354	16.8561	0.0057	-16.653
0.17535	16.7094	0.0064	-18.598
0.18672	16.5665	0.0063	-21.513
0.19767	16.4310	0.0066	-23.035
0.20822	16.3001	0.0073	-24.818
0.21837	16.1719	0.0058	-27.913
0.22815	16.0500	0.0060	-29.919
0.23756	15.9311	0.0046	-32.884
0.24663	15.8183	0.0047	-34.704
0.25535	15.7082	0.0036	-37.465
0.26375	15.6023	0.0026	-40.067
0.27183	15.5002	0.0014	-42.757
0.27961	15.4013	-0.0005	-45.794
0.28710	15.3058	-0.0025	-48.923
0.29430	15.2141	-0.0043	-51.886
0.30123	15.1250	-0.0069	-55.303
0.30790	15.0397	-0.0090	-58.392
0.31432	14.9597	-0.0089	-59.999
0.32048	14.8770	-0.0146	-65.405
		$\langle\sigma P/kPa\rangle$ = .0073	

TABLE 25

VAPOR PRESSURE P, AND LN(P/P_{IDEAL}) FOR ($xn\text{-}C_9H_{20}+(1-x)n\text{-}C_8H_{18}$) AT 323.15 K; P = P(OBS.) - P(CALC.); LOOP VOLUME, 0.062 ML

($xn\text{-}C_9H_{20}+(1-x)n\text{-}C_8H_{18}$)			
X x 10^3	P/kPa	σP/kPa	$+\ln(P/P_R) \times 10^4$
0	6.7069	-	-
1.554	6.7008	0.0015	0.8531
3.101	6.6948	0.0011	1.827
4.642	6.6888	0.0007	2.764
6.177	6.6829	0.0003	3.743
7.707	6.6774	0.0003	5.443
0.230	6.6716	0.0000	6.467
10.746	6.6655	-0.0006	7.134
12.257	6.6622	0.0015	8.250
13.762	6.6548	-0.0005	10.520
15.261	6.6489	-0.0009	11.398
16.754	6.6437	-0.0008	13.242
18.241	6.6385	-0.0006	15.010
19.723	6.6327	-0.0010	15.980
21.198	6.6273	-0.0011	17.436
22.667	6.6224	-0.0007	19.583
24.131	6.6169	-0.0009	20.767
25.589	6.6120	-0.0006	22.885
27.041	6.6068	-0.0006	24.363
28.849	6.6015	-0.0007	25.581
29.928	6.5965	-0.0005	27.659
31.363	6.5915	-0.0002	29.518
32.793	6.5868	0.0002	31.668
34.217	6.5815	0.0000	33.015
35.635	6.5770	0.0007	35.462
37.047	6.5716	0.0004	36.538
38.454	6.5667	0.0005	38.269
39.856	6.5614	0.0003	39.398
41.252	6.5570	0.0008	41.794
42.642	6.5520	0.0009	43.425
44.027	6.5467	0.0006	44.452

$\langle \sigma P/kPa \rangle$ = .0008

TABLE 26

VAPOR PRESSURE P, AND LN(P/P_{IDEAL}) FOR ($xn\text{-}C_9H_{20}+(1-x)n\text{-}C_7H_{16}$) AT 323.15 K; P = P(OBS.) - P(CALC.); LOOP VOLUME, 0.062 ML

($xn\text{-}C_9H_{20}+(1-x)n\text{-}C_7H_{16}$)			
X x 10^3	P/kPa	σP/kPa	$\ln(P/P_R)$ x 10^4
0	18.8740	-	-
1.452	18.8514	0.0020	0.655
2.898	28.8289	0.0014	1.358
4.336	18.8063	0.0006	1.958
5.768	18.7840	0.0000	2.626
7.192	18.7619	-0.0006	3.321
8.610	18.7401	-0.0010	4.148
10.020	18.7187	-0.0009	5.167
11.424	18.6978	-0.0006	6.342
12.822	18.6771	-0.0002	7.567
14.212	18.6557	-0.0005	8.415
15.596	18.6345	-0.0007	9.276
16.973	18.6134	-0.0001	10.137
18.343	18.5925	-0.0012	11.006
19.707	18.5722	-0.0008	12.199
21.064	18.5525	0.0000	13.625
22.415	18.5321	0.0000	14.635
23.759	18.5115	-0.0001	15.518
25.097	18.4918	0.0004	16.778
26.429	18.4726	0.0013	18.272
27.754	18.4531	0.0019	19.568
		<σP/kPa> = .0010	

TABLE 27

VAPOR PRESSURE P, AND LN(P/P_{IDEAL}) FOR ($xn\text{-}C_9H_{20}+(1-x)n\text{-}C_8H_{18}$) AT 323.15 K; P = P(OBS.) - P(CALC.); LOOP VOLUME, 0.402 ML

($xn\text{-}C_9H_{20}+(1-x)n\text{-}C_8H_{18}$) [.4015 cm^3]			
X	P/kPa	σP/kPa	$\ln(P/P_R) \times 10^3$
0	6.7069	-	-
0.00170	6.6689	0.0022	1.196
0.02117	6.6313	0.0028	2.316
0.03141	6.5939	0.0029	3.346
0.04143	6.5586	0.0042	4.542
0.05122	6.5230	0.0044	5.578
0.06081	6.4878	0.0042	6.534
0.07018	6.4528	0.0035	7.392
0.07934	6.4178	0.0020	8.130
0.08831	6.3863	0.0032	9.269
0.09707	6.3516	0.0006	9.796
0.10565	6.3200	0.0003	10.688
0.11403	6.2885	-0.0005	11.477
0.12223	6.2568	-0.0023	12.102
0.13024	6.2251	-0.0047	12.607
0.13808	6.1966	-0.0046	13.509
0.14575	6.1694	-0.0038	14.513
0.15324	6.1419	-0.0039	15.362
0.16057	6.1147	-0.0043	16.144
0.16773	6.0886	-0.0043	16.992
0.17473	6.0624	-0.0048	17.732
0.18158	6.0379	-0.0043	18.630
0.18827	6.0136	-0.0041	19.469
0.19481	5.9904	-0.0034	20.383
		$\langle\sigma P/kPa\rangle$ = .0010	

TABLE 27 (CONTINUED)

$(xn\text{-}C_9H_{20}+(1-x)n\text{-}C_8H_{18})$ [.4015 cm^3]			
X	P/kPa	σP/kPa	$\ln(P/P_R) \times 10^3$
0.20121	5.9670	-0.0034	21.153
0.20746	5.9438	-0.0038	21.869
0.21357	5.9219	-0.0033	22.711
0.21955	5.9003	-0.0031	23.502
0.22539	5.8787	-0.0033	24.199
0.23109	5.8586	-0.0026	25.053
0.23667	5.8385	-0.0024	25.816
0.24212	5.8209	0.0000	26.924
0.24745	5.8137	0.0122	29.737
0.25266	5.7822	0.0002	28.285
0.25775	5.7630	0.0008	28.858
0.26272	5.7457	0.0001	29.672
0.26758	5.7270	0.0008	30.171
0.27233	5.7089	0.0016	30.681
0.27698	5.6937	0.0002	31.625
0.28151	5.6787	0.0018	32.539
0.28594	5.6633	0.0025	33.284
0.29028	5.6483	0.0034	34.048
0.29451	5.6334	0.0040	34.737
0.29864	5.6187	0.0044	35.403
0.30260	5.6043	0.0048	36.044
0.30663	5.5915	0.0064	34.901
		$\langle\sigma P/kPa\rangle$ = .0038	

TABLE 28

VAPOR PRESSURE P, AND LN(P/P_{IDEAL}) FOR ($xn\text{-}C_6H_{14}+(1-x)n\text{-}C_7H_{16}$) AT 323.15 K; P = P(OBS.) - P(CALC.); LOOP VOLUME, 0.402 ML

($xn\text{-}C_6H_{14}+(1-x)n\text{-}C_7H_{16}$)			
X	P/kPa	σP/kPa	$\ln(P/P_{IDEAL})$
0	18.8740	-	-
0.02098	19.8425	0.0636	0.01170
0.04111	20.7194	0.2150	0.01950
0.06045	21.2039	0.0025	0.00969
0.07903	21.7684	-0.1033	0.00532
0.09689	22.4372	-0.0782	0.00400
0.11405	23.0657	-0.0683	0.00790
0.13054	23.6603	-0.0685	0.00832
0.14641	24.2442	-0.0564	0.00921
0.16167	24.8095	-0.0412	0.01017
0.17635	24.3535	-0.0264	0.01106
0.19047	25.8894	0.0003	0.01236
0.20407	26.3800	0.0008	0.01261
0.21716	26.8547	0.0035	0.01293
0.22976	27.3160	0.0105	0.01338
0.24190	27.7666	0.0236	0.01403
0.25359	28.1959	0.0314	0.01447
0.26485	28.6172	0.0467	0.01516
0.27570	29.0065	0.0447	0.01522

TABLE 29

VAPOR PRESSURE P, AND LN(P/P_{IDEAL}) FOR ($xn\text{-}C_7H_{16}+(1-x)n\text{-}C_8H_{18}$) AT 323.15 K; P = P(OBS.) - P(CALC.); LOOP VOLUME, 0.062 ML

($xn\text{-}C_7H_{16}+(1-x)n\text{-}C_8H_{18}$)			
X x 10^3	P/kPa	σP/kPa	$\ln(P/P_R)$ x 10^4
0	6.7069	-	-
3.571	6.7528	0.0006	3.609
7.113	6.7990	0.0033	8.178
10.625	6.8414	0.0025	7.635
14.108	6.8838	0.0020	7.609
17.563	6.9251	0.0008	6.544
20.990	6.9662	-0.0003	5.602
24.388	7.0069	-0.0014	4.623
27.757	7.0478	-0.0019	4.474
31.103	7.0882	-0.0027	4.045
34.420	7.1287	-0.0029	4.270
37.709	7.1695	-0.0026	5.322
40.972	7.2103	-0.0019	6.811
44.209	7.2506	-0.0015	7.992
47.420	7.2895	-0.0021	7.765
50.604	7.3301	-0.0007	10.154
53.763	7.3687	-0.0009	10.406
36.897	7.4090	0.0008	13.233
60.006	7.4485	0.0020	15.367
63.090	7.4871	0.0027	16.815
66.149	7.5260	0.0040	19.018

$\langle \sigma P/kPa \rangle$ = .0022

TABLE 30

VAPOR PRESSURE P, AND LN(P/P_{IDEAL}) FOR ($xn\text{-}C_6H_{14}+(1-x)n\text{-}C_7H_{16}$) AT 323.15 K; P = P(OBS.) - P(CALC.); LOOP VOLUME, 0.062 ML

($xn\text{-}C_6H_{14}+(1-x)n\text{-}C_7H_{16}$)			
X x 10^3	P/kPa	σP/kPa	$\ln(P/P_R) \times 10^4$
0	18.8740	-	-
2.283	18.9711	0.0213	8.836
4.548	19.0402	0.0072	3.279
6.976	19.1090	-0.0066	-2.108
9.026	19.1821	-0.0153	-4.852
11.240	19.2474	-0.03158	11.377
13.432	19.3724	0.0131	13.453
15.607	19.4564	0.0173	17.265
17.765	19.5353	0.1070	18.765
19.906	19.5948	-0.0022	10.614
22.031	19.6636	-0.0114	7.561
24.140	19.7372	-0.0153	7.259
26.230	19.8326	0.0034	18.307
28.305	19.8902	-0.0152	10.516
30.363	19.9750	-0.0060	16.700
32.405	20.0596	0.0036	22.998
34.431	20.1225	-0.0079	18.789
36.439	20.2222	0.0181	33.125
38.432	20.2849	0.0075	29.348
40.410	20.3593	0.0093	31.633
42.373	20.4155	-0.0065	25.274
		$\langle\sigma P/kPa\rangle$ = .0145	

TABLE 31

VAPOR PRESSURE P, AND LN(P/P_{IDEAL}) FOR ($xn\text{-}C_7H_{16}+(1-x)n\text{-}C_8H_{18}$) AT 323.15 K; P = P(OBS.) - P(CALC.); LOOP VOLUME, 0.402 ML

($xn\text{-}C_7H_{16}+(1-x)n\text{-}C_8H_{18}$) [.4015]			
X x 10^3	P/kPa	σP/kPa	$\ln(P/P_{IDEAL})$ x 10^3
0	6.7069	0.0246	-
0.02769	7.0359	0.0186	-1.131
0.05412	7.3567	0.0053	-1.172
0.07934	7.6554	0.0015	-2.198
0.10342	7.9495	-0.0046	-1.978
0.12642	8.2279	-0.0139	-2.093
0.14840	8.4905	-0.0119	-2.590
0.16941	8.7523	-0.0115	-1.800
0.18949	9.0011	-0.0115	-1.261
0.20870	9.2387	-0.0108	-0.809
0.22707	9.4667	-0.0110	-0.322
0.24465	9.6840	-0.0068	0.037
0.26148	9.8963	-0.0090	0.798
0.27759	10.0933	-0.0040	0.889
0.29301	10.2888	-0.0038	1.632
0.30778	10.4719	-0.0001	1.937
0.32192	10.6506	0.0055	2.518
0.33548	10.8239	0.0048	3.258
0.34846	10.9839	0.0055	3.391
0.36091	11.1386	0.0046	3.634
0.37284	11.2852	0.0045	3.721
0.38427	11.4265	0.0048	3.866
0.39524	11.5625	0.0082	4.044
0.40575	11.6958	0.0081	4.462
0.41587	11.8238	0.0114	4.865
		$\langle\sigma P/kPa\rangle$ = .0103	

TABLE 32

VAPOR PRESSURE P, AND LN(P/P_{IDEAL}) FOR ($xn\text{-}C_7H_{16}+(1-x)n\text{-}C_8H_{18}$) AT 303.15 K; P = P(OBS.) - P(CALC.); LOOP VOLUME, 0.062 ML

($xn\text{-}C_7H_{16}+(1-x)n\text{-}C_8H_{18}$) [303.15 K]					
X x 100	P/kPa	σP/kPa	X x 100	P/kPa	σP/kPa
0	2.4554	-	0	2.4554	-
2.413	2.5234	-0.0091	2.480	2.5183	-0.0366
4.816	2.5461	0.0004	4.946	2.5585	-0.0118
7.206	2.5595	0.0007	7.398	2.5796	-0.0059
9.584	2.5767	0.0047	9.837	2.6079	0.0071
11.950	2.5844	-0.0006	12.263	2.6271	0.0115
14.303	2.6016	0.0037	14.676	2.6437	0.0127
16.644	2.6107	-0.0001	17.076	2.6597	0.0137
18.973	2.6240	0.0004	19.464	2.6727	0.0118
21.290	2.6364	0.0000	21.839	2.6860	0.0103
23.595	2.6497	0.0006	24.202	2.6991	0.0086
25.888	2.6622	0.0006	26.553	2.7109	0.0058
28.169	2.6747	0.0005	28.891	2.7240	0.0042
30.439	2.6872	0.0005	31.218	2.7361	0.0018
32.697	2.6996	0.0004	33.532	2.7485	-0.0002
34.943	2.7122	0.0007	35.834	2.7618	0.0013
34.177	2.7243	0.0005	38.124	2.7745	0.0029
39.400	2.7363	0.0003	40.403	2.7868	0.0048
41.611	2.7483	0.0001	42.660	2.7993	0.0065
43.812	2.7603	0.0000	44.925	2.8115	0.0083
46.000	2.7714	-0.0010	47.168	2.8250	0.0089
48.178	2.7830	-0.0014			
50.345	2.7943	-0.0020			
	<σP/kPa> = .0025			<σP/kPa> = .0121	

TABLE 33

SUMMARY OF HENRY'S LAW CONSTANTS AND LOGARITHMS OF LIMITING ACTIVITY COEFFICIENTS

X_2	$(1-X_2)$	K_H/kPa	P_2^o	$\ln\gamma_2^o$
		(323.15 K)		
C_6H_{14}	C_5H_{12}	35.5856 ± .2554	54.0363	-0.4177
C_7H_{16}	C_6H_{14}	16.1004 ± .0432	18.8740	-0.1589
C_8H_{18}	C_7H_{16}	7.1898 ± .0321	6.7069	-0.0695
C_8H_{18}	C_7H_{16}	6.7558 ± 1642	6.7069	-0.0073
C_8H_{18}	C_7H_{16}	6.4110 ± .0123	6.7069	-0.0451
C_9H_{20}	C_7H_{16}	3.7340 ± .0280	2.4087	0.4384
C_9H_{18}	C_8H_{18}	3.0989 ± .0109	2.4087	0.2520
C_9H_{18}	C_8H_{18}	3.0509 ± .0054	2.4087	0.2365
C_6H_{14}	C_7H_{16}	55.5885 ± .2597	54.0363	0.0283
C_6H_{14}	C_7H_{16}	55.0730 ± .0418	54.0363	0.0190
C_7H_{16}	C_8H_{18}	19.0104 ± .0254	18.8740	0.0072
C_7H_{16}	C_8H_{18}	19.0383 ± .0138	18.8740	0.0087
		(303.15 K)		
C_7H_{16}	C_8H_{18}	8.0233 ± .0364	7.7776	0.0311

$$g/x_1x_2 = A_{21}x_1 + A_{12}x_2 \qquad 60$$

$$\ln \gamma_1 = x_2^2[A_{12} + 2(A_{21}-A_{12})x_1] \qquad 61$$

$$\ln \gamma_2 = x_1^2[A_{21} + 2(A_{12}-A_{21})x_2], \qquad 62$$

where the parameters A_{12} and A_{21} are the logarithms of the activities at infinite dilution of the solvent and solute respectively. The activities at infinite dilution obtained with the two parameter Margules equation and those obtained with the pressure fit, equation 59, agreed to better that ±0.01 kPa, the same precision as was obtained with the other methods of data reduction. As shown in Tables 34 through 37, the excess free energies, G^E, were determined to a precision of ±0.1 J mol^{-1}. Although the data was precisely analyzed, there were no literature values with which to directly test the accuracy. The implications of the VLE measurements and the excess volume measurements will be discussed in detail in the following section.

TABLE 34

VAPOR PRESSURE P, AND EXCESS GIBBS FREE ENERGY G^E FOR
$(xn\text{-}C_6H_{14}+(1-x)n\text{-}C_7H_{16})$ AT 323.15 K;
P = P(OBS.) - P(CALC.),
LOOP VOLUME, 0.402 ML

$(xn\text{-}C_6H_{14}+(1-x)n\text{-}C_7H_{16})$ [.4015 ml]			
X	P/kPa	σP/kPa	G^E/J mol^{-1}
0	18.8740	-	-
0.02098	19.8425	0.1821	0.0489
0.04111	20.7194	0.3078	0.1802
0.06045	21.2039	0.0732	0.3745
0.07903	21.7684	-0.0587	0.6157
0.09689	22.4372	-0.0413	0.8906
0.11405	23.0657	-0.0443	1.1886
0.13054	23.6603	-0.0550	1.5017
0.14641	24.2442	-0.0513	1.8214
0.16167	24.8095	-0.0427	2.1438
0.17635	25.3535	-0.0329	2.4641
0.19047	25.8894	-0.0096	2.7790
0.20407	26.3800	-0.0114	3.0857
0.21716	26.3847	-0.0097	3.3826
0.22976	27.3160	-0.0029	3.6680
0.24190	27.7666	0.0109	3.9411
0.25359	28.2959	0.0202	4.2013
0.26485	28.6172	0.0376	4.4480
0.27570	29.0065	0.0384	4.6814

$\langle \sigma P/kPa \rangle$ = .0974

TABLE 35

VAPOR PRESSURE P, AND EXCESS GIBBS FREE ENERGY G^E FOR
$(xn\text{-}C_7H_{16}+(1-x)n\text{-}C_8H_{18})$ AT 323.15 K;
P = P(OBS.) - P(CALC.),
LOOP VOLUME, 0.402 ML

$(xn\text{-}C_7H_{16}+(1-x)n\text{-}C_8H_{18})$ [.4015]			
X	P/kPa	σP/kPa	G^E/J mol^{-1}
0	6.7069	-	-
0.02769	7.0359	0.0019	-0.0411
0.05412	7.3567	0.0074	-0.1369
0.07934	7.6554	0.0025	-0.2564
0.10342	7.9495	0.0045	-0.3789
0.12642	8.2279	0.0022	-0.4910
0.14840	8.4905	-0.0046	-0.5847
0.16941	8.7523	-0.0015	-0.6559
0.18949	9.0011	-0.0009	-0.7028
0.20870	9.2387	-0.0012	-0.7258
0.22707	9.4667	-0.0014	-0.7259
0.24465	9.6840	-0.0028	-0.7052
0.26148	9.8963	-0.0001	-0.6660
0.27759	10.0933	-0.0038	-0.6108
0.29301	10.2888	-0.0007	-0.5421
0.30778	10.4719	-0.0018	-0.4622
0.32192	10.6506	0.0003	-0.3734
0.33548	10.8239	0.0045	-0.2778
0.34846	10.9839	0.0024	-0.1771
0.36091	11.1386	0.0018	-0.0730
0.37284	11.2852	-0.0003	0.0331
0.38427	11.4265	-0.0015	0.1401
0.39524	11.5625	-0.0020	0.2468
0.40575	11.6958	0.0004	0.3525
0.41584	11.8238	0.0030	0.4565

$\langle P/kPa \rangle$ = .0029

TABLE 36

VAPOR PRESSURE P, AND EXCESS GIBBS FREE ENERGY G^E FOR
($xn\text{-}C_8H_{18}+(1-x)n\text{-}C_7H_{16}$) AT 323.15 K;
P = P(OBS.) - P(CALC.),
LOOP VOLUME, 0.402 ML

($xn\text{-}C_8H_{18}+(1-x)n\text{-}C_7H_{16}$)			
X	P/kPa	σP/kPa	$-G^E$/J mol^{-1}
0	18.8740	-	-
0.01777	18.6581	0.0061	0.0275
0.03490	18.4495	0.0099	0.1128
0.05141	18.2304	0.0061	0.2571
0.06731	18.0506	0.0054	0.4595
0.08264	17.8613	0.0040	0.7167
0.09741	17.6781	0.0036	0.0246
0.11164	17.5024	0.0015	1.3779
0.12535	17.3312	0.0017	1.7713
0.13856	17.1683	-0.0001	2.1992
0.15129	17.0091	-0.0012	2.6560
0.16354	16.8561	-0.0013	3.1365
0.17535	16.7094	-0.0027	3.6355
0.18672	16.5665	-0.0016	4.1484
0.19767	16.4310	-0.0008	4.6709
0.20822	16.3001	-0.0019	5.1993
0.21837	16.1719	-0.0010	5.7299
0.22815	16.0500	-0.0016	6.2598
0.23756	15.9311	-0.0002	6.7863
0.24663	15.8183	-0.0001	7.3070
0.25535	15.7082	0.0003	7.8200
0.26375	15.6023	0.0007	8.3236
0.27183	15.5002	0.0007	8.8165
0.27961	15.4013	0.0005	9.2975
0.28710	15.3058	0.0004	9.7656
0.29430	15.2141	0.0005	10.2202
0.30123	15.1250	-0.0001	10.6608
0.30790	15.0397	-0.0001	11.0840
0.31432	14.9597	0.0020	11.4985
0.32048	14.8770	-0.0014	11.8954

$\langle P/kPa \rangle$ = .0032

TABLE 37

VAPOR PRESSURE P, AND EXCESS GIBBS FREE ENERGY G^E FOR
$(xn\text{-}C_9H_{20}+(1-x)n\text{-}C_8H_{18})$ AT 323.15 K;
P = P(OBS.) - P(CALC.),
LOOP VOLUME, 0.402 ML

$(xn\text{-}C_9H_{20}+(1-x)n\text{-}C_8H_{18})$ [0.4015]			
X	P/kPa	σP/kPa	G^E/J mol^{-1}
0	6.7069	-	-
0.0107	6.6689	0.0015	0.0678
0.02117	6.6313	0.0016	0.2624
0.03141	6.5939	0.0031	0.5716
0.04143	6.5586	0.0048	0.9836
0.05122	6.5230	0.0054	1.4876
0.06081	6.4878	0.0055	2.0734
0.07018	6.4528	0.0051	2.7316
0.07934	6.4178	0.0039	3.4535
0.08831	6.3863	0.0053	4.2309
0.09707	6.3516	0.0029	5.0563
0.10565	6.3200	0.0028	5.9230
0.11403	6.2885	0.0021	6.8244
0.12223	6.2568	0.0004	7.7547
0.13024	6.2251	-0.0020	8.7086
0.13808	6.1966	-0.0018	9.6812
0.14574	6.1694	-0.0010	10.6681
0.15324	6.1419	-0.0011	11.6652
0.16057	6.1147	-0.0016	12.6688
0.16773	6.0886	-0.0016	13.6756
0.17473	6.0624	-0.0023	14.6826
0.18158	6.0379	-0.0019	15.6871
0.18827	5.0136	-0.0019	16.6867
0.19481	5.9904	-0.0013	17.6792

TABLE 37 (CONTINUED)

$(xn\text{-}C_9H_{20}+(1-x)n\text{-}C_8H_{18})$ [0.4015]			
X	P/kPa	σP/kPa	G^E/J mol^{-1}
0.20121	5.9670	-0.0016	18.6627
0.20746	5.9438	-0.0021	19.6355
0.21357	5.9219	-0.0019	20.5962
0.21955	5.9003	-0.0018	21.5434
0.22539	5.8787	-0.0023	22.4761
0.23109	5.8586	-0.0019	23.3932
0.22667	5.8385	-0.0018	24.2939
0.24212	5.7822	0.0002	25.1775
0.24745	5.7630	0.0122	26.0436
0.25266	5.7457	-0.0005	26.8915
0.25775	5.7270	-0.0014	27.7210
0.26272	5.7089	-0.0008	28.5317
0.26758	5.6937	-0.0020	29.3236
0.27233	5.6787	-0.0031	30.0964
0.27698	5.6633	-0.0016	30.8501
0.28151	5.6483	-0.0002	31.5848
0.28594	5.6334	0.0002	32.3005
0.29028	5.6187	0.0008	32.9973
0.29451	5.6483	0.0011	33.6754
0.29864	5.6334	0.0012	34.3349
0.30268	5.6043	0.0013	34.9761
0.30663	5.5915	0.0025	35.5993

CHAPTER IV

DISCUSSION

A survey of the recent literature on the thermodynamics of n-hydrocarbons and their binary mixtures, shows that the experimental investigations have largely become tools for testing the various theoretical developments now in vogue. The choices of the systems to be investigated and the properties to be measured have been biased by the assumption that the fundamental thermodynamic behavior of the n-hydrocarbons had been satisfactorily established. Thus, systems which exhibit the largest and consequently, the more easily measured thermodynamic effects, have received the greatest scrutiny with an almost total exclusion of those systems which have been unintentionally deemed, experimentally "unenlightening". The development of innovative instrumentation and experimental techniques, by which the thermodynamics of these substances might be explored extensivitively has almost reached a standstill. Not since the development of Brønsted's "Concept of Congruence",[1] has there been any attempt to correlate and phenomenologically explain the existing thermodynamic data. These facts are most unfortunate, for complete understanding of the thermodynamics of n-hydrocarbons is extremely important to the field of solution thermodynamics and to solution chemistry as a whole. Analysis of our data presented in the preceding chapter and discussed below has revealed several interesting experimental observations which we feel provide new insights into the thermodynamic behavior of n-hydrocarbons and which we hope will stimulate new theoretical investigations.

Contrary to the established notions,[77-82] it was observed that the excess volume curves, $\partial V^E/\partial x$, for the measured binary n-hydrocarbon systems, were not parabolic,[15] but in fact, S-shaped, albeit highly skewed. The excess volumes were positive at low concentrations of the shorter components. Furthermore, it was found that our V^E data and the available literature data[61-63,77,78] for all binary systems at 0.5 mole fraction and 298.15 K, i.e., near the maxima, could be correlated with a simple function containing only the respective pure substance molar volumes, V_1^0 and V_2^0, and the carbon numbers, n_1 and n_2. The continuous dilution vapor pressure apparatus provided the means for the direct determination of limiting activity coefficients, γ°, for binary systems never before measured. As was the case with the excess volumes, we were able to correlate the literature values of γ° for n-hydrocarbon mixtures[27,40,63,83,84] and the γ°'s obtained in this investigation by assuming the limiting activity coefficients to be a function of the solute and solvent carbon numbers and the temperature. However, two completely different correlation curves were obtained, depending upon whether the solute was the shorter or longer component.

The following discussion will not be centered on the individual thermodynamic measurements. Instead, it will be based on the trends we have observed experimentally, and, where applicable, in conjunction with the available literature data.

A. POSITIVE V^E IN N-ALKANE SYSTEMS

Experimentally, the excess volumes of binary n-hydrocarbon mixtures had, until now, been found to be negative over the entire concentration range, with the V^E versus x curves skewed toward high concentrations of the shorter component.[61-63,77-82] The literature measurements had been made over the entire concentration range at various convenient concentrations, and the resulting V^E curves extrapolated to zero concentration. The results obtained from our measurements were consistent with the general features of the literature findings, with one very important exception. Our results, (for example, see Figure 11, p 53), show that, at least for the systems measured at 298.15 K, binary n-hydrocarbon mixtures do not form totally regular solutions. The excess volumes are positive at low concentrations of the shorter component, a finding which is totally new to the volumetric properties of binary mixtures of n-alkanes. These observations will have profound implication on the theoretical reasoning now applied to the solution thermodynamics of binary n-alkane mixtures. The simple solute-solvent interactions which have dominated the theories of n-hydrocarbon mixtures will undoubtedly require reformulation.

S-shaped V^E curves have been found for other systems,[85-88] i.e., p-dioxane + n-C_5 or 2-methylbutane and cycloheptane + n-C_7. The rationale used to explain this phenomenon can be expanded to possibly explain the S-shaped V^E curves observed for the binary n-alkane mixtures in question. Theoretically, the excess volume is assumed to originate from the energetic effect associated with the replacement of (1-1) and (2-2) contacts by (1-2) contacts.[89]

According to the Prigogine-Flory theories,[21,90] there is also a contribution resulting from the volume changes occuring during the mixing of liquids of different degrees of thermal expansion or free volume, X_{12}. A third effect, employed by Patterson and co-workers[46,88] considers the reduced pressure, P*, contribution to the excess volume. P* is related to the thermal pressure coefficient (γ) or internal pressure (γT) through the relation,

$$P^* = (\gamma T)\tilde{V}^2 \qquad 63$$

where tilde refers to the reduced quantity. Using expressions from the Flory model,[90] Patterson[88] defined the three contributions to the excess volume as,

$$V^E/x_1V_1^* + x_2V_2^* = (\tilde{V}^{1/3}-1)\tilde{V}^{2/3}/(4/3\tilde{V}^{-1/3}-1)\cdot\Psi_1\theta_2X_{12}/P_1^* \quad \text{(interactional)}$$

$$-(\tilde{V}_1-\tilde{V}_2)^2(14/9\tilde{V}^{1/3}-1)/4/3\tilde{V}^{1/3}-1)\tilde{V}\cdot\Psi_1\Psi_2(\tilde{V}\text{ curvature})$$

$$+(\tilde{V}_1-\tilde{V}_2)(P_1^*-P_2^*)/(P_2^*\Psi_1 + P_1^*\Psi_2)\cdot\Psi_1\Psi_2(P^*\text{ effect}) \qquad 64$$

where θ are the surface fraction and Ψ are contact-energy fractions. It is this P* contribution that Patterson and coworkers[88] used to qualitatively explain their S-shaped V^E curves for mixtures of hexane isomers, and that we will expand to our systems.

The P* contribution may be positive or negative, depending on the difference of the thermal pressure coefficients or internal pressures of the components. The P* term often dominates V^E, particularly when one component is of higher internal pressure and lower thermal expansion coefficient that the other, leading to negative V^E values.

Patterson and Costas[88] performed experiments where component 1, e.g., cyclopentane, cyclohexane, or benzene, had a higher value of P* than component 2, an n-alkane. They found that typically, V^E was positive and large for alkanes of large n, but as n decreased, V^E became negative passing through zero as a S-shaped curve against composition. They attributed this to an effect of the P* contribution. For all systems, $P_1^* > P_2^*$ and $\tilde{V}_1 > V_2^*$ for large n, leading to a positive P* contribution in V^E, while $\tilde{V}_1 < \tilde{V}_2$ for small n, leading to a negative P* contribution and negative V^E. This approach was also used to interpret the magnitudes and concentration dependence of V^E for components of high P* with hexane and lower alkane isomers and in systems involving branched alkane isomers. They concluded that the effect of alkane branching on V^E was due to the decrease of P* of the alkane and consequently, the increase of the negative P* term. They further rationalized that the S-shaped V^E (x) curves could have also arose from the slightly different composition dependencies of the negative P* and positive X_{12} terms, both of which are large.

Corresponding states theories, such as that of Flory,[4] predict generally that if the excess volume becomes zero at any composition, it will have a S-shaped composition dependence, with the negative V^E values lying at high concentration of the component having the larger P* parameter. Patterson and coworkers[87] derived the expression,

$$1/V_2^* \left(\frac{dV^E}{dx_2}\right)_{x_2=0} = \frac{V_2^\infty - V_2^o}{V_2^*}$$

$$= X_{12}/P_1^* \; S_2/S_1 \tilde{\alpha}\tilde{V}_1\tilde{T}_1 + (\tilde{V}_1-\tilde{V}_2)-(\tilde{T}_1-\tilde{T}_2)\tilde{\alpha}_1\tilde{V}_1(P_2^*/P_1^*) \qquad 65$$

for the slope dV^E/dx_2 at $x_2 = 0$; the volume change on mixing component 2 at infinite dilution in component. S_1 and S_2 are the surface/volume ratios of components 1 and 2, respectively. Thus, by expanding $\tilde{V}_2$ around $\tilde{V}_1$ and choosing a value of X_{12} so that the slope dV^E/dx_2 is zero at $x_2 = 0$, they arrived at the expression, for the slope dV^E/dx_1, at $x_2 = 1$

$$1/V_1^*\left(\frac{dV^E}{dx_1}\right)_{x_2=1} = \frac{\bar{V}_1^\infty - V_1^o}{V_1^*} = \tilde{\alpha}_2\tilde{V}_2\,\frac{(\tilde{T}_2-\tilde{T}_1)}{\tilde{T}_1}\,\frac{P_1^*-P_2^*}{P_2^*} \qquad 66$$

From the mathematical development it follows, that V^E is negative for $P_2^* > P_1^*$. Similarly, if dV^E/dx_1 is put equal to zero at $x_2 = 1$, then dV^E/dx_2 at $x_2 = 0$ is positive for $P_2^* > P_1^*$. Thus V^E must have an S-shaped composition dependence with the negative part at high concentration of the component having the higher P^*.

To test the applicability of this approach to the V^E measurements of this work, consider the n-C_8 +n-C_{10} system at 298.15 K. Since the substances are different by only two methylene units, the internal energies per carbon are of almost the same magnitude, and as depicted by the small V^E values, the volume changes occuring during mixing are small. It is therefore logical to attribute the bulk of the volumetric effects on the excess volume to the P* contribution. The internal pressures of octane(1) and decane(2) are 439 and 448 J/cm^3 respectively; $P_2^* > P_1^*$.[6,32] Thus, if the approach described above is utilized, an S-shaped composition dependence with the negative part at high concentration of n-C_8, the component having the higher P*, is predicted. Experimentally, in accordance with the formulism, S-shaped

composition dependences were observed for the n-C_8 + n-C_{10}, n-C_9 + n-C_{10}, n-C_9 + n-C_{11} and n-C_9 + n-C_{13} systems at 298.15 K, with negative excess volumes at concentrations greater than 0.07 mole fraction.

The P* contribution provides a general theoretical explanation for the S-shaped composition dependences for the binary n-alkane systems measured in this investigation. However, it does not predict the magnitude of the excess volumes or quantitatively explain the experimental observations. A careful examination of the available V^E data for binary n-alkane and various other systems will also allow a purely intuitive prediction of S-shaped V^E curves. If one first considers systems which have more or less symmetric S-shaped V curves[86] and goes to systems which exhibit more unsymmetrical V^E curves,[88] it is readily obvious that as the components become closer in size, the area under the curve which is negative, increases. It is therefore logical to conclude that in binary n-hydrocarbon systems, where the V^E curves are skewed toward the longer component, there should exist a finite area where the excess volumes are positive, although small when compared to the total V^E curve.

The possible reasons why, until now, this V^E effect has not been observed in binary n-hydrocarbon mixtures are two-fold. As will be shown in the following section, the main features of the volumetric properties of n-hydrocarbon mixtures are thermodynamically consistent between laboratories, and thus such an effect was unlooked for. Second, and more importantly, the measurements in this work were performed on systems where the components were separated by only one or two methylene units, with special emphasis paid to end effects. The

question whether this effect is unique to the systems measured, or is a general feature of binary n-alkane mixtures, dictates that more extensive V^E measurements be performed.

B. CORRELATIONS WITH CARBON NUMBER

As described in Chapter I, the goal of the various theoretical developments on n-alkane solution thermodynamics, is to predict the equilibrium properties of the mixtures. Furthermore, any comprehensive theory should relate the properties of the mixtures to the properties of the pure constituents themselves.[82] The logical experimental extension of this ideal would be to establish what fundamental relationships exist between the physical characteristics of the components and the measured thermodynamic properties. Using the results obtained in this work and the corresponding literature data for the excess volumes at equal mole fraction, and limiting activity coefficients for binary n-alkane mixtures, we were able to correlate the properties with the carbon numbers of the mixture components. A correlation between the component carbon numbers and the limiting partial molar volumes was not made because the slopes of the excess volume curves for the low concentration measurements were not defined well enough to allow determination. Thus, the correlations will be discussed separately.

A plot of V^E at 0.5 mole fraction versus the difference in the component carbon numbers, $n_{Shorter} - n_{Longer}$, at 298.15 K was presented in Chapter III, Figure 12, p 56, in order to compare our values to those of the literature.[61-63,77-82] The slopes of the resulting lines, for solutes 6, 7, etc., decreased with increasing

solute carbon number. By correlating the excess volumes at 0.50 mole fraction and the logarithm of the ratios of the carbon numbers and pure component molar volume, $\ln(V_s^o/n_s \cdot n_L/V_L^o)$, we were able to reduce all the available data to a single curve, Figure 22. Notice that the correlation is of the type desired; a property of the mixture is related directly to the properties of its pure components. $(V_s^o/n_s \cdot n_L/V_L)$ is actually the pure component molar volume per carbon number of the shorter component divided by the molar volume per carbon number of the longer component. Since a plot of the logarithm of pure n-alkane molar volumes per carbon versus 1/n results in a straight line, Figure 6, p 45, the fact, that V^E of all the binary systems at 298.15 K and 0.5 mole fraction can be expressed simply as a function of the pure component molar volumes per carbon number, is particularly interesting. Without invoking any theoretical assumptions, it may be concluded, that for equal molar concentrations, the excess volume of n-alkane mixtures is an explicit functions of the molar volumes per carbon number of the pure components. This conclusion is fortunately in exact agreement wiuth the conclusion of the most recent theoretical developments on the volumetric properties of liquid pure n-alkanes and their binary mixtures.[81-82]

Attempts at correlating the limiting activity coefficients, those obtained in our measurements and those available from the literature, with the component carbon numbers and temperature revealed a totally unexpected phenomenon. Two distinctly different correlations exist; the correlation depending upon whether the solute was the shorter or longer component. Based on our data it may be concluded that at

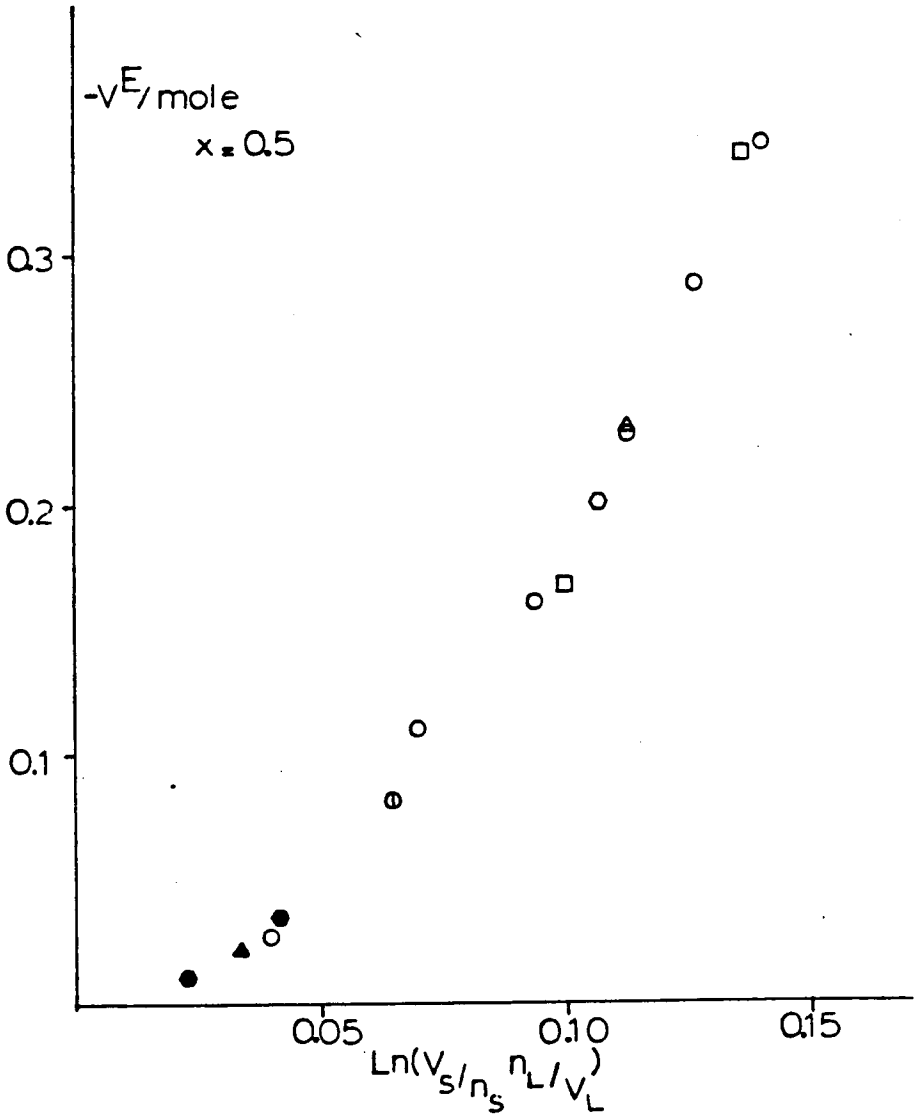

Figure 22. Correlation curve for V^E (0.50 mole fraction) as a function of the logarithm of the carbon numbers and pure component molar volumes. O-(References 48, 72); []-References 7, 64); ⬡ -(Reference 63); Δ and ◐-(Reference 7). Filled shapes, this work.

infinite dilution, depending upon the relative length of the solvent and solute, there exist two totally different solute-solvent interactions in binary n-alkane systems.

The literature limiting activity coefficients were obtained from g.l.c. measurements.[27,40,63,84,91] Thus previously, only values for systems where the solvent was much longer than the solute were available. However, the continuous dilution vapor pressure apparatus developed in this laboratory, allowed us to determine limiting activity coefficients not only for systems where the solute was shorter than the solvent by only one or two methylene units, but also for systems where the converse was true. Using only ln γ° values for shorter into longer, a plot of RTln γ° versus $\ln(n_S/n_L)/T(K)$, Figure 23, shows that, within experimental error, the data can be reduced to a single curve. The ratio of carbon numbers was divided by the temperature so that the limiting activity coefficients at the different temperatures could be represented on the same plot. The currently expressed belief that all limiting activity coefficients for binary n-alkane systems are negative,[10] is obviously incorrect. The correlation curve, Figure 23, clearly predicts the existence of positive ln γ°'s, and our data for the n-C_6 + n-C_7 and n-C_7 + n-C_8 systems confirm this prediction.

The limiting activity coefficient data, for the systems where the solute chain length was greater than that of the solvent, do not fit into the correlation described above. This is perplexing. All of the VLE measurements made in this work were performed with the same meticulous care, and the data for the systems where the solute was the longer component were, as explained in Chapter III, the more precise, Figure

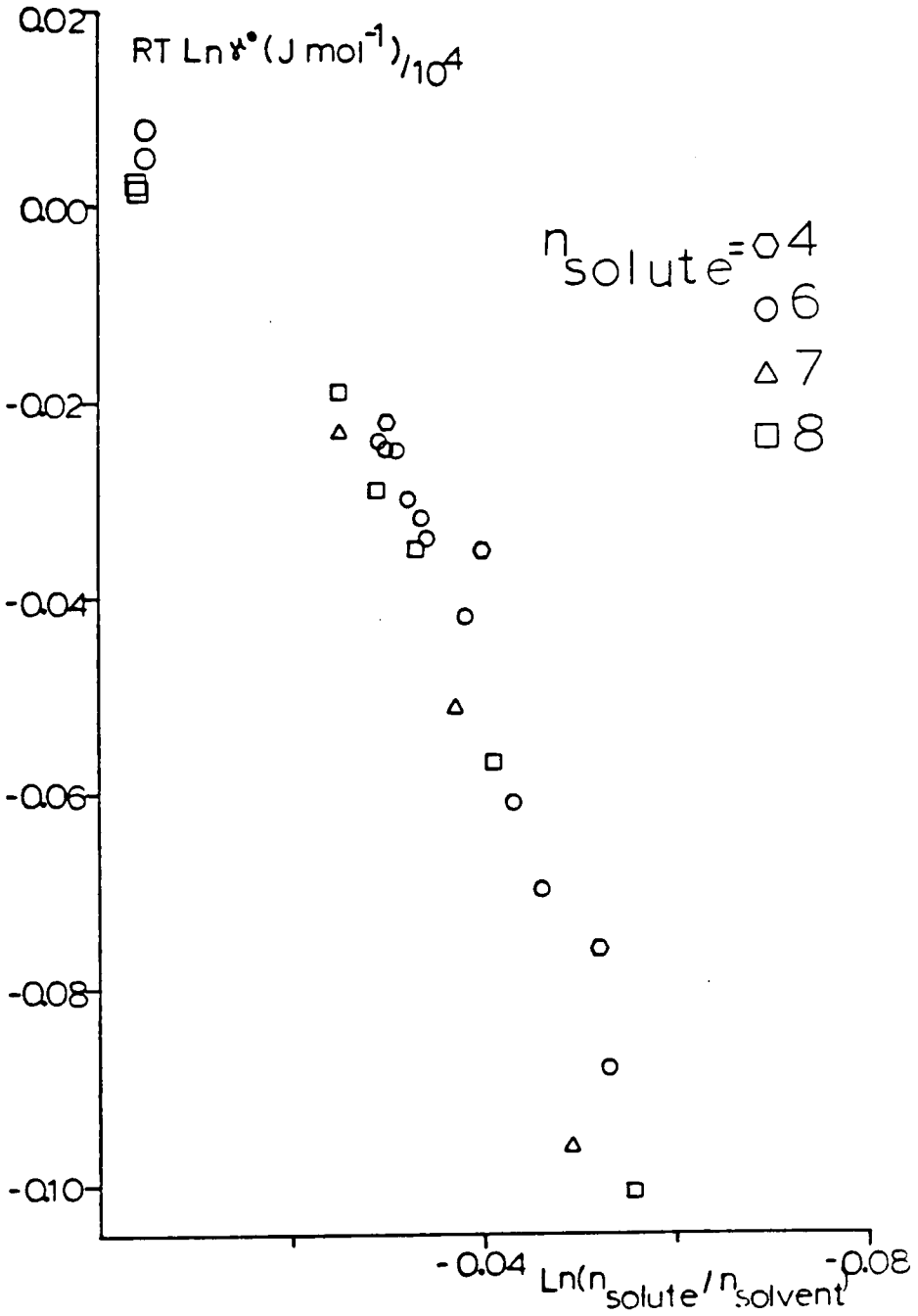

Figure 23. Correlation curve for RT ln γ° for shorter into longer component as a function of the carbon numbers and temperature. ⬡, 0, Δ and [] literature values, References 27, 40 and 63. Larger shapes, this work.

21, p 86. Even though there exist no literature data with which to compare our longer into shorter component ln γ°'s, the shorter into longer data compare favorably with other workers. Thus there was no reason for believing the data to be incorrect. A plot of ln γ° /Δn versus the solute carbon number for the longer into shorter component ln γ° data, readily reduced to a straight line, Figure 24. However, if all the available limiting activity coefficient data are divided by the temperature and Δn, ln γ°/ΔnT(K), and are plotted against the solute carbon number, the discontinuity between the longer into shorter and shorter into longer correlation curves is immediately evident, Figure 25.

In a previous analysis of ln γ° data,[10] it was noted theoretically, that there exist two contributions to the activity coefficients for lower n-alkanes at infinite dilution in higher n-alkanes; the configurational and non-combinatorial terms. The configurational contribution to ln γ°, which is associated with the difference of molecular sizes of the components, is negative, whereas the non-combinatorial terms is positive. The quasi-lattice theory,[89,92] extended by Cruickshank and collaborators,[27] gives an "interactional interpretation to the non-combinatorial term, associating it with a difference in force fields around the methyl ends and methylene interior segments of the chains. For our data the configuration contribution to ln γ° would be decreased and the interactional term's influence increased, relative to the magnitudes of the contributions present in the systems with large Δn values. It should be remembered that the limiting activity coefficients we obtained were for systems

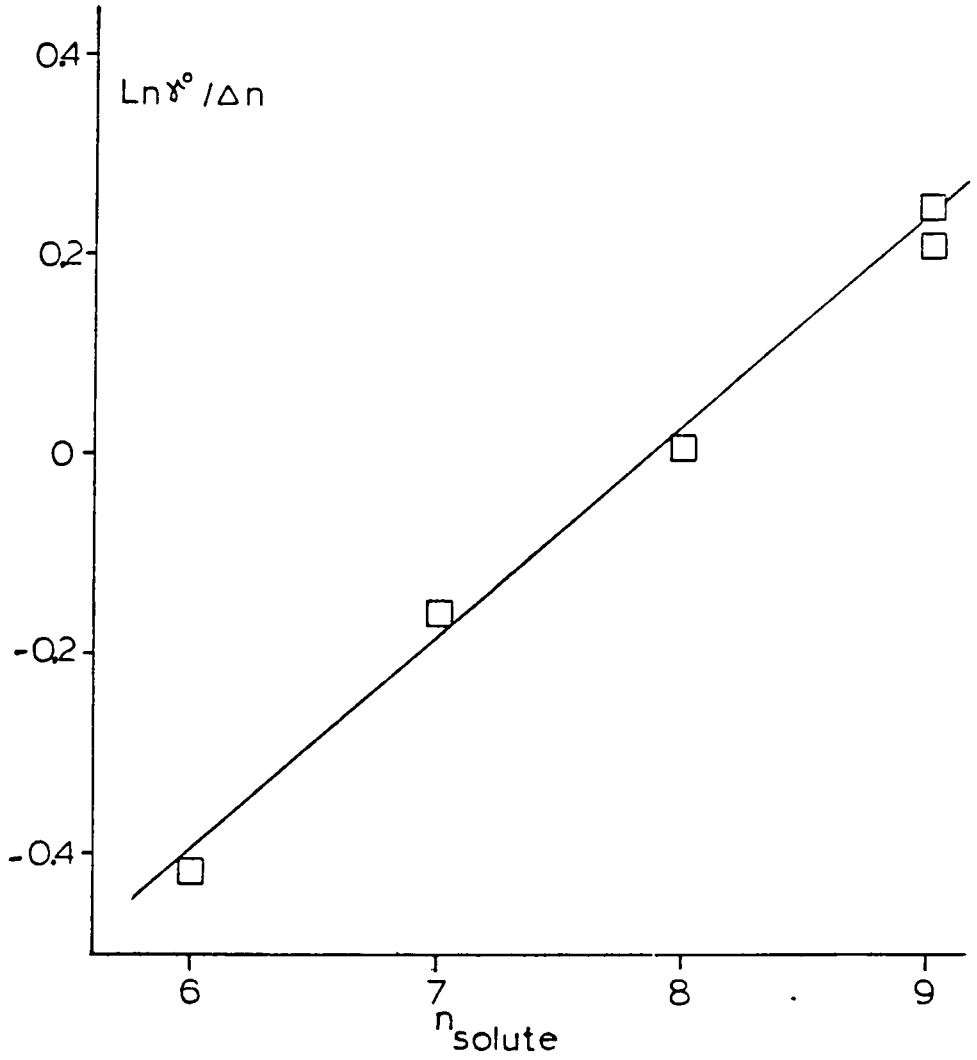

Figure 24. Correlation curve for ln $\gamma^\circ/\Delta n$ for longer into shorter component as a function of the carbon number.

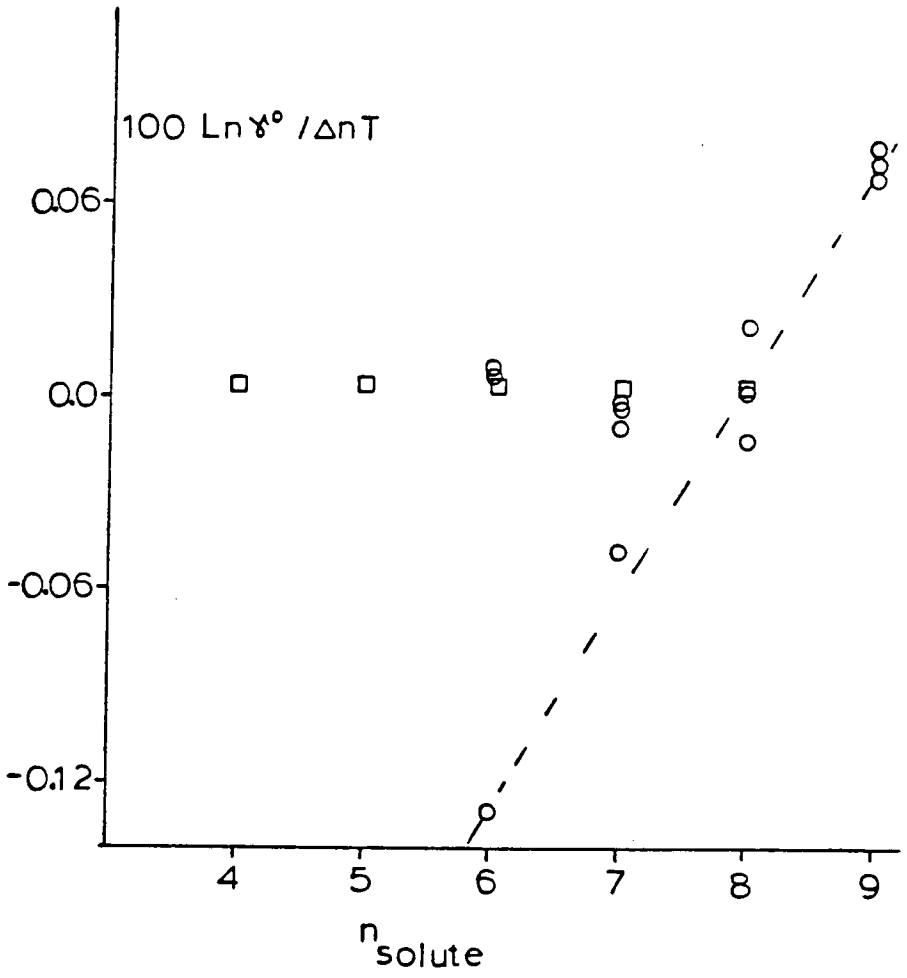

Figure 25. Correlation curves for all available ln γ° data as a function of carbon number. []-literature values, References 27, 40 and 63. O, this work.

that were separated by, at most, only two methylene units. Thus, the differences in segment force fields, i.e. n-C_8 or the reverse situation, are small. It was therefore decided that a simple interactional lattice calculation might provide some insight into the observations.

For an n-alkane at infinite dilution in another n-alkane, there will be three distinct contact interactions; end-end, EE, middle-end, ME, and middle-middle, MM. If j and n are the number of carbon atoms of the solute and solvent respectively, and c the coordination number, the external interaction may be expressed as

$$I_{EXT} + [4(c-1)/n]EE + [(2(c-1)(n-2) + 2(j-2)(c-2))/n]EM + [(j-2)(n-2)/n]MM \qquad 67$$

The formal derivation is presented in Appendix 2. Calculations for the coefficients of EE, EM, and MM were performed for coordination numbers 6, 10, and 14; solutes 6, 8, and 10; and solvents 5 through 16. As shown in Figure 26, this simple lattice calculation failed to explain the experimental observations. However, this result was not wholly unexpected. More sophisticated lattice calculations on the excess chemical potentials for mixtures of dissimilar n-hydrocarbons,[16,24,38,92,93] where entropy effects had been taken into consideration had also proved to be inadequate.

A quantitative explanation of the experimental observations may require more than a more sophisticated version of the existing theories[94-96] but possibly a totally new view of the limiting activity coefficients and the other thermodynamic properties for binary n-alkane mixtures. Also, as exemplified in the following section, new

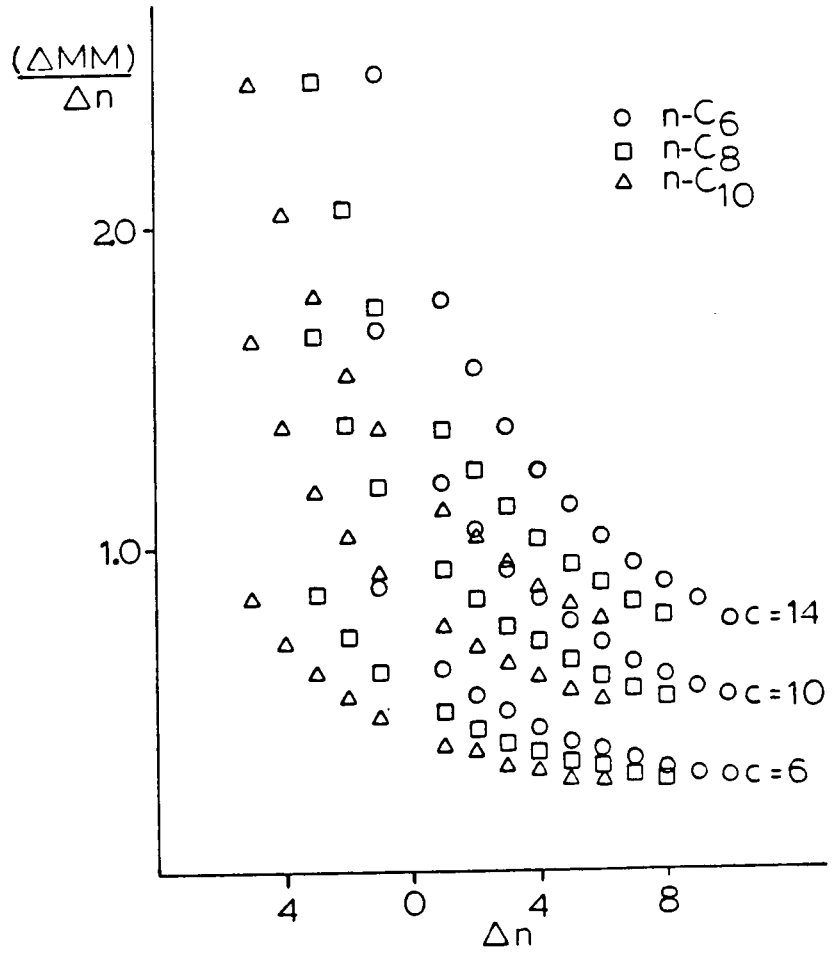

Figure 26. Plots of Δ(MM)/Δn versus Δn for the simple lattice calculation.

experimental investigations, unencumbered by an expectation of what should happen theoretically, must be implemented.

C. CONCLUSION

For the binary n-hydrocarbon systems studied in this investigation, we observed that; at low concentration of the shorter component ($x < 0.07$), the excess volume is positive; positive limiting activity coefficients, γ°, exist for certain systems; and the behavior of $\ln \gamma^\circ$ is governed by whether the longer or shorter component is approaching infinite dilution. Furthermore, the excess volumes and the limiting activity coefficients for all the available data may be represented as simple functions of the carbon numbers. Although some of our findings may be contrary to certain theoretical conjectures; experimentally, they are simply new and are not, as shown in Figures 22 through 25, contradictory.

As alluded to throughout this work, quantitatively understanding the thermodynamics of n-alkanes and their mixtures is of importance to the field of solution chemistry. It is hoped that the observations made in this work have added to that understanding and will generate new experimental investigations.

LIST OF REFERENCES

LIST OF REFERENCES

1. J. N. Brϕnsted and J. Koefoed, Kgl. Danske. Videnskab. Selskab, Mat. Phys. Medd. 22, 1, (1946).

2. K. S. Pitzer, J. Chem. Phys., 7, 583 (1939).

3. E. A. Guggenheim, J. Chem. Phys., 13, 253 (1945).

4. P. J. Flory, R. A. Orwoll and A. Vrij, J. Am. Chem. Soc., 86, 3507 (1964).

5. P. J. Flory, R. A. Orwoll and A. Vrij, J. Am. Chem. Soc., 86, 3515 (1964).

6. P. J. Flory and R. A. Orwoll, J. Am. Chem. Soc., 89, 6814 (1967).

7. P. J. Flory and R. A. Orwoll, J. Am. Chem. Soc., 89, 6822 (1967).

8. D. Patterson and J. M. Bardin, Trans. Faraday Soc., 66, 321 (1970)

9. D. Patterson and G. Delmas, Disc. Faraday Soc., 49, 98 (1970).

10. D. Patterson, Y. B. Tewari, and H. P. Schreiber, J.C.S. Faraday II, 68, 885 (1972).

11. G. D. Patterson and P. J. Flory, J.C.S. Faraday II, 68, 1098 (1972).

12. J. Hildebrand, J. Am. Chem. Soc., 59, 794 (1937).

13. R. H. Fowler and G. S. Rushbrooke, Tran. Far. Soc., 33, 1272 (1937).

14. J. Hijmans and TH. Holleman, Mol. Phys., 4, 91 (1961).

15. J. S. Rowlinson, Liquids and Liquid Mixtures, 2ned., (Butterworth and Comp. London, 1969), 123.

16. T. H. Van der Waals and J. J. Hermans, Rec. Trav. Chem., 69, 971 (1950).

17. M. L. McGlashan and K. W. Morcom, Trans. Faraday Soc., 57, 581 (1961).

18. C. Harrison and J. Winnich, J. Chem. Eng. Data, 12, 176 (1967).

19. TH. Holleman, Physica, 29, 585 (1963).

20. I. Prigogine, A. Bellemans, and Naar-Colin, J. Chem. Phys., 26, 751 (1957).

21. I. Prigogine, Molecular Theory of Solutions, (Interscience Publishers Inc., New York, 1957), 337.

22. TH. Holleman and J. Hijmans, Physica, 28, 602 (1962).

23. J. Hijmans, Physica, 27, 433 (1961).

24. J. N. Van der Waals, Trans. Faraday Soc., 52, 916 (1956).

25. M. J. Sims and J. Winnick, J. Chem. Eng. Data, 14, 164 (1969).

26. A. G. Williamson and R. L. Scott, Trans. Faraday. Soc., 66, 335 (1970).

27. A. J. B. Cruickshank, B. W. Gainey and C. L. Young, Trans. Faraday Soc., 64, 337 (1968).

28. P. Bothorel, J. Colloid Sc., 27, 529 (1968).

29. K. Nagai, J. Chem. Phys., 47, 4690 (1967).

30. B. Lemaire, G. Fourche and P. Bothorel, Compt. Rend, 274, 1481 (1972).

31. H. Quinones and P. Bothorel, Compt. Rend., 277, 133 (1973).

32. D. Patterson, P. Tancrede, V. T. Lam and P. Picker, J.C.S. Faraday II, 69, 1465 (1973).

33. P. Bothorel and G. Fourche, J.C.S. Faraday II, 69, 441 (1973).

34. M. Barbe and D. Patterson, J. Phys. Chem., 82, 40 (1978).

35. D. Patterson and M. Barbe, J. Phys. Chem., 80, 2435 (1976).

36. G. D. Patterson, A. P. Kennedy, and J. P. Latham, Macromolecules, 10, 667 (1977).

37. S. N. Bhattacharyya and D. Patterson, J. Phys. Chem., 83, 2979 (1979).

38. A. Heintz and Rüdiger N. Lichtenthaler, Angew. Chem. Int. Ed. Engl., 21, 184 (1982).

39. H. Klunder, W. E. Hammers and C. L. de Ligny, J. Soln. Chem., 7, 475 (1978).

40. A. T. Rodriguez and D. Patterson, J. Chem. Soc., Faraday Trans. 2, 78, 501 (1982).

41. S. N. Bhattacharyya and D. Patterson, J. Phys. Chem., 9, 247 (1980).

42. A. T. Rodriguez and D. Patterson, J. Chem. Soc., Faraday Trans 2, 78, 491 (1982).

43. G. Dessauges, N. Miljevic, and W. A. Van Hook, J. Phys. Chem., 84, 2587 (1980).

44. O. K. Yohara and G. C. Benson, Can. J. Chem., 51, 2489 (1973).

45. G. S. Kell, J. Phys. Chem. Ref. Data, 6, 1109 (1977).

46. H. T. Van and D. Patterson, J. Soln. Chem., 11, 783 (1982).

47. A. J. Treszczanowicz, O. Kiyohara and G. C. Benson, J. Chem. Thermodynamics, 13, 253 (1981).

48. J. R. Goates, J. B. Ott, and R. B. Grigg, J. Chem. Thermodynamics, 13, 907 (1981).

49. H. Hala, J. Pick, V. Fried and O. Vilim, Vapor-Liquid Equilibrium, 2d. ed. (Pergomon, Oxford, 1967).

50. H. C. Van Ness and M. M. Abbott, Int. DATA. Ser. Selec. Data Mixtures Ser A., 1977, pp 7-9.

51. Gy. Jakli and W. A. Van Hook, J. Phys. Chem., 85, 3480 (1981).

52. G. Jakli, P. Tzias, and W. A. Van Hook, J. Chem. Phys., 68, 3177 (1978).

53. M. K. Dutta-Choudhury, G. Dessauges and W. A. Van Hook, J. Chem. Phys., 86, 4068 (1982).

54. G. Jansco and W. A. Van Hook, J. Chem. Phys., 68, 3191 (1978).

55. J. D. Worley, Can. J. Chem., 45, 2465 (1967).

56. S. Goldman, Can. J. Chem., 52, 1668 (1974).

57. S. Goldman and T. R. Krishnan, J. Soln Chem., 5, 693 (1976).

58. E. E. Tucker, and S. D. Christan, J. Phys. Chem., 83, 426 (1979).

59. M. K. Dutta-Choudhury, N. Miljevic, and W. A. Van Hook, J. Phys. Chem., 86, 1711 (1982).

60. P. Backx and S. Goldman, J. Phys. Chem., 85, 2975 (1981).

61. A. J. Trezczanwoicz and G. C. Benson, J. Chem. Thermodynamics, 9, 1189 (1977).

62. J. B. Ott, K. N. Marsh, and R. H. Stokes, J. Chem. Thermodynamics, 13, 371 (1981).

63. G. M. Janini and D. E. Matire, J. Chem. Soc. Faraday Trans 2, 70, 837 (1974).

64. K. N. Marsh, J. B. Ott, and M. J. Costigain, J. Chem. Thermodynamics, 12, 343 (1980).

65. G. Scatchard, S. Wood, and J. Mochel, J. Am. Chem. Soc., 61, 3206 (1939).

66. E. R. Brewster and M. L. McGlashan, J. Chem. Soc Faraday Trans. I., 69, 2046 (1973).

67. J. Stecki and A. W. Jackowski, J. Chem. Thermodynamics, 8, 1095 (1976).

68. K. Elliot and C. J. Wormald, J. Chem. Thermodynamics, 8, 881 (1976).

69. S. Murakami and G. C. Benson, J. Chem., Thermodynamics, 1, 559 (1969).

70. B. H. Stokes, K. N. Marsh, and R. P. Tomlins, J. Chem. Thermodynamics, 1, 211 (1969).

71. K. Y. Hsu and H. L. Clever, J. Chem. Thermodynamics, 7, 435 (1975).

72. C. G. Boissonnas, Helv. Chim. Acta, 22, 541 (1939).

73. H. C. Van Ness and M. M. Abbott, Classical Thermodynamics of Nonelectrolyte Solutions, (McGraw-Hill Book Company, N. York; 1982), 336.

74. G. M. Wilson, J. Am. Chem. Soc., 86, 127 (1964).

75. J. A. Barker, Aust. J. Chem., 6, 207 (1953).

76. M. B. Ewing and K. N. Marsh, J. Chem. Thermodynamics, 5, 651 (1973).

77. A. Desmyter and J. H. van der Waals, Rec. Trav. Chim., 77, 53 (1958).

78. J. D. Gomez-Ibanez and C. T. Liu, J. Phys. Chem., 67, 1388 (1963).

79. M. Diaz Pena and M. Benitez de Sota, Anales Real Soc. Espan. Fis. Quim. (Madrd). Ser B., 61, 1163, (1965).

80. R. Battino, Chem. Rev., 71, 5 (1971).

81. E. Liebermann, Chem. Eng. J., 22, 159 (1981).

82. L. Ernst Liebermann, Chem. Eng. J., 24, 111 (1982).

83. D. Patterson, Y. B. Tewari, H. P. Schreiber and J. E. Guillet, Macromolecules, 4, 356 (1971).

84. E. R. Thomas, B. A. Newman, T. C. Long, D. A. Wood and C. A. Eckert, J. Chem. Eng. Data., 27, 399 (1982).

85. M. L. Martin and L. Symons, J. Chem. Thermodynamics, 13, 81 (1981).

86. M. A. Leiva, J. P. Greenberg, and C. M. Knobler, J. Chem. Eng. Data., 24, 208 (1979).

87. R. S. Chahal, W. P. Kao, and D. Patterson, J.C.S. Faraday I, 69, 1834 (1979).

88. M. Costas and D. Patterson, J. Soln. Chem., 11, 807 (1982).

89. F. A. Guggenheim, Mixtures, (Oxford University Press, 1952).

90. P. J. Flory, J. Am. Chem. Soc., 87, 1833 (1965).

91. D. W. Arnold, R. A. Greenkorn and K. C. Chao, J. Chem. Eng. Data, 27, 123 (1982).

92. M. L. McGlashan, K. W. Morcum and A. G. Williamson, Trans. Faraday Soc., 57, 601 (1961).

93. M. L. McGlashan and A. G. Williamson, Trans. Faraday Soc., 52, 916 (1956).

94. W. Brostow, Phys. Chem. Liq., 3, 91 (1972).

95. T. Nitta, E. A. Turek, R. A. Greenkorn and K. C. Chao, AICHE J., 23, 144 (1977).

96. V. P. Villar, R. Bravo, and I. I. Paz Androde, J. de Chim. Phys., 80, 2 (1983).

APPENDICES

APPENDIX 1

METHOD OF BOISSONNAS

The method of Boissonnas[72] is readily derived from the Gibbs-Duhem equation,

$$x_1 \, \partial \ln\gamma_1/\partial x_2 + x_2 \, \partial \ln\gamma_2/x_2 = 0 \qquad \text{A-1-1}$$

or

$$\partial \ln\gamma_1/\partial x_2 = -x_2/(1-x_2) \, \partial \ln\gamma_2/\partial x_2 \qquad \text{A-1-2}$$

Since $\partial \ln x/\partial y = 1/x \, \partial x/\partial y$, equation 2 becomes

$$1/\gamma_1 \, \partial\gamma_1/\partial x_2 = -x_2/(1-x_2) \, 1/\gamma_2 \, \partial\gamma_2/\partial x_2 \qquad \text{A-1-3}$$

Now if it is assumed that the partial pressure of the solvent also depends on the mole fraction of the solute, and that the activity coefficients may be written as $\gamma_i = P_i/x_i P_i^0$, then equation 3 becomes,

$$\partial\gamma_1/\partial x_2 = ((\partial P_1/\partial x_2)x_1 + P_1)/P_1^0(1-x_2)^2 \qquad \text{A-1-4}$$

Differentiating equation (4) with respect to x_2 and simplifying, we obtain

$$\partial\gamma^2/\partial x_2 = [(\partial P_2/\partial x_2)x_2 - P_2]/x_2^2 P_2^0 \qquad \text{A-1-5}$$

By substituting equations 4 and 5 into equation 3, it becomes,

$$(\partial P_1/\partial x_2) = -P_1/P_2 \, (\partial P_2/\partial x_2)x_2/x_1 \qquad \text{A-1-6}$$

Now if the vapor phase is assumed to be ideal, i.e., $P_1 = P_T - P_2$, and

$$\partial P_1/\partial x_2 = \partial P_T/\partial x_2 - \partial P_2/\partial x_2 \qquad \text{A-1-7}$$

then equation 6 becomes

$$\partial P_T/\partial x_2 - \partial P_2/\partial x_2 = -P_1/P_2(\partial P_2/\partial x_2)x_2/x_1 \qquad \text{A-1-8}$$

Thus by rearranging equation 8, we obtain a relationship which is identical to the method of Boissonnas;

$$\partial P_2/\partial x_2 = [1/(1-P_1x_2/P_2x_1)]\cdot\partial P_T/\partial x_2 \qquad \text{A-1-9}$$

APPENDIX 2

SIMPLE LATTICE MODEL

For an n-alkane molecule consisting of j carbon atoms at infinite dilution in a solvent of n carbon atoms, and with a coordination number, c, there will be three types of possible interactions; end-end, EE, middle-end, ME, and middle-middle, MM. In the pure component, there are j-1 internal interaction. The numbers of external interactions will be the difference between the total number of interactions, j•c, and the internal interactions,

$$j \cdot c - (j-1) = j(c-1) + 1 \qquad \text{A-2-1}$$

The EE interactions per solute molecule would be defined as

$$\text{End-End} = 4(c-1)/n, \qquad \text{A-2-2}$$

where c-1 represents the number of end interactions per solute $-CH_3$ group. The coefficients of EM, ME and MM will be defined, respectively, as

$$\text{END-MIDDLE} = 2(c-1)(n-2)/n \text{ EM} \qquad \text{A-2-3}$$

$$\text{MIDDLE-END} = 2(j-2)(c-2)/n \text{ ME} \qquad \text{A-2-4}$$

and

$$\text{MIDDLE-MIDDLE} = (j-2)(n-2)(c-2)/n \text{ M.M.} \qquad \text{A-2-5}$$

The total external interactions would then be defined as

$$I_{Total} = [4(c-1)/n]EE + [(2(c-1)(n-2) + (j-2)(c-2))/n]EM + [(j-2)(n-2)(c-2)/n]MM \qquad A\text{-}2\text{-}6$$

By taking several values of c, n and j, we were able to define a set of coefficients for EE, EM and MM. The values were then used to generate a simple contact energy profile, Figure 26, pp 125.

Richard Steward Hutchings was born in Nashville, Tennessee on June 21, 1956. He graduated from Jones County High School, Gray, Georgia, in June 1974 and entered Mercer University of Macon, Georgia. In June 1978, he received the B.S. degree in chemistry and a major in physics.

He entered graduate school at The University of Tennessee at Knoxville in September 1978 and received the Doctor of Philosophy degree with a major in chemistry in March 1984.